BAG3 myofibrillar myopathy: model creation and characterization of a defect in mechanotransduction

By

Rebecca Robertson

Department of Human Genetics
McGill University, Montreal
February, 2022

A thesis submitted to McGill in partial fulfillment of the requirements of the degree of Doctor of Philosophy

ABSTRACT

BAG3 myofibrillar myopathy (MFM) is a rare and severe form of childhood muscular dystrophy. Typically caused by the pathogenic Pro209Leu substitution in the BAG3 protein, this myopathy results in progressive muscle weakness, spinal rigidity and peripheral neuropathy. Cardiomyopathy, and respiratory failure typically occur in the second decade of life and this is often the cause of death in these patients. BAG3 is a multifunctional protein, perhaps best known for its role as a co-chaperone to HSP70 as a part of the chaperone assisted selective autophagy (CASA) complex. CASA is of particular importance to skeletal and cardiac muscle due to the high rate of protein turnover in these tissues owing to the mechanical stress it experiences. The Pro209Leu variant stalls this complex, inducing toxic aggregate formation and preventing cargo processing, making it a toxic gain of function leading to loss of function. We have developed a murine model of this disease, the first with both whole body expression of the protein and an appreciable phenotype that recapitulates that seen in human patients. This model has one knock-in allele with an analogous varniant to the human variant, Pro215Leu, and one knock-out allele. This was chosen due to the lack of phenotype in the homozygous knock-in, and the presumed loss of functional BAG3 due to aggregation. The skeletal muscle of this model shows pathological changes characteristic of BAG3 MFM, including aggregates, inflammation, moth-eaten fibers, ragged red fibers and Z-disk streaming. Their phenotype is relatively mild, displaying only a lack of voluntary movement. Changes to the nuclei of these mice were also noted, such as abnormal envelopes, intranuclear accumulations which contained BAG3 and lamin A/C and increased heterochromatin. This led us to investigate the role of the nucleus and mechanosensing in the pathophysiology of this disease. Using fibroblasts from a patient bearing the P209L variant, we showed defects in both the nuclear envelope and cytoskeleton. The nucleus, which is significantly larger than that of controls but smaller than expected for their large cell body size, fails to change in size in response to extracellular matrix stiffness changes and does not change in size with the cell body at the same rate as control. These cells show disorganization of the cytoskeleton and nuclear damage which worsens with increases in tension. The accumulation of cytoskeletal components appears to be affecting the cells' ability to migrate as shown in a wound healing assay, and this defect was rescued by the inhibition of myosin through blebbistatin. Indeed, we observed poor actin turnover in fluorescence recovery after

photobleaching (FRAP) and an increase in active myosin light chain in the space surrounding the nucleus. An apparent consequence of this was the lack of activation of the mechanosensitive transcriptional co-activator YAP, with its lower nuclear entry in cells. This suggests that the changes in morphology are in relation to changes in mechanotransduction within the cell, and reducing this connection reduces the aberrant signaling. This thesis presents both an original model of BAG3 myofibrillar myopathy, as well as proposes a novel aspect of the pathophysiology of ths MFM, a defect in mechanosensing caused by defects to and uncoupling of the cytoskeleton and nuclear envelope.

RÉSUMÉ

La myopathie myofibrillaire BAG3 (MFM) est une forme rare et sévère de dystrophie musculaire infantile. Typiquement causée par la substitution pathogénique Pro209Leu, cette myopathie se traduit par une faiblesse musculaire progressive, une rigidité vertébrale et une neuropathie périphérique. La cardiomyopathie et l'insuffisance respiratoire surviennent généralement au cours de la deuxième décennie de vie et sont souvent cause de décès. BAG3 est une protéine multifonctionnelle bien connue pour son rôle co-chaperon de HSP70 dans le cadre du complexe d'autophagie sélective assistée par chaperon (CASA). CASA est d'une importance primordiale pour les muscles squelettiques et cardiaques en raison du taux élevé de renouvellement des protéines causées par les stress mécaniques. La mutation Pro209Leu bloque ce complexe, induisant la formation d'agrégats toxiques et empêchant le traitement de la cargaison. Cet enchaînement crée donc un gain de fonction toxique entraînant une perte de fonction. Nous avons développé un premier modèle murin de cette maladie avec une expression de la protéine dans tout le corps et un phénotype imitant celui observé chez les patients humains. Ce modèle a un allèle knock-in avec une mutation analogue à la mutation humaine, Pro215Leu, et un allèle knock-out. Cela a été choisi en raison de l'absence de phénotype dans le knock-in homozygote et de la perte présumée de BAG3 disponible par agrégation. Le muscle squelettique de ce modèle montre des changements pathologiques caractéristiques de BAG3 MFM comprenant des agrégats, une inflammation, une distribution irrégulière du réseau myofibrillaire résultant à des espaces vacants, des fibres musculaires rouges «déchiquetées» et des dommages diffus aux disques Z. Leur phénotype est modéré, ne montrant qu'un manque de mouvement volontaire. Des modifications des noyaux de ces souris ont également été notées, telles que des enveloppes anormales, des accumulations intranucléaires contenant BAG3 et Lamin A/C ainsi qu'une augmentation de l'hétérochromatine. Cela nous a conduit à étudier le rôle du noyau et de la mécanosensibilité dans la physiopathologie de cette maladie. En utilisant des fibroblastes d'un patient porteur de la mutation P209L, nous avons montré des défauts à la fois dans l'enveloppe nucléaire et dans le cytosquelette. Le noyau, qui est significativement plus gros que celui des contrôles mais plus petit qu'envisagé, ne change pas de taille en réponse aux changements de rigidité de la matrice extracellulaire et ne change pas de taille avec le corps cellulaire au même rythme que le contrôle. Ces cellules montrent une désorganisation du cytosquelette qui s'aggrave

avec les augmentations de tension, créant des agrégats positifs pour BAG3 et l'actine. L'accumulation de composants cytosquelettiques semble affecter la capacité des cellules à migrer, comme le montre un test de cicatrisation des plaies, et ce défaut a été sauvé par l'inhibition de la myosine par la blébbistatine. En effet, nous avons observé un faible renouvellement de l'actine dans la récupération de fluorescence après photoblanchiment (FRAP) et une augmentation de la chaîne légère de myosine active dans l'espace entourant le noyau. Une conséquence apparente a été le manque d'activation du coactivateur transcriptionnel mécanosensible YAP, avec son entrée nucléaire plus faible dans les cellules. Cela suggère que les changements de morphologie sont liés aux changements de la mécanotransduction dans la cellule et que la réduction de cette connexion réduit la signalisation aberrante. Cette thèse présente à la fois un modèle original de myopathie myofibrillaire BAG3 et propose un nouvel aspect de la physiopathologie de la MFM, un défaut de mécanodétection causé par des défauts à la fois du cytosquelette et de l'enveloppe nucléaire.

Table of Contents

LIST OF ABBREVIATIONS

AMOTL1/2: Angiomotin Like 1/2

ANOVA: analysis of variance

BAF: barrier to autointegration factor

BAG3: BCL-2-associated athanogene 3

BCL-2: B-cell lymphoma 2

BMD: Becker muscular dystrophy

bp: base pair

C57Bl/6: C57 black six

Cas9: CRISPR associated protein 9

CASA: chaperone assisted selective autophagy

CD45: cluster of differentiation 45

CK: creatine kinase

CMT: Charcot-Marie-Tooth

CNBP: cellular nucleic acid binding protein

COX: cytochrome c oxidase

CRISPR: clustered regularly interspaced short palindromic repeats

COX: Cytochrome c oxidase

DCM: dilated cardiomyopathy

DGC: dystophin glycoprotein complex

DM1: myotonic dystrophy type 1

DM2: myotonic dystrophy type 2

DMD: Duchenne muscular dystrophy

DMEM: Dulbecco's modified Eagle's medium

DMPK: dystrophia myotonica protein kinase

DMSO: dimethylsulfoxide

ECM: extracellular matrix

EDL: extensor digitorum longus

EDMD: Emery-Dreifuss muscular dystrophy

FRAP: fluorescence recovery after photobleaching

FBS: fetal bovine serum

FLNC: filamin C

H&E: hematoxylin and eosin

HSF1: heat shock factor 1

HSP: heat shock protein

HSP70: heat shock protein 70

HSPB1: Heat Shock Protein Family B (Small) Member 1

HSPB6: Heat Shock Protein Family B (Small) Member 6

HSPB8: Heat Shock Protein Family B (Small) Member 8

IgG: Immunoglobulin G

IgM: Immunoglobulin M

INM: inner nuclear membrane

IPV: Ile-Pro-Val

kDa: kilodalton

KI: knock-in

KO: knock-out

LAD: lamina associated domains

LATS1/2: Large Tumor Suppressor Kinase 1/2

LEM: LAP2, Emerin and MAN1

LGMD: limb girdle muscular dystrophy

LINC: Linker of Nucleoskeleton and Cytoskeleton

LMNA: lamin A/C

mg: milligram

MHC: myosin heavy chain

mL: milliliter

mM: millimolar

mTOR: mechanistic target of rapamycin

mTORC1: mechanistic target of rapamycin complex 1

NADH: nicotinamide adenine dinucleotide (NAD) + hydrogen (H)

NE: nuclear envelope

NEF: nucleotide exchange factor

ONM: outer nuclear membrane

p62: SH2 domain of 62 kDa

PAX7: paired box 7

PFA: paraformaldehyde

PNS: perinuclear space

PQC: protein quality control

PxxP: proline rich region

RRF: ragged-red fiber

SD: standard deviation

SEM: standard error of the mean

SUN: Sad1 and UNC84 domain-containing protein

SYNOP2: synaptopodin- 2

TA: tibialis anterior

TAZ: transcriptional coactivator with PDZ-binding motif

TEAD: transcriptional enhancer factor TEF

TEM: transmission electron microscopy

TSC: tubular sclerosis protein

UTR: untranslated region

VPS: vacuolar protein sorting

WT: wildtype

WW: tryptophan-tryptophan

YAP: Yes-associated protein

μm: micrometers

μM: micromolar

LIST OF FIGURES

Chapter 1

Chapter 2

Chapter 3

Chapter 4

ACKNOWLEDGEMENTS

This thesis was supported by the Pigini family (Fondazione Roby) and the Bellini family (The Bellini Foundation), and a scholarship from the Fondation du Grand Défi Pierre Lavoie.

I want to thank my supervisor, Dr. Bernard Brais, for accepting me into his lab and teaching me to be a creative and independent researcher. I also want to extend my gratitude to Dr. Josée Lavoie who, despite the geographical distance, ended up being a huge source of support for the second half of this thesis. Chapter 3 would not be half the quality it is without the generous contributions of her time, knowledge and materials.

I would like to thank so many of the people on the 6th floor who have gladly put up with my constant annoyances, nonsense, and food theft. It's been a blast. So, thank you to many members of the Brais, Armstrong, Shoubridge and McBride labs, past and present. Special thanks to my lab mothers, Marie-Josée and Mai, for their constant support and advice. Thanks to Talita for training and supporting me at the beginning of my PhD when this was all very new and scary, and thanks to Hana for whipping this thesis into shape at the end. Thanks to the members of Josée's lab for supporting me through my visit there, which was unfortunately cut short by the arrival of the pandemic.

Thank you to my committee members, Dr. Eric Shoubridge and Dr. Gary Armstrong. Their guidance and understanding was essential to the completion of this degree, and I thank them for being always approachable and available and for letting me cry in their offices.

I am grateful to my partner, Ernesto, who has been with me from the start, supporting me with unending patience and kindness through all of the tough moments. I wouldn't have made it without you. And thanks to our fat furry cat son, Miko, who has been a lovely creature and constant source of comfort and entertainment. Thanks to my parents and my friends for their support throughout this.

Thanks to whoever discovered coffee.

PREFACE

This thesis is written in accordance with the guidelines of the McGill University Graduate and Postdoctoral Studies Office, and is presented in a manuscript-based format. The studies described were performed under the supervision of Dr. Bernard Brais. This thesis

This thesis is composed of 5 chapters. **Chapter 1** is a general introduction which reviews key literature relevant to the thesis. **Chapter 2** presents a manuscript which describes the generation and characterization of a mouse model of BAG3 MFM which was published in *The American Journal of Pathology*. **Chapter 3** is a manuscript in preparation, which describes how the BAG3 P209L variant affects nuclear-cytoskeletal coupling and mechanotransduction.

Chapter 4 provides a discussion of the previous chapters and **Chapter 5** presents a general conclusion and future directions.

Contribution to original knowledge

The work described in this thesis provides an original contribution to the understanding of BAG3 MFM, a rare and severe childhood disease with no known treatment or cure. Prior to this work, no murine model of the disease which developed a phenotype existed.

Chapter 2 describes the development and characterization of a mouse model of BAG3 myofibrillar myopathy. We demonstrate that a compound heterozygous mouse, with one knock-out and one allele with a mP215L variant homologous to the human P209L, recapitulates the human form of the disease. This work demonstrates that development of a phenotype requires both a decrease in BAG3 protein level and a gain of function caused by the missense mutation, as neither knock-in/knock-in mice nor heterozygous knockout animals show the same phenotype. While this phenotype is mild, we believe that this may be useful to study early stages of the disease, as by the time most patients are biopsied the disease has progressed too far and damage to muscle has become extensive. With this work we provide a useful new tool to study this MFM which formerly lacked a mammalian model.

Chapter 3 presents data which shows a possible role for nuclear-cytoskeletal coupling and mechanotransduction in BAG3 MFM, a disease thought of as primarily due to Z-disk damage. We show that our mice develop nuclear deformities in the absence of extensive proximal muscle damage, suggesting a role for the nucleus in pathophysiology of disease. We also show that tension worsens both the nuclear and cytoskeletal defects *in vitro*, even in non myogenic cell lines. This work proposes a new facet to the pathophysiology of this disease, and a potential contributor to the severity of BAG3 MFMF compared to other myofibrillar myopathies. It also demonstrates how mechanical stress may contribute to increasing disease severity.

Contribution of authors

Chapter 2: This study was carried out with the following contributors: Rebecca Robertson, Talita C Conte, Marie-Josée Dicaire, Vladimir V Rymar, Abbas F Sadikot, Robert J Bryson-Richardson, Josée N Lavoie, Erin O'Ferrall, Jason C Young, Bernard Brais

I managed the colony, did the immunofluorescent labeling, histology, imaging and quantification, western blotting, performed the behavioural phenotyping, designed the experiments, interpreted the data and wrote the paper.

T.C.C. established the colony and aided in the generation of preliminary data for histology, immunofluorescent labeling, and pilot phenotyping. M.J.D. helped carry out the behavioral phenotyping and western blotting. V.V.R. and A.F.S. contributed the equipment for and aided in carrying out the grip strength experiments. E.F. helped with imaging interpretations. R.J.B., J.N.L and J.C.Y. were members of the BAG3 MFM collaboration, contributing intellectually and reviewing the manuscript. B.B. contributed to experimental design and writing of the paper.

Chapter 3: This study was carried out with the following contributors: Rebecca Robertson, Marie-Josée Dicaire, Josée N Lavoie, Bernard Brais

I did the cell culture, immunofluorescent labeling, imaging and quantification, designed the experiments, interpreted the data and wrote the paper.
M.J.D. managed the colony and helped with the experiments. B.B. and J.N.L. contributed to experimental design and writing of the paper.

CHAPTER 1: General introduction

BAG3 myofibrillar myopathy (MFM) is a disease that is both severe and extremely rare [1], with childhood onset and leading to death by the second or third decade of life. Most cases of BAG3 MFM are caused by the Pro209Leu (P209L) variant, resulting from the recurrent *BAG3* 626C>T mutation. It is almost always *de novo* in nature, with the exception of one known case in which the father was a mosaic who carried the mutation in his germ line[2]. The BAG3 protein is essential for the process of chaperone assisted selective autophagy, which is essential in muscle for its maintenance and proper functioning[3]. Defects in this process, like those in BAG3 MFM, can have severe consequences for the integrity of the muscle. In this thesis we developed a murine model of BAG3 MFM, which we used in conjunction with other tools, to study the pathophysiology of this disease.

In the first part of this introduction I will detail the cellular roles of BAG3 and the BAG family of proteins, as well as what is currently known of the effects of mutations to site Pro209, including the P209L mutation. I will also give background on myofibrillar myopathies at large, and their molecular and clinical effects. The first part of my thesis, chapter 2, will focus on the generation and characterization of a mouse model of this disease[4].

The third part of my thesis, chapter 3, presents original investigations on defective mechanotransduction in this disease. In the second part of my introduction, I will outline the mechanisms behind mechanotransduction and the current known role of BAG3 in maintenance of the nuclear envelope. I will also discuss how defects to the nuclear envelope which lead to impaired mechanosignaling, such as in Emery-Dreifuss muscular dystrophy (EDMD) and laminopathies, affect the cell as well as the muscle at large.

1.1 Muscular Dystrophy

1.1.1 The skeletal muscle

Skeletal muscle is a highly organized tissue, making up 40% of body weight and accounts for 50-75% of the proteins in the human body, making it the most abundant of tissues in the human body[5]. Proper functioning of this tissue is essential to our ability to generate force and movements. As such it is required for us to move, maintain our posture, breathe and also generate heat. It also serves an important metabolic function, serving as an important reservoir of amino acids for other tissues that becomes all the more essential in times of stress, illness or starvation[6]. Loss of this tissue leads to a loss of quality of life, and eventually life itself, as evident in those suffering from sarcopenia later in life[7]. As such, a proper maintenance of this tissue is essential.

The skeletal muscle is composed of muscle fibers; long, polynucleated post-mitotic cells which are up to 100 μm in diameter and 30 cm in length, individually wrapped in a membrane called the sarcolemma. These are grouped together into bundles called fascicles, and these bundles make up the larger muscle. Three layers of connective tissue define these structures: the epimysium around the muscle, the perimisium around the fascicles and the endomysium around the individual fibers[5 8]. In the endomysium lies the capillaries and nerves required to support the muscle fibers. This triple layer of connective tissue provides tensile support to the muscle tissue during mechanical stress[5]. This connective tissue, as well as the tendons, become thicker in comparison to fiber size in larger muscles and depending on size of the species in question due to the increased stress that comes with increased size[9].

Within the muscle fiber are the striated myofibrils, the contractile units of the muscle composed of sarcomeres, which contain the locomotory proteins actin and myosin (Figure 1.1). The costamere, composed primarily of the dystrophin-glycoprotein and the integrin-vinculin-talin complexes, tethers the sarcolemmal membrane to the Z-disk of the sarcomere through filamin-C. It is similar to the focal adhesion complexes within cells, transmitting lateral force from sarcomere to sarcolemma to the extracellular matrix. This allows for force to be transduced

from one myofibril to an adjacent one, and also helps maintain the structural integrity of the myofibril[10].

The sarcomeres are separated by the Z-disk, a lattice that serves to anchor the thin filaments actin, tropomyosin and troponin in place and transmit mechanical signals[11]. While this structure is generally of fixed width, muscle injury or disease can lead to loss of integrity and characteristic Z-disk "streaming" [12]. The area surrounding the Z-disk, which can be visualized as a band of lighter color on electron microscopy, is called the I-band. This band changes in size during contraction as myosin, which defines the adjacent M-band, overlaps the thin filaments. Titin, the largest protein in the human body, spans the sarcomere and provides support to this complex machinery[5]. Usage of ATP at the ATPase site in the myosin heads allows myosin to detach from actin and form new cross bridges on actin as the sites are exposed by tropomyosin, allowing it to move itself across actin[5]. This process, called bridge cycling, is the basis for contraction.

The muscle fibers can be divided into two main types: slow (type I) and fast (type II) twitch fibers. There are differences in myosin heavy chain (MHC) type and energy usage between the fiber types, and a further spectrum of subdivisions of fiber types exist. The most common types in human muscle are pure type I, type 2X, and type 2A, and intermediate between the two. Type I fibers are fatigue resistant, relying on aerobic respiration. They are commonly found in postural muscles that provide constant support and are also called "red" fibers due to their colouration from increased myoglobin content. The fast twitch fibers are fast and powerful, relying on glycolytic stores to provide bursts of power. The type 2X fibers are best suited to sudden movements like jumping or sprinting; the intermediate type 2A being used in repetitive movements like chewing[13]. Fiber type is determined by the type of motor nerve innervation, and damage or loss of motor nerves can result in a phenomenon called fiber type grouping.

1.1.2 Muscular dystrophies

Muscular dystrophies are a group of inherited myogenic diseases defined by muscle wasting and weakness. It is a highly heterogeneous group of diseases, varying in age of onset,

mode of transmission, degree of severity and distribution of the affected muscles. Diagnosis is typically done through physical examination, testing of creatine kinase (CK) levels, as this enzyme is released into the blood when muscle is damaged, and muscle biopsy to assess damage to fibers and fibrosis or fatty replacement of tissue. Genetic testing can determine the causative gene, as the most prevalent mutations are known[14]. While our knowledge of the genetics and pathophysiology of many forms is extensive, treatments are still largely lacking although many patients are able to live decades longer with advances in supportive therapies[15].

The most common and well known of the muscular dystrophies is Duchenne Muscular Dystrophy (DMD), a disease that primarily affects young boys that was first described in 1849 by Guillaume-Benjamin Duchenne (unpublished), and the first case series published in 1851[16] by Edward Meryon. DMD, and its milder form Becker muscular dystrophy (BMD) are caused by mutations to dystrophin. This X-linked recessive disorder results in the total absence of dystrophin in DMD, and a truncated version of the protein in BMD[17]. Part of the dystrophin glycoprotein complex (DGC) adheres the cytoskeleton of the muscle cell to the basal lamina and is thought to act as a stabilizer and prevent contraction induced damage. Without it, this stability is lost and damage occurs, resulting in muscle wasting[15]. Onset begins in early childhood as patients develop difficulties walking as primarily proximal muscle weakness progresses, and most are wheelchair bound by 12 years of age. Respiratory and sometimes cardiac involvement eventually develop, and this is often the eventual cause of death[14]. Mutations to other components of the DGC can lead to a different kind of muscular dystrophy, limb girdle muscular dystrophy (LGMD). LGMDs are a highly heterogeneous group, defined by their clinical characteristics. They all primarily affect the pelvic and shoulder girdles, although progression and onset varies. Their classification is separated by inheritance type, autosomal dominant (D) or autosomal recessive (R)[18]. While a number of subtypes are caused by variants in different sarcoglycans and other members of the DGC[19], over 50 causative genetic loci have been identified[20], making this a highly heterogenous group of diseases without clear common mechanism of damage.

Another form of dystrophy, which has later relevance to this thesis, is Emery Dreifuss muscular dystrophy (EMDM). This is either an X-linked disease, caused by mutations in *EMD*,

or an autosomal dominant version caused by mutations in *LMNA*, both of which encode for components of the inner nuclear membrane. While this disease has clinically heterogeneous presentation, most present first with joint contractures at the ankles and elbows, slowly progressing muscle weakness and wasting that begins with a humero-peroneal distribution, and later heart conduction defects[21]. While the skeletal muscle weakness is rarely severe, cardiac involvement is typically present by age 30, becoming apparent in the second decade of life. This can result in sudden death in patients, including those who lack obvious muscle weakness or females who are carriers of the X-linked version[22]. While the muscle shows typical myopathic traits, what sets this dystrophy apart is the nuclear phenotype. Ultrastructural examination of the nuclei of these patients show heterogenous changes, including fragility and breakdown, nuclear rupture, chromatin reorganization, shrunken nuclei, aberrant structure, loss of peripheral heterochromatin, highly hyperchromatic nuclei, chromatin leakage and nuclear pockets containing sarcoplasmic material[23–25]. Despite this broad range of defects, they all suggest the same thing: a loss of nuclear stability. This makes the nuclei particularly vulnerable to damage in tissues where they are subject to mechanical stress, such as the muscle.

1.1.3 Myofibrillar myopathies

The myofibrillar myopathies (MFM) are a group of muscular dystrophies characterized by myofibrillar disintegration that begins at the Z-disk, resulting in inclusions of accumulated proteins[26,27]. While the onset, severity and clinical features vary, histologically they share this distinct morphological characteristic. Ultrastructurally, streaming of the Z-disk is seen as one of the earliest changes as well as granulous accumulations. This loss of stability at the Z-disk results in the disintegration of the myofilaments. As this progresses, the sarcomere becomes unrecognizable and is replaced by granulofilamentous material. Organelles, dislocated from their original membrane bound positions, accumulate in the voids created and eventually are degraded themselves [26,27]. Histological evaluations often reveal vacuoles, aggregates, atrophic and angular fibers, cytochrome *c* oxidase (COX) and nicotinamide adenine dinucleotide +hydrogen (NADH) deficient fibers, atrophic fibers and ectopic expression of Z-disk proteins as well as sarcoglycans, ubiquitin and gelsolin[28].

The early Z-disk damage seen in MFMs gives a hint as to the causative genes in these dystrophies; almost all are Z-disk proteins. The genes so far identified are *DES*[29] , *CRYAB*[30], *ZASP*[31], *FLNC*[32], *MYOT*[33], *FHL1*[34], *TTN*[35] and *BAG3*[1]. Clinically, there are some similarities between the MFMs, with all showing progressive muscle weakness which often begins distally, and most have abnormally high creatine kinase (CK) values. Neuropathy and cardiac involvement is also a frequent finding in myofibrillar myopathies, and the onset is usually in adulthood. There is, however, a very variable clinical spectrum between the subtypes[26]. The most commonly mutated gene in MFM is *Desmin* (*DES)*, with 50 known pathogenic mutations[28].

Desminopathies are the largest subset of MFMs. Desmin is a muscle-specific intermediate filament of 53.5 kDa, located at the Z-disk periphery. It spans the Z-disk, acting as a scaffold that connects the contractile apparatus to the costameres as well as tethering organelles such as the nucleus and mitochondria in place. As such, it is important for maintaining the integrity of the sarcomere, as well as defining the proper shape and position of the nucleus and mitochontria[36]. Loss of desmin results in the loss of the costameres, along with some loss of the Z-disc domains. This effect varies between muscles with tibialis anterior (TA) and extensor digitorum longus (EDL) being more affected than the quadriceps or gastrocnemius, and this may be based on the differential usage patterns of the muscles, and as such most cases have distal involvement of the lower limbs[37]. Most cases of desminopathy are autosomal dominant with adult onset, and the long term prognosis depends on severity of cardiac involvement in most cases, with all types of cardiomyopathy being part of the desminopathy spectrum[28]. Like most other muscular dystrophies, it is progressive in nature.

The other MFMs are somewhat heterogeneous in nature. While desminopathy, αB-crystallinopathy and ZASPopathy are predominantly distal, the rest are mixed or proximal in nature. Peripheral neuropathy is a more common finding in ZASPopathy, filaminopathy and BAG3 MFM[38]. Uniquely, some αB-crystallin MFM mutations also cause cataracts[39]. Morphological findings also vary; filamentous bundles are common in myotilinopathy and zaspopathy, while granulofilamentous accumulations are more common in desminopathies and αB-crystallinopathies. Apoptotic changes are typically only present in αB-crystallinopathies and

BAG3 MFM, and prominent necrosis in those with myotilin mutations as well as vacuoles[1,28]. Despite what is known about MFMs and the differences in their presentations, they can still be difficult to diagnose due to the focal nature of lesions, nonspecific changes to the muscle and unclear boundaries as to what constitutes an MFM[28].

1.2 BAG3 and its molecular roles

1.2.1 BAG3

BAG3 (BCL-2-associated athanogene 3) is a highly multifunctional protein best known for its role as a co-chaperone to heat-shock proteins. The *BAG3* gene is encoded on chromosome 10, spanning 26,440 base pairs (bp). It was first discovered in 1999 through yeast two-hybrid screening, using the ATPase domain of heat-shock factor 70 (HSP70) as bait[40], which binds its BAG domain. BAG3 is part of a larger family of proteins, all defined by the presence of a BAG domain (Figure 1.2). They are considered to be "pro-survival" proteins due to their anti-apoptotic properties and heat-shock protein co-chaperoning. The BAG family as well as the domain which was responsible for BCL-2 binding was named for this interaction. The second part of the name, anthanogene, was derived from the latin word athánatos, meaning "against death". This came from the anti-apoptotic properties of the first BAG protein[41]. This family is well conserved across eukaryotic species, with homologues being found in *C. elegans*, yeast species[40], Drosophila[42], and even plants[43].

BAG3 is primarily expressed as a full length gene product, an ubiquitous protein of 75kDa. A shorter, 40kDa, version has been found which lacks a part of the C-terminal that is only expressed in synaptosomes[44], and thus far it has been poorly characterized. The full length protein contains the aforementioned BAG domain at the C-terminus, a tryptophan-tryptophan (WW) domain at the N terminus, a proline rich repeat region (PxxP) and two adjacent Ile-Pro-Val (IPV) motifs (Figure 1.3). The BAG domain, as previously mentioned, is important for both binding to BCL-2 and Hsp70. When bound to BCL-2 it works to prevent Bax and Fas mediated apoptosis[45]. The PxxP region is essential to BAG3's interaction with dynein, a cytoskeletal motor protein. Binding to the dynein motor complex allows for the transport of cargo by the CASA complex to the aggresome for degradation[46]. The WW domain binds to proline rich

regions of other proteins, such as that of synaptopodin-2 (SYNPO2), and this interaction helps drive autophagosome formation[47]. Finally, the two IPV motifs bind to small heat-shock proteins (HSP), with the highest affinity for HSPB8 and HSPB6[48].

Despite being most well known for its anti-apoptotic, which derives from its interaction with B-cell lymphoma 2 (BCL2), stabilizing BCL2 so that it may prevent the pro-apoptotic activity of Bak and Bax through direct interaction[45], and autophagic activities (Chapter 1.2.2.), BAG3 has a number of other roles. It has a transcriptional impact through its interaction with members of the Hippo signaling pathway. It binds to Large Tumor Suppressor Kinase (LATS) 1/2 as well as Angiomotin Like (AMOTL)1/2 through its WW domain, preventing the phosphorylation and cytoplasmic retention of the transcriptional regulators Yes Associated Protein (YAP) and transcriptional coactivator with PDZ-binding motif (TAZ)[49]. Without inhibition by LATS1/2 and AMOTL1/2, YAP/TAZ can translocate to the nucleus and activate expression of a wide variety of proteins including filamin, cytoskeletal components, cell cycle regulators, repair pathways and anti-apoptotic genes[50].

The WW domain is also important for BAG3's regulation of the mechanistic target of rapamycin (mTOR) pathway. Tubular sclerosis 1 (TSC1) and tubular sclerosis 2 (TSC2) proteins are inhibitors of the mTOR complex 1 (mTORC1). BAG3 interacts with the proline rich domains of TSC1 and TSC2 with its WW domain. Under mechanical strain BAG3 recruits the TSC1/2 to actin stress fibers to locally inhibit mTORC1 activity, initiating autophagy. As a consequence mTORC1 can function uninhibited in the cytoplasm as its inhibitors are now localized to the stress fibers, which initiates protein translation. This effect was evident by the localization of TSC1 both *in vivo* and in human muscle biopsied post-exercise[51]. This WW domain also appears to contribute to cell adhesion, as Cos7 cells lacking the BAG3 WW domain lose adhesion and motility[52].

BAG3 also has mitotic functions through the regulation of actin dynamics. Mitosis involves significant changes in cellular tension as well as mitotic cytoskeletal remodeling. During mitotic entry BAG3 becomes hyperphosphorylated and localizes to centrosomal regions, forms a complex with HSPB8 without HSP70, and shows increased association with p62.

Through this interaction it appears to guide mitotic spindles to their correct orientation through the actin-rich retraction fibers through remodeling of the fibers. Depletion of the BAG3-HSPB8 complex results in disorganization of the retraction fibers as well as nuclear blebbing, impaired mitotic rounding, multinucleation and improper chromosomal segregation[53]. It also appears to impact F-actin remodeling, with knock-down of members of the complex resulting in an aberrant segregation between daughter cells at telophase and ultimately failed cytokinesis[54]. It also plays a role in the capping of F-actin with CapZβ1, promoting its association with HSP70 and regulating its structural stability in this way[55]. This shows an additional protein quality control (PQC) role for BAG3 outside of the CASA complex that is essential for proper mitotic remodeling.

1.2.2 Chaperone assisted selective autophagy

BAG3 is well known for its role in PQC. This is primarily accomplished through its role in chaperone mediated selective autophagy (CASA). CASA is a type of macroautophagy distinct from chaperone mediated autophagy due to its selective nature and because cargo is not directly transported to lysosomes. BAG3 acts as a scaffold for this complex, linking together components. The CASA complex consists of HSP70, HSP40, CHIP, p62 (SQSTM1), HSPB8, SYNPO2 and BAG3[3,47,56]. HSP70 serves as a selective chaperone for misfolded proteins which have been ubiquitinated by the ubiquitin ligase C-terminus of Hsc70-interacting protein (CHIP). BAG3 acts as a nucleotide exchange factor (NEF) through the interaction between its BAG domain and HSP70s ATPase domain, allowing it to bind and release cargo[57]. HSP40 helps to modulate this ATPase activity of HSP70 through its J-domain, inducing the binding of substrate[58]. ATP cycling is important to proper interaction and management of HSP70's client proteins, driving its activity as a chaperone and inducing client refolding to reduce insolubility[59,60]. Other members of the CASA complex, such as HSPB8, serve to aid this process by stabilizing proteins in their soluble state.

Small HSPs, particularly HSPB8, are brought into the complex through their interaction with BAG3's two IPV motifs. Small HSPs typically form large oligomers, and within the context of PQC they act to stabilize non native proteins. While they do not have ATPase activity like larger HSPs, small HSPs all share an α-crystallin domain. This domain is what stabilizes

these non-native proteins in a soluble state, preventing them from becoming insoluble and forming aggregates. This activity increases the efficiency of the refolding process undertaken by larger HSPs, such as that of HSP70 in the CASA complex[61]. These stabilized, refolded proteins are then transported for disposal.

The damaged proteins that are sequestered by the CASA compex are actively transported to perinuclear aggresomes. This is accomplished through BAG3 binding to dynein, a microtubule motor protein, via its PxxP domain[46]. Once at the aggresome, BAG3 stimulates the formation of autophagosomes through its interaction with SYNPO2 and p62. When the WW domain of BAG3 interacts with SYNPO2 it tethers to a vacuolar protein sorting (VPS) complex, specifically that of VPS18. This VPS complex is involved in the tethering of phagophore membranes, which are precursors to autophagosomes. On this membrane is LC3; once p62, an autophagic ubiquitin adaptor, recognizes the ubiquitinated cargo carried by the CASA complex it interacts with LC3. This stimulates engulfment of the cargo and formation of the autophagosome from the phagophore membrane[62]. From there, autophagosomes eventually fuse with lysosomes for degradation.

In most tissues under physiological conditions BAG1 replaces BAG3 in the complex; however, this induces proteasomal degradation instead of autophagic. The loss of expression of one BAG induces the expression of the other, and, during increased stress such as that experienced through aging, the ratio of BAG3 to BAG1 increases as PQC needs to be increased, acting as an adaptive molecular switch between proteosomal and autophagic pathways[63]. As such, BAG3 expression is upregulated in response to overloading of the proteosomal system[64] and of all the BAG proteins, it has the highest affinity for the ATPase site of HSP70, likely due to its importance during stress[59]. Through this, BAG3 upregulation allows for the switch to autophagy to occur. BAG3 expression is controlled by heat shock factor 1 (HSF1), which interacts with heat shock-responsive elements in the *bag3* promotor and is part of a larger family of heat shock factors that control the expression of stress inducible genes[65]. BAG3 is also responsible for shuttling HSF1 to the nucleus, actively translocating there during periods of stress and helping to drive the heat shock response responsible for its own transcription[66].

CASA is essential for the maintenance of muscle through PQC at the Z-disk, a force-bearing structure which is subject to significant stress during contraction. Filamin, a force-bearing Z-disk protein which anchors actin and unfolds under mechanical stress, is a target of particular importance for CASA. Successful turnover of this protein is essential for maintenance of the Z-disk, and impairment of CASA leads to Z-disk disintegration[47]. In line with this, BAG3 expression is highest in skeletal muscle where it is constitutively expressed. Mechanical tension also induces the expression of BAG3, and in turn this helps maintain normal tension in the tissue as well as normal mechanotransduction[62]. This process also appears to be important in neuronal maintenance, having been linked to the clearance of pathological forms of huntingtin[67], the Alzheimer's protein tau[68], and oxidatively damaged proteins associated with aging[63]. This suggests that BAG3 is important in maintaining protein homeostasis, preventing toxic accumulations within neurons.

1.2.3 BAG3 myofibrillar myopathy: morphological and clinical characteristics

BAG3 MFM is typically caused by the recurrent Pro209Leu variant in one of two IPV motifs. First described by Selcen *et al.* (2009)[1] in three patients, this MFM is a severe autosomal dominant disease with childhood onset. Its severity and early onset makes it extremely rare, as the mutation is almost always *de novo* in nature[27], except in one case where the father was known to be a mosaic and passed the mutation to his two children[2]. This makes the allele's frequency in the population essentially zero[69]. This MFM shares the same classical features that other MFMs exhibit. Z-disc streaming, granulofilamentous accumulations, aggregates, atrophic fibers, vacuoles and "rubbed out" fibers on NADH staining, indicating myofibrillar disruption, are frequent findings in this myopathy[27,70]. Unique in this myopathy is the findings of increased nuclear apoptosis, a feature shared only with αB-crystallinopathy[27], giant axonal neuropathy[71] and rigid spines[1]. Clinically, BAG3 MFM stands out in its severity and early onset. It may begin proximally or distally and is often accompanied by cardiomyopathy, peripheral neuropathy or a rigid spine. Onset is typically in early childhood, with patients showing signs such as toe walking due to contractures, progressive muscle weakness, atrophy and easy fatigability. As the course of disease progresses, which occurs rapidly, respiratory insufficiency and cardiomyopathy develops[1]. Many develop peripheral neuropathy, with or without giant axons[71,72]. Some patients

require heart transplant in their second decade of life[1,2,72], and death usually results in the second or third decade from respiratory or cardiac failure[1,2,72]. The cardiomyopathy present in patients is typically either restrictive cardiomyopathy or hypertrophic cardiomyopathy[1,2,73]. Although these are the most common clinical symptoms there is some variation in the clinical spectrum. While most patients demonstrate the typical symptoms described above, a number of atypical cases have been reported in literature. Some patients present with a phenotype that resembles Charcot-Marie-Tooth disease (CMT)[74,75] due to the presence of sensory-motor axonal neuropathy, lack of cardiomyopathy, and a myopathic phenotype that was mild compared to other patients carrying the P209L mutation. Cardiomyopathy preceding skeletal muscle symptoms has also been observed[72]. The cause for these deviations from the typical BAG3 MFM phenotype is not known.

While the P209L mutation is the predominant BAG3 MFM causing mutation, rarely other mutations leading to MFM or neuropathy occur. Interestingly, these often occur at the same site. A Pro209Gln mutation has been identified, with age of onset at 34 and no respiratory or cardiac involvement[76(p3)]. Pro209Ser has been reported to cause a late-onset CMT disease[77]. Additionally, a Pro470Ser mutation has been reported in two unrelated individuals with no family history of myopathy, with onset at 35 and 28 years of age[78]. Most other mutations in BAG3 do not result in myofibrillar myopathy or CMT, but rather cardiomyopathy.

1.2.4 Pathophysiology of BAG3 myofibrillar myopathy

Early theories about the mechanism of disease involved a direct effect in binding at the affected IPV site[79]. It was thought that this would affect HSPB8 binding, however it has been shown that there is only a minor loss of affinity at the site, and a complete loss of HSPB8 does not induce the characteristic aggregates of BAG3 MFM[78]. Work done in a zebrafish model showed that the mutant is indeed functional to a degree, rescuing knock-out fibers. It was also shown that only expression of the mutant, not reduction of autophagy, results in aggregation[80]. From this work it was theorized that the mutation must be a toxic gain of function mutation leading to a loss of function, rather than just a loss of function, inducing the formation of

aggregates which then prevent CASA activity[80]. More in depth molecular analysis has since provided an explanation for the aggregate formation.

The P209L mutation is predicted to cause a shift in local secondary structure from a random coil structure to a β-sheet, and indeed it was found that there is increased hydrophobicity at the region which in turn induces the formation of non-native oligomers, whereas the wildtype exists only as a monomer[78]. Additionally, its interaction with HSP70 is impaired; binding to the ATPase domain but failing to release and cycle as a NEF normally would. This stalls HSP70 thus stalling its co-chaperoning activity and failing to deliver client proteins for disposal. This stalled complex appears to attract other PQC proteins and complexes as well as the wildtype form of the protein, likely due to the presence of trapped ubiquitinated client proteins. It is proposed that this is the mechanism by which aggregates form in BAG3 MFM[78,81]. These aggregates can be classified as aggresomes due to the presence of ubiquitinated proteins, multiple PQC systems and of HDAC6 and vimentin[81], common markers for aggresomes[82]. Aggresomes are a cellular response to PQC systems failing to handle the burden of misfolded proteins, accumulating them in one place to reduce cellular toxicity[82,83]. The Pro209Ser and Pro209Gly disease causing mutations share similar pathophysiology, demonstrating stalling of the CASA complex, despite the milder MFM phenotypes in affected patients.

1.2.5 BAG3 in heart disease

BAG3 has been repeatedly implicated in dilated cardiomyopathy (DCM), with most reported *BAG3* mutations resulting in DCM rather than MFM. DCM is characterized by dilation of the left ventricle and systolic dysfunction. It is usually progressive in nature, eventually leading to heart failure. Other adverse events include ventricular arrhythmias, thromboembolisms and conduction system abnormalities. While often due to a genetic cause, some cases may be idiopathic[84]. *BAG3* mutations which cause DCM are often highly penetrant, usually with early onset and high risk of progression to end stage heart failure. Men have both earlier onset and worse prognosis. Although the risk of serious arrhythmia is low in these patients, the risk of adverse cardiac events is relatively high and the overall course of disease is aggressive[85]. A loss of BAG3 in mice results in DCM associated with reduced stability of small HSPs[86], and

contractile impairment in human heart failure is associated with a loss of BAG3 and thus BAG3 mediated PQC of the sarcomere. This failure of sarcomeric proteostasis of the heart directly affects the function of the cardiomyocytes, impacting their tension generation[87]. Many *BAG3* DCM mutations are associated with a reduction of BAG3 levels in the heart, and are often truncating in nature with large deletions[85,88,89]. Even patients with idiopathic DCM often show a decrease in overall BAG3 levels, strongly linking BAG3 levels to heart failure[88].

1.2.6 Animal models of BAG3 mutations

A number of animal models carrying BAG3 mutations have been developed prior to this date. The earliest were two knockout models in 2006[90] and 2008[91], and they focused on the early and severe phenotype of homozygous knockout animals. While they are born with normal appearance and histology, their muscle quickly degenerates and they fail to gain weight, dying between 2-3 weeks of age[90,91]. Massive degeneration of the muscle occurs by two weeks and extensive apoptosis occurs by 20 days, with little sign of attempted regeneration. Degenerative changes are most severe in antigravity muscles such as the soleus, and muscles under continual use such as the diaphragm, suggesting that use may be driving degeneration[90]. A reduction in the size of thymus and spleen, as well as significant hypoglycemia was seen[91]. Both studies suggest that these mice ultimately die due to an inability to properly latch and feed[90,91], although an exact cause of death has not been determined.

While these studies reported that the haploinsufficient littermates of these mice were normal, the studies did not follow the mice past a few weeks of age and focused on histological findings. A 2018 study showed that haploinsufficient mice do in fact develop a heart specific phenotype. By ten weeks of age, haploinsufficient animals develop a cardiac phenotype, showing an increased heart size and reduced left ventricular ejection fraction. Additionally, myocytes had a significantly decreased response to β-adrenergic stimulation, as well as dysregulated apoptosis and increased autophagy[92]. BAG3 directly interacts with β1-adrenergic receptors in ventricular myocytes, helping to regulate contraction during β-adrenergic stimulation[93], which may contribute to this phenotype.

Zebrafish Bag3 knockout models also exist. One study characterizing a CRISPR Cas9 knock-out model reported no phenotypic or histological changes to skeletal muscle or heart, even in homozygous knock-outs. They hypothesized that this was due to a compensation from Bag2 due to a 2.2 fold increase in the protein[94]. However, morpholino based knock-down resulted in myofibrillar disintegration with severe skeletal muscle and cardiac defects[80,94].

In addition to models which focus on the reduction of BAG3 levels, a number of models have attempted to mimic BAG3 MFM. The first, in 2016, was a mouse model with cardiomyocyte specific expression. These mice had the human version of the gene inserted with a cardiomyocyte specific promoter, resulting in a twofold expression over the endogenous protein. These mice developed systolic dysfunction by 8 months of age, as evidenced by decreased fractional shortening and ejection fraction. They also showed thickening of the anterior wall and activation of p38 signalling[95]. Another study has shown that overexpression of BAG3 on its own can induce a heart phenotype that includes decreased fractional shortening[96]. The overexpression of BAG3 leads to increased turnover of small heat shock proteins and increased activation of autophagy and mitophagy, suggesting that this may be toxic for cardiomyocytes[96]. It is therefore difficult to draw any conclusions about how the mutation may have contributed to the phenotype, as they did not have a wildtype transgene control.

Another mouse model of BAG3 MFM was published, this time with the endogenous protein mutated. This mouse carried a P215L variant, the same as our knock-in mice[4], on a C57BL/6 background[97]. The hearts of these mice were characterized up to 16 months of age, however neither morphological, histological nor molecular investigations showed any defect and electrocardiogram (ECG) readings were consistently normal[97]. The lack of phenotype, something also observed in our knock-in animals[4] is not unusual for mouse models of muscle disease, as many show mild or absent phenotypes compared to humans[9,98]. The increased muscle size and length in humans results in increased mechanical tension and morphological adaptations to handle force, such as thicker tendons and more fibrous septa[9]. There are also differences in the timing of inflammation post-injury, as well as the activation of satellite cells, with both peaking days faster in mice, contributing to repair faster[99]. The satellite cells themselves also exhibit differences in differentiation as well as temporal differences in the expression of myogenic

markers[100]. Additionally, there may be compensation by other genes within the mice that does not occur in humans, such as the case with utrophin in *mdx* mice which compensate for the lack of dystrophin, resulting in a milder phenotype[101]. In the case of the BAG3 MFM mice, it is possible that there is another autophagy complex compensating for failures of BAG3 P209L.

1.3. The nuclear envelope

1.3.1 Nuclear-cytoskeletal coupling: Structure and role in mechanosignaling

Under the sarcolemma of the muscle fibers along their periphery are the nuclei. They are tethered to the cytoskeleton through the Linker of Nucleoskeleton and Cytoskeleton (LINC) complex, which connects to the nuclear envelope (NE) (Figure 1.4). The NE is a double membraned structure, with a gap of 50nm called the perinuclear space. The two membranes of the NE, while both phospholipid bilayers, are distinctly different in composition. The outer nuclear membrane (ONM) is continuous with the membrane of the endoplasmic reticulum. It contains two giant actin binding proteins, Nesprin 1 and 2[102]. Their localization on the ONM is dependent on Sad1 and UNC84 domain-containing protein(SUN) 1 and SUN2, proteins of the inner nuclear membrane (INM) that bind to Nesprin in the perinuclear space, effectively linking the two membranes and maintaining the size of the PNS. SUN1/2 also interact with the nuclear lamins on the other face of the INM[103]. These proteins make up the core components of the LINC complex that tether the nucleus to the cytoskeleton.

The INM is unique in its makeup, with many of the proteins which are uniquely enriched in the NE being found here[104]. On the nuclear face of the inner membrane lies the nuclear lamina, composed of type A (A and C) and type B (B1 and B2) lamins which are intermediate filaments that help to maintain its structure[102]. Lamin A and C are both encoded by *LMNA* and the B-types are encoded by *LMNB1* and *LMNB2*. They form a lattice which strengthens the nucleus and protects it from mechanical strain by increasing rigidity[102,105]. Several proteins with LEM (LAP2, Emerin and MAN1) domains are also present; these connect the lamins to BAF, a DNA bridging protein involved in chromosome organization, which binds to the heterochromatin at lamina associated domains (LAD)[106]. This tethering of envelope and lamina to the DNA points to its role in chromatin organization, gene expression and ultimately cell fate decisions. This

connection of cytoskeleton to nuclear envelope to the chromatin is what turns mechanical signals into cellular response.

Mechanotransduction, the process by which mechanical forces are turned into molecular signals, plays an important role in cell function and cell fate decisions[107]. All cells are mechanosensitive; without this property they would not respond to physical forces. This includes cells involved in dynamic response, such as those implicated in hearing, balance and touch sensation; and those relying on it to control tissue maintenance such as muscle and bone[105]. This process begins at the cell adhesion sites, where the cell connects to the extracellular matrix (ECM) through integrins, and the actomyosin filaments. From there, the signal is carried from the aforementioned LINC complex to the nuclear envelope which is tethered to the chromatin through BAF. Defects to mechanosensitivity are implicated in a number of diseases, including many muscular dystrophies, cardiomyopathies, deafness, and cancer[105]. Mechanically stressed tissue relies on this process to react quickly to changes in stress[105], thus the large number of muscle oriented diseases associated with disruption in this process.

The nuclear envelope uses mechanical signals to modulate transcriptional activity through its connection to the chromatin. Changes or defects to this system in adult tissue can impact homeostasis, resulting in pathological developments including dystrophies, cardiomyopathies, osteoporosis, premature aging and the progression of cancer[105]. YAP and TAZ are two important proteins in this process. YAP/TAZ are canonically known as effectors of the Hippo pathway, however the regulation by mechanical stress appears to be independent of this[108,109]. Mutations in *LMNA* change YAP signaling, and result in cells that do not correctly respond to changes to the extracellular matrix or mechanical stress, showing a link between NE and the YAP pathway[110].

YAP and TAZ are both transcriptional coactivators and orthologs of the same *Drosophila* gene Yorkie, and as such there are many redundancies between the two proteins. As they do not bind DNA directly, their activity is dependent on the transcriptional enhancer factor TEF (TEAD) family of transcription factors. YAP/TAZ have an N-terminal domain that binds TEAD transcription factors. With increased tension, YAP/TAZ localizes to the nucleus, although this

process is poorly understood. It appears to rely at least in part on F-actin levels and polymerization, which increases during tension. ARID1A under normal conditions binds to YAP/TAZ and blocks its interaction with TEAD, but instead binds to F-actin when it undergoes tension induced changes, allowing YAP/TAZ to function[111]. The mechanosensitive properties of YAP/TAZ are implicated in development, with ECM stiffness influencing cell fate decisions in stem cells, as well as homeostasis and regeneration in mature tissue[112]. YAP/TAZ is an important regulator of both mass and function in skeletal muscle, both at the stage of myoblast differentiation and proliferation and the growth of the mature fiber, as it influences the expression of myogenic factors[113]. YAP specifically maintains a population of PAX7+ and MYOD+ satellite cells when constitutively expressed, and its knockdown reduces this population. This population is proliferative but not differentiative, and as such a balance in YAP levels is necessary for maintaining normal activity of the satellite cells so that they may ultimately contribute to repair[114].

1.3.2 The nuclear envelope in disease

Mutations to nuclear envelope associated proteins have been associated with a number of diseases. Mutations in *LMNA* result in disorders associated with skeletal muscle, peripheral neuropathy, lipodystrophies and accelerated aging disorders such as progeria[115]. These disorders are broadly categorized as "laminopathies". Laminopathies are often referred to as diseases of the skeletal or cardiac muscle despite the mutations affecting all tissues of the body. Mutations in emerin (*EMD)*, like those in *LMNA,* most commonly cause muscle disease; specifically the X-linked form of Emery-Dreifuss muscular dystrophy (EDMD), a connection first made in 1994[116]. This may be due to the increased mechanical stress in muscle tissue, making nuclear rigidity and mechanotransduction of high importance in both protecting the nucleus and transmitting mechanical signals that stimulate growth and repair[113,117]. While mice with emerin null mutations have very little phenotype, showing only an age related atrioventricular conduction defect, cells with the same mutation display altered nuclear shape and dynamics, as well as a sensitivity to mechanical strain that results in increased apoptosis[118].

Cells that lack lamin A/C have increased deformability as well as fragility. This leads to a loss of stability and stiffness and an increase in nuclear ruptures, which means mechanical tension can lead to nuclear deformity or rupture and cell death[119]. Mice that carry these null mutations have a severe cardiac and skeletal myopathy, dying within weeks after birth[120,121]. Loss of lamin A/C has implications for mechanosensing, cytoplasmic and cytoskeletal mechanics, and cell polarization due to disruptions in the connection between nucleus and cytoskeleton[106]. This is also true of Lamin A/C mutations that result in myopathy, which show increased nuclear deformability, making them vulnerable to mechanical tension[110,122,123]. These myopathic mutations can result in loss of the nuclei but also defective mechanotransduction and thus aberrant transcription[110,117], which negatively affects maintenance and repair of the tissue. While these mutations do not primarily cause a lack of lamin, they are likely causing defects to the higher order assembly of lamin into filaments, primarily through disruption of head to tail assembly[119]. Mutations that have no effect on nuclear stiffness can also have similar end results through disruption of coupling of the nucleus to the cytoskeleton. If mutations to lamin or other NE or LINC components disrupt this, force transmission is impaired regardless of NE stiffness[119]. The curious class of age-accelerating disorders, which includes Hutchinson-Gilford syndrome, have a slightly different pathophysiology; instead of affecting assembly or resulting in a loss of tension, these mutations in *LMNA* result in an increased nuclear stiffness. This results in increased sensitivity to mechanical tension[124,125], possibly due to the lamina's inability to dissipate force and rearrange under stress.

1.3.3 BAG3 in the nucleus

While limited work has been done on the role of BAG3 in the nucleus, BAG3's presence in the nucleus and interaction with components of the NE have been shown. It is typically considered a cytoplasmic protein, but has been shown in the past to be capable of actively translocating to the nucleus during the shuttling of HSF1[126]. Additionally, it has been found at low levels in the nuclei of neuronal cells[127]. Recent work has shown that it also plays a role in maintenance of the nuclear envelope through lamin B1 turnover. During proteotoxic stress, such as that induced by MG132 treatment,a proteosomal inhibitor, lamin B1 accumulated perinuclearly where it colocalized with BAG3 and BAG3 levels increased in the nuclear fraction.

Additionally, both MG132 treatment and BAG3 knockdown resulted in the formation of lamin B positive micronuclei. Overexpression of BAG3 ameliorated the pathological nuclear findings in the cells undergoing proteotoxic stress, and immunoprecipitation of BAG3 showed it was bound to lamin B[128]. This evidence points to a PQC role for BAG3 in the nucleus, specifically in maintenance of the nuclear envelope during stress.

While a role for BAG3 at the nucleus has been established, a link between this function and disease has not been explored. In the following chapters, I will provide data on a new murine model of BAG3 MFM which repaticulates the human form of the disease, and show how the BAG3 MFM mutation may impact the nuclear envelope and its mechanosensitive functioning.

Figures

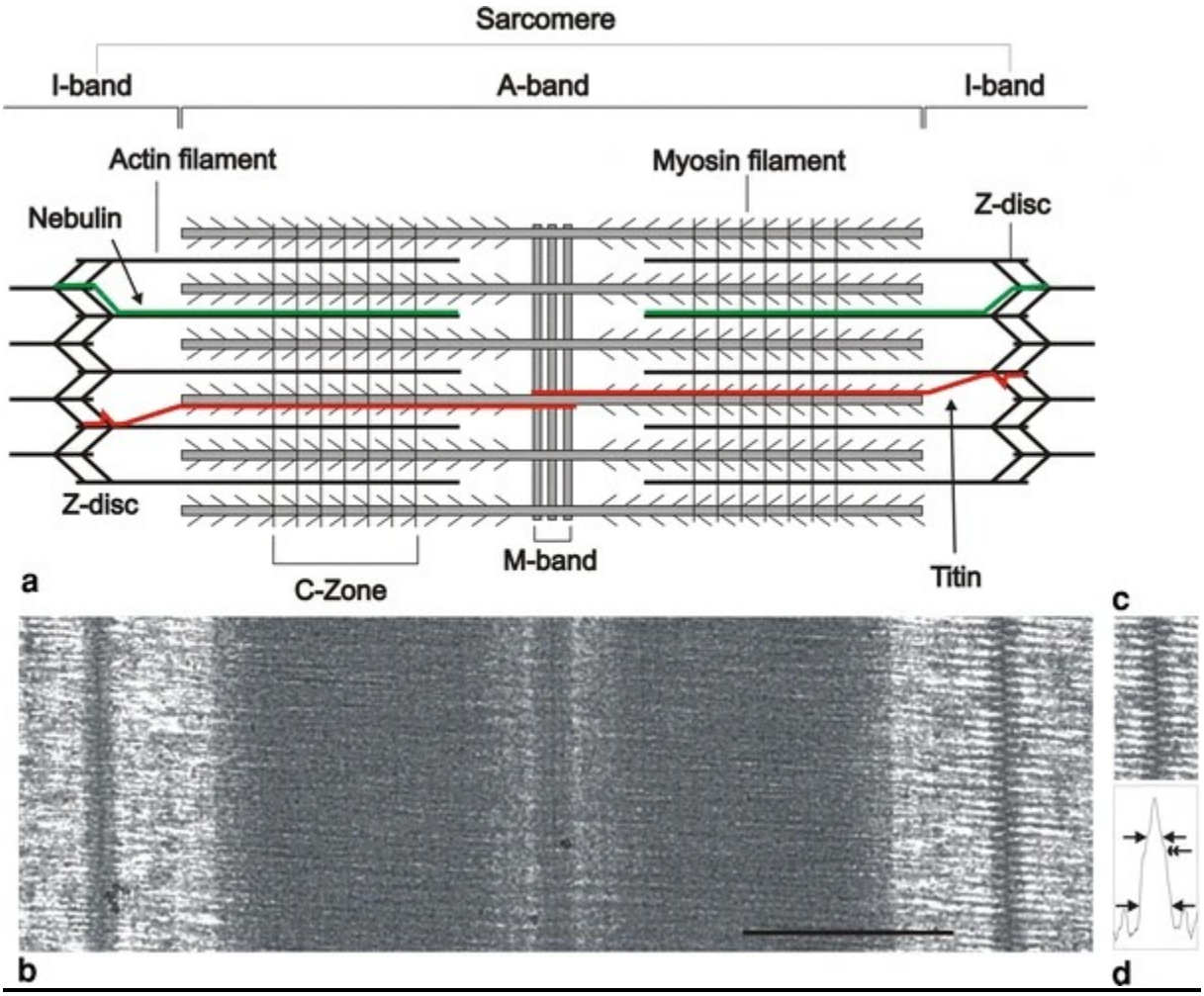

Figure 1.1 The sarcomere. A) A diagram showing the structure of the sarcomere. The A-band is composed of myosin filaments with the M-band assembly at the center. At the Z-disk Thin actin filaments are tethered at their capped end and interact with the thick myosin filaments in the A-band. Two giant proteins (Titin (in red) and Nebulin (in green)) contribute to the structure of the Z-disc. B) Electron micrograph of a longitudinal section of a muscle sarcomere. For the right-hand Z-disc, also reproduced partly in c, favourable alignment of the lattice gives the characteristic zigzag. (Scale bar = 500 nm) C) the Z-disk and its profile plot (D). Reproduced from doi: 10.1007/s10974-009-9189-6

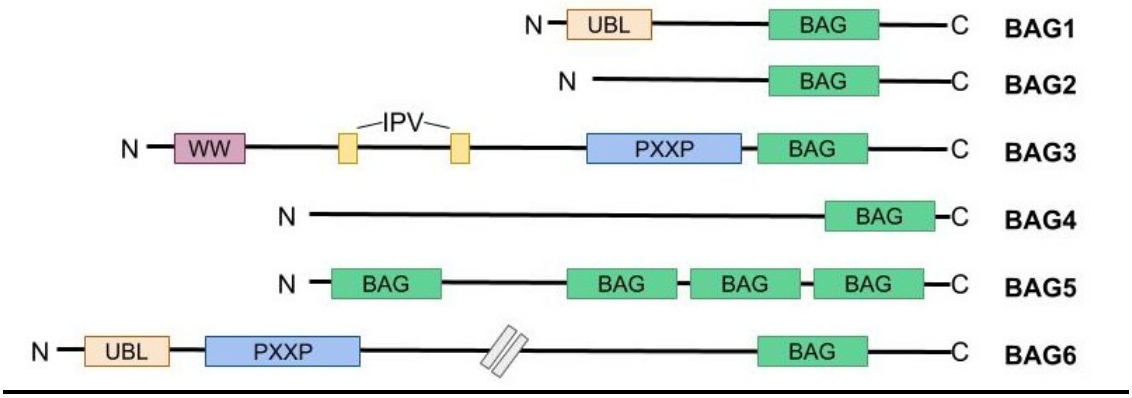

Figure 1.2 The BAG family of proteins. The BAG family of proteins consists of six proteins, which all contain the BAG domain which allows them to act as nucleotide exchange factors to Hsp70. Abbreviations: BAG: Bcl-2-associated athanogene domain; UBL: ubiquitin-like domain; PxxP: proline-rich region; WW: tryptophan–tryptophan domain, IPV: Ile-Pro-Val motif.

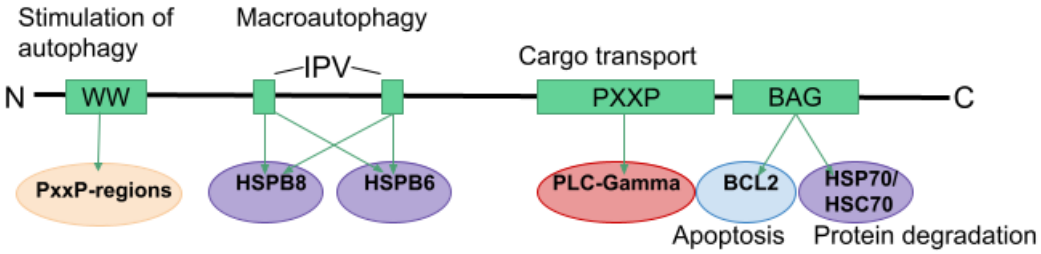

Figure 1.3 Domains and functions of BAG3. The BAG3 protein has three domains: a BCL2-associated anthanogene (BAG) domain at the C-terminus, a tryptophan-tryptophan (WW)

domain at the N terminus, and a proline rich repeat region (PxxP). It also has two adjacent Ile-Pro-Val (IPV) motifs which bind to small heat shock proteins.

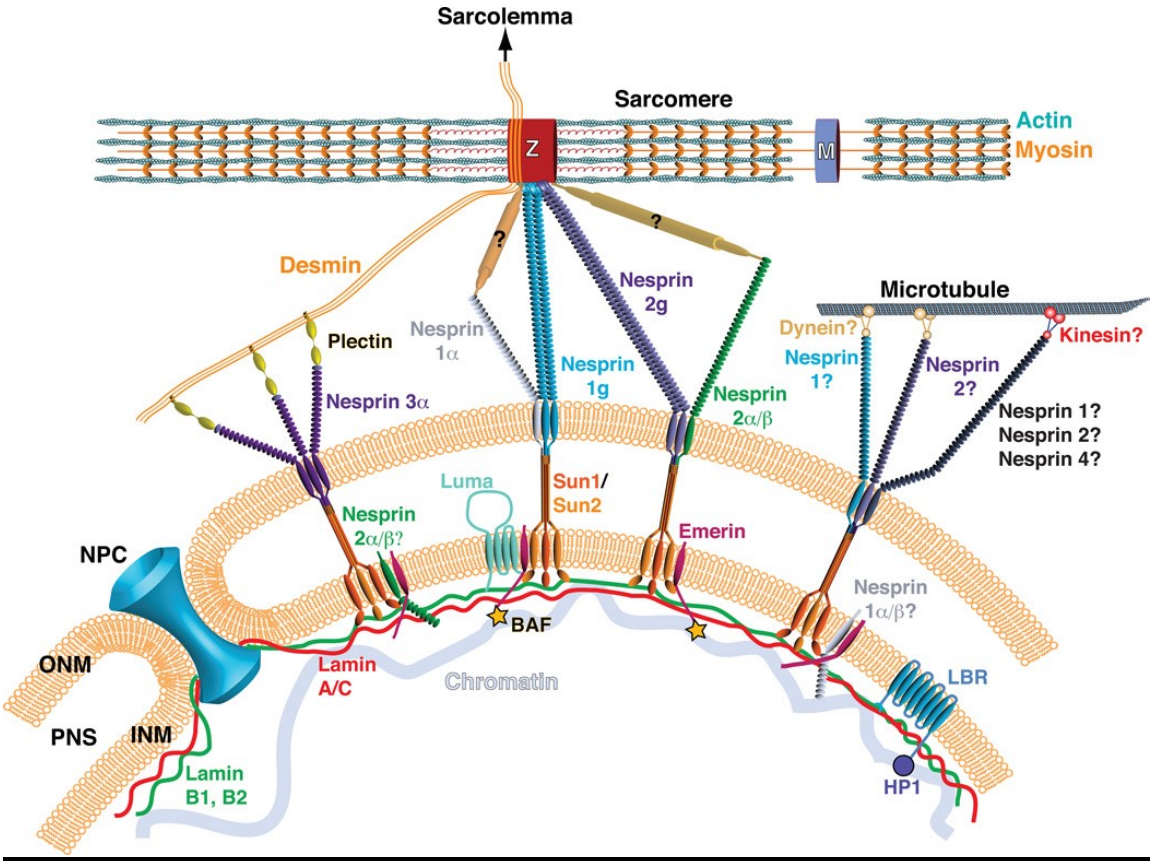

Figure 1.4. Nuclear envelope and LINC complex in muscle cells. The nuclear envelope is a double membraned structure. The LINC complex connects the nuclear envelope to the cytoskeleton. Nesprins connect the cytoskeleton, linking directly to the Z-disk in muscle, back to Sun1/2 at the outer nuclear membrane (ONM). Sun1/2 spans the perinuclear space (PNS), tethering ONM to the inner nuclear membrane (INM). Emerin connects the INM to the chromatin through BAF. A and B type lamins span the interior surface of the INM, providing structural support to the nucleus. Reproduced from doi:10.1161/CIRCRESAHA.114.301236

RATIONAL, HYPOTHESIS AND OBJECTIVES

BAG3 myofibrillar myopathy is a severe disease and currently without effective treatment. Those affected typically die in the second decade of life. While there now exists a body of work studying the molecular nature of the mutation and describing case studies, very little work has been done towards finding a treatment and many holes exist in our understanding of the pathophysiology of this disease. Despite attempts to model this disease, there has been very little success in animal models with the exception of one Zebrafish model[80] and our own knock-in model was without a phenotype. Given that the P209L variant appears to be a toxic gain of function that ultimately results in BAG3 insufficiency due to aggregation, and that the mutant protein is semi functional, ***we hypothesised that loss of BAG3 protein is required to drive the MFM phenotype.*** Therefore, the **first objective** of this thesis was to **create and characterize a model of BAG3 MFM through the creation of a knock-in/knock-out model to overcome the weak phenotype seen in murine knock-in models.**

BAG3, unlike most other MFM causing proteins, is not a structural protein but rather one of autophagy. BAG3 MFM is also markedly more severe than many other MFMs and with earlier onset. These differences led us to consider that this disease was not one of increased damage, but rather failure to repair from normal damage leading to instability. ***We hypothesised that, given BAG3's role in PQC and the myopathic phenotype of the P209L mutation, pathophysiology is driven by muscle injury and mechanical tension in the context of faulty BAG3 dependent repair.*** **The second objective was to determine the effect of mechanical tension on the progression of the phenotype.**

While canonical BAG3 MFM has been thought to be a disease of the Z-disk due to the sarcomeric damage seen, recent evidence has shown that BAG3 plays a role in maintenance of the nuclear envelope, a structure influenced by mechanical strain. Patients with BAG3 MFM also show increased nuclear apoptosis and nuclear abnormalities. ***We hypothesised that the PQC issues have implications for the integrity of the nucleus, which, in conjunction with damage to cytoskeletal components, leads to defects in mechanotransduction***. The **third objective** was to **characterize the nuclear defect in BAG3 MFM and the related tension-based defects.**

PREFACE TO CHAPTER 2

This project began as a collaborative effort between four laboratories: That of Dr. Bernard Brais, Dr. Robert J Bryson-Richardson, Dr. Josée N Lavoie and Dr. Jason Young. The goal of this project was to further the understanding of BAG3 P209L myofibrillar myopathy and to work towards a potential treatment. The Brais lab has had much experience with the development and characterization of mouse models, and as such the development of the mouse model was undertaken here. Chapter 2 describes the generation and characterization of this model.

CHAPTER 2: BAG3$^{P215L/KO}$ Mice as a Model of BAG3^{P209L} Myofibrillar Myopathy

Rebecca Robertson [1], Talita C Conte [1], Marie-Josée Dicaire [2], Vladimir V Rymar [3], Abbas F Sadikot [3], Robert J Bryson-Richardson [4], Josée N Lavoie [5], Erin O'Ferrall [6], Jason C Young [7], Bernard Brais [8]

Affiliations:

1. Neurogenetics of Motion Laboratory, Department of Neurology and Neurosurgery, Montreal Neurological Institute, McGill University, Montreal, Quebec, Canada; Department of Human Genetics, McGill University, Montreal, Quebec, Canada.
2. Neurogenetics of Motion Laboratory, Department of Neurology and Neurosurgery, Montreal Neurological Institute, McGill University, Montreal, Quebec, Canada.
3. Cone Laboratory, Department of Neurology and Neurosurgery, Montreal Neurological Institute, McGill University, Montreal, Quebec, Canada.
4. School of Biological Sciences, Monash University, Melbourne, Australia.
5. Centre de Recherche sur le Cancer, l'Université Laval, Québec, Quebec, Canada; Oncology Axis, Centre de Recherche du Centre Hospitalier Universitaire (CHU), Québec-Université Laval, Québec, Quebec, Canada; Département de Biologie Moléculaire, Biochimie Médicale et Pathologie, l'Université Laval, Québec, Quebec, Canada.
6. Rare Neurological Diseases Group, Montreal Neurological Institute, McGill University, Montreal, Quebec, Canada.
7. Department of Biochemistry, McGill University, Montreal, Quebec, Canada.
8. Neurogenetics of Motion Laboratory, Department of Neurology and Neurosurgery, Montreal Neurological Institute, McGill University, Montreal, Quebec, Canada.

Published in

Am J Pathol. 2020 Mar;190(3):554-562. doi: 10.1016/j.ajpath.2019.11.005. Epub 2020 Jan 14.

Reproduced with permission.

Abstract

BCL-2-associated athanogene 3 (BAG3) is a co-chaperone to heat shock proteins important in degrading misfolded proteins through chaperone-assisted selective autophagy. The recurrent dominant BAG3-P209L mutation results in a severe childhood-onset myofibrillar myopathy (MFM) associated with progressive muscle weakness, cardiomyopathy, and respiratory failure. Because a homozygous knock-in (KI) strain for the mP215L mutation homologous to the human P209L mutation did not have a gross phenotype, compound heterozygote knockout (KO) and KI mP215L mice were generated to establish whether further reduction in BAG3 expression would lead to a phenotype. The KI/KO mice have a significant decrease in voluntary movement compared with wild-type and KI/KI mice in the open field starting at 7 months. The KI/KI and KI/KO mice both have significantly smaller muscle fiber cross-sectional area. However, only the KI/KO mice have clear skeletal muscle histologic changes in MFM. As in patient muscle, there are increased levels of BAG3-interacting proteins, such as p62, heat shock protein B8, and αB-crystallin. The KI/KO mP215L strain is the first murine model of BAG3 myopathy that resembles the human skeletal muscle pathologic features. The results support the hypothesis that the pathologic development of MFM requires a significant decrease in BAG3 protein level and not only a gain of function caused by the dominant missense mutation.

Introduction

Muscular dystrophy is a heterogeneous group of diseases characterized by progressive muscle weakness. Myofibrillar myopathies (MFMs) are a subset of muscular dystrophy that share pathologic features that may also present with cardiac muscle involvement and neuropathies. Symptoms and age at onset vary among the different MFMs, although most forms affect adults(Selcen, Ohno, and Engel 2004). Histologically and structurally, they all share similar features: Z-disk streaming and disruption, aggregation of Z-disk–associated proteins, abnormal fiber size(D. Selcen, Ohno, and Engel 2004), and mitochondrial abnormalities.(Jackson et al. 2015; Vincent et al. 2016) In MFM, the broken-down filaments of the myofibers aggregate with membranous organelles and ectopic proteins (Selcen, Ohno, and Engel 2004; Olivé et al. 2011). Mutations in the genes *DES, MYOT, FLNC, LDB3, FHL1, CRYAB,* and *BAG3* cause MFMs and their proteins to localize to the Z-disk (Ferrer and Olivé 2008).

BCL-2–associated athanogene 3 (BAG3) is one of six BAG proteins in humans. The BAG proteins share the BAG domain that binds to the ATPase domain of heat shock protein (HSP) 70 and as such are considered to be co-chaperones to HSPs and prosurvival in nature (Rauch and Gestwicki 2014). BAG3 in particular is important to muscle and its maintenance because of its role in chaperone-assisted selective autophagy (CASA), an ubiquitin-dependent system operating at the Z-disk that leads to the autophagic degradation of damaged cytoskeletal proteins (Arndt et al. 2010). It fulfills this role through the aforementioned association with HSP70, as well as HSPB8 and HSPB6 at BAG3's Ile-Pro-Val motifs. BAG3 also plays a role in the regulation of the stability of actin in conjunction with heat shock cognate protein 70 through interaction with the actin capping protein CapZ (a barbed-end actin capping protein from the Z line of skeletal muscle) (Hishiya, Kitazawa, and Takayama 2010). Furthermore, it also plays an antiapoptotic role because of its association with B-cell lymphoma 2, an antiapoptotic protein localized to the mitochondria (Hockenbery et al. 1990

The recurrent proline to leucine mutation in one of the Ile-Pro-Val motifs, P209L, results in a severe, childhood, autosomal-dominant MFM (Selcen et al. 2009). Morphologically similar to other MFMs, these motifs display Z-disk streaming, aggregates of Z-disk proteins, abnormal fiber size, ragged red fibers (RRFs), abnormal mitochondrial morphologic features, and

regenerating and splitting fibers (Selcen et al. 2009). Clinically, affected patients begin experiencing symptoms in childhood, such as toe walking, that progress into more generalized muscle weakness, with spinal rigidity and a peripheral neuropathy in many patients. Respiratory insufficiency and cardiomyopathy usually develop by the second decade of life, often necessitating heart transplant and eventually leading to death (Selcen et al. 2009; Odgerel et al. 2010). Because of the severity of the disease, the P209L mutation is usually *de novo*, with only one published case of it being inherited from a mosaic father (Odgerel et al. 2010). This finding makes this disease extremely rare, with only 19 published cases (Selcen et al. 2009; Odgerel et al. 2010; Jaffer et al. 2012; Noury et al. 2018; Kim et al. 2018; Hockenbery et al. 1990; Lee et al. 2012; Konersman et al. 2015; Kostera-Pruszczyk et al. 2015; Schänzer et al. 2018).

One of the initial hypotheses concerning the mechanism of disease is that mutated BAG3 protein impairs autophagy (Arimura et al. 2011), resulting in aggregates of misfolded proteins. This theory, however, has been disputed. Experiments in a zebrafish model found that suppression of autophagy is not enough to induce the formation of aggregates. Instead, only the expression of mutated BAG3 protein produces the aggregates, which also sequesters the wild-type (WT) protein, other Z-disk proteins, and autophagy-associated proteins. These results suggest that there is a toxic gain of function that leads to BAG3 insufficiency because the protein is now bound within aggregates and therefore unavailable to function (Ruparelia et al. 2014), Indeed, the mutated protein stalled the HSP70 autophagy machinery because its activity as a nucleotide exchange factor is impaired. This finding leads to the formation of insoluble aggregates, which are composed of both the HSP70 system and other autophagic systems that accept the same clients (Meister-Broekema et al. 2018), preventing degradation and leading to their accumulation (Meister-Broekema et al. 2018; Guilbert et al. 2018).

Mice were generated with three different genotypes on C57Bl/6 background, carrying one [knock-in (KI)/ WT] or two copies of the P215L mutation analogous to the human P209L mutation (KI/KI), as well as mice with one copy of P215L and a knockout (KO) allele (KI/KO). A full characterization of heterozygote (KO/WT) mice was not completed because two other groups, both also using C57Bl/6 mice, independently reported that they did not develop a phenotype (Youn et al. 2008; Homma et al. 2006), Extensive phenotypic, histologic, and

molecular characterization of the KI/WT, KI/KI, and KI/KO mice was performed. KI/KO crosses were of the greatest interest because the KI/KI and KI/WT had little or no phenotype (Fang et al. 2019), Further supporting the relevance of this cross are the results in zebrafish, which indicate that a reduction of protein quantity in addition to the P215L mutation may result in a muscle phenotype that is more severe than KI alone (Ruparelia et al. 2014; 2020) because the P209L mutation results in a lack of available and active BAG3 (Meister-Broekema et al. 2018). In addition, a reduction in BAG3 levels has been noted in patients (Kostera-Pruszczyk et al. 2015; D'Avila et al. 2016). We hypothesized that reducing the protein quantity through a KI/KO cross would overcome the weak phenotype seen in KI/WT and KI/KI crosses in a manner that still reflected this dominant MFM on a molecular level. Indeed, KI/KO mice develop myopathic changes that are not present in the other strains. The BAG3-P215L KI/KO mice are the first model of P209L-BAG3 MFM with full-body expression of the mutant protein.

Materials and Methods

Generation of BAG3 P215L and KO Mice

Mice were generated by the Toronto Center for Phenogenomics using CRISPR-Cas9 on a C57Bl/6 background. The KI mice contain the change c.644_645CC>TG, which results in the P215L mutation. The KO mice have a 7-bp deletion, c.639_645delCATCCCC, causing a premature stop codon. The sequences were confirmed via Sanger sequencing using the primers 5′-GGTGTCTGGTGGCTATTTGG-3′ (forward) and 5′-ATCTGCAGAACCTCTCAGCC-3′ (reverse) (Supplemental Figure S2.1). The absence of protein was confirmed in the KO homozygote mice via Western blot using a polyclonal BAG3 antibody (LP11) (Guilbert et al. 2018).

Western Blots

Mouse gastrocnemius muscles were dissected and snap frozen in liquid nitrogen. Muscles were finely ground using a mortar and pestle, suspended in radioimmunoprecipitation assay buffer, and then sonicated. The resulting extract was spun at 10,000 × g for 5 minutes at 4°C and the supernatant collected. Protein quantification was performed using the DC colorimetric assay (Bio-Rad, Hercules, CA). Aliquots of 5, 20, and 40 μg were separated onto a NuPAGE 4% to 12% Bis-Tris gel (Life Technologies, Carlsbad, CA) and transferred onto a nitrocellulose membrane (Bio-Rad). The resulting blots were incubated with the following primary antibodies: BAG3 (LP11),(Guilbert et al. 2018) p62 (catalog number 610832; BD Biosciences, San Jose, CA), HSPB8 (catalog number 3C12-H11; StressMarq, Victoria, BC), αB-crystallin (catalog number ADI-SPA-222; Enzo); HSPB1 (catalog number 5D12-A12; StressMarq), glyceraldehyde-3-phosphate dehydrogenase (catalog number GT239; GeneTex, Irvine, CA), HSP70 (clone C92F3A-5; Enzo Life Sciences, Farmingdale, NY), sarcomeric α-actinin (clone EA-53; Abcam, Cambridge, MA). This was followed by incubating membranes with a horseradish peroxidase secondary antibody and visualized using chemiluminscence (Intas Science Imaging, Göttingen, Germany). Bands were quantified using ImageJ software version 1.52 (NIH, Bethesda, MD; http://imagej.nih.gov/ij), and levels were normalized to glyceraldehyde-3-phosphate dehydrogenase and sarcomeric α-actinin.

Histologic Analysis

Cryostat sections of 10 μm were fixed with 4% paraformaldehyde for 10 minutes at room temperature and stained using the following stains: hematoxylin and eosin (H&E), Gomori trichrome, NADH, and immunohistochemical staining. For immunostaining, antigens were initially demasked in serial sections using target retrieval solution (catalog number S1699; Dako Agilent, Santa Clara, CA) at 95°C for 45 minutes. Peroxidases were inactivated using 0.6% hydrogen peroxide for 15 minutes, followed by avidin and biotin blocking (catalog number SP-2001; Vector Laboratories, Burlingame CA) for 15 minutes. Blocking and permeabilization were performed with a -buffered saline solution that contained 5% goat serum and 0.25% Triton X-100 for 1.5 hours. Primary antibodies were incubated overnight at 4°C. Biotinylated secondary antibodies (Vector Laboratories) were incubated for 1 hour. Complex A + B (catalog number PK-6100; Vector Laboratories) was incubated for 1 hour, followed by diaminobenzidine solution (catalog number SK-4100; Vector Laboratories) for 5 minutes. Nuclei were stained briefly using hematoxylin and then mounted with xylene mounting medium (catalog number 245-691; Protocol, Waltham MA). Primary antibodies consisted of the following: BAG3 (LP11) (Guilbert et al. 2018), desmin (catalog number M0760; Dako), and filamin C (catalog number NBP1-89300; Novus Biologicals, Centennial CO).

Counting of the RRFs, defined as fibers that have an irregularly thick or ragged contour, was performed using the Gomori trichrome–stained whole gastrocnemius sections. This counting was performed by an individual (R.R.) blind to the genotype associated with each section. The number of RRFs was quantified as a percentage of total fiber number.

Immunofluorescence

Cryostat cross-sections of 10 μm were fixed with 4% paraformaldehyde for 10 minutes at room temperature. They were blocked and permeabilized for 1 hour in a -buffered saline solution that contained 5% normal donkey serum, 0.25% Triton X-100, and 0.1 mol/L glycine. Cells were incubated overnight at 4°C with anti-CD45 primary antibody. The secondary antibody, mixed with 488 Alexa Fluor wheat germ agglutinin, was applied for 1 hour at room temperature, followed by Hoescht staining for 5 minutes. Slides were mounted with ProLongTM Gold antifade reagent (Thermo Fisher, Waltham, MA). Fiber-type staining immunolabelling was performed as previously described (Gouspillou et al. 2014), with the following primary antibody

cocktail: anti–major histocompatibility complex (MHC) type I (BA-F8, 1:25), mouse IgG1 monoclonal anti-MHC type IIa (SC- 71, 1:25), mouse IgM monoclonal anti–type 2× MHC (6H1, 1:25), and a rabbit IgG polyclonal anti-laminin (catalog number L9393; Sigma-Aldrich, St. Louis, MO). The MHC monoclonal antibodies were obtained from the Developmental Studies Hybridoma Bank, created by the Eunice Kennedy Shriver National Institute of Child Health and Human Development of the NIH and maintained at Department of Biology, The University of Iowa (Iowa City, IA; developed by Stefano Schiaffino).

Electron Microscopy

Male mice at 7 months of age, three per genotype used, were perfused with phosphate-buffered saline followed by 4% glutaraldehyde in 0.2 mol/L cacodylate buffer. The gastrocnemius muscle was dissected out, cut into 1 × 2-mm pieces, and left in the same glutaraldehyde mixture for 24 hours. Sections were postfixed in osmium tetroxide for 1 hour and embedded is epoxy resin. Sections were stained using uranyl acetate and lead citrate and then imaged using a FEI Tecnai G2 Spirit Twin 120 kV Cryo-TEM at the Facility of Electron Microscopy Research at McGill University.

Behavioral Phenotyping

Motor behavior in mice was tested using rotarod, force transducers for grip strength, inverted grid, and open field. Fifteen male mice per genotype were used. Balance and coordination were tested using the rotarod. Mice were subjected to 3 days of training, gradually increasing the maximum Rpm through the training sessions and returning mice to the rotarod after falling unless exhaustion had been reached. The actual testing was composed of five sessions, with the speed increasing from 5 to 40 Rpm during that time. The time at which the mice fell from the rod was recorded, and adequate rest was given between rounds. For inverted grid, mice were placed on the grid, which was then inverted over a padded surface for a maximum of 5 minutes. The time at which the mice fell was recorded. Grip strength testing was performed using forelimbs only, with the peak force at the point of failure recorded for five trials. All values for rotarod, grip strength, and inverted grid were normalized to body weight, and these tests were repeated at 3, 6, and 9 months of age. For testing of spontaneous locomotion in open field, mice were allowed to acclimate to the testing room 30 minutes before testing while still in their home cages.

They were then placed in a 50 × 50-cm field in a quiet, low-light room for 10 minutes and recorded using a ceiling-mounted camera and HVS Image Software version 2016.6 (HVS Image Software Ltd., Buckingham, UK). Testing was repeated at 5, 7, and 10 months of age. Individuals performing the testing were blind to genotype throughout the trials (R.R., M.-J.D.).

Statistical Analysis

Analyses that consisted of multiple genotypes were performed using two-way analysis of variance. If $P < 0.05$ was reached, post hoc testing (Dunnett multiple comparisons test) was performed to identify which group was different from WT.

Results

Reduction of Voluntary Movement in KI/KO Mice

KI/WT, KI/KI, and KI/KO mice were clinically assessed using rotarod, inverted grid, grip strength, and open field tests to assess their strength, endurance, and movement. Inverted grid, rotarod, and weighing were performed at 3, 6, and 9 months, and grip strength and open field were performed at 4, 7, and 10 months. No significant difference among KI/WT, KI/KI, and WT mice was seen for any measure (Figure 2.1A). The KI/KO mice did not have any coordination, endurance, or strength deficit as measured by rotarod, inverted grid, or grip strength tests up to 9 months of age, and there were no differences in weight. However, the mice did have a significant reduction in voluntary movement (Figure 2.1B). Open field measurements revealed a significant decrease in movement, which became apparent at 7 months of age, moving a mean of 15.1 m compared with the 20.5 m by WT (total path and total entries $P < 0.05$) during a period of 10 minutes. This measurement decreased more at 10 months, moving 11.9 m compared with 17.85 m and moving 43% less of the time (total path $P < 0.01$, total entries and time moving $P < 0.001$). There was a decrease in overall movement and lower use of the field.

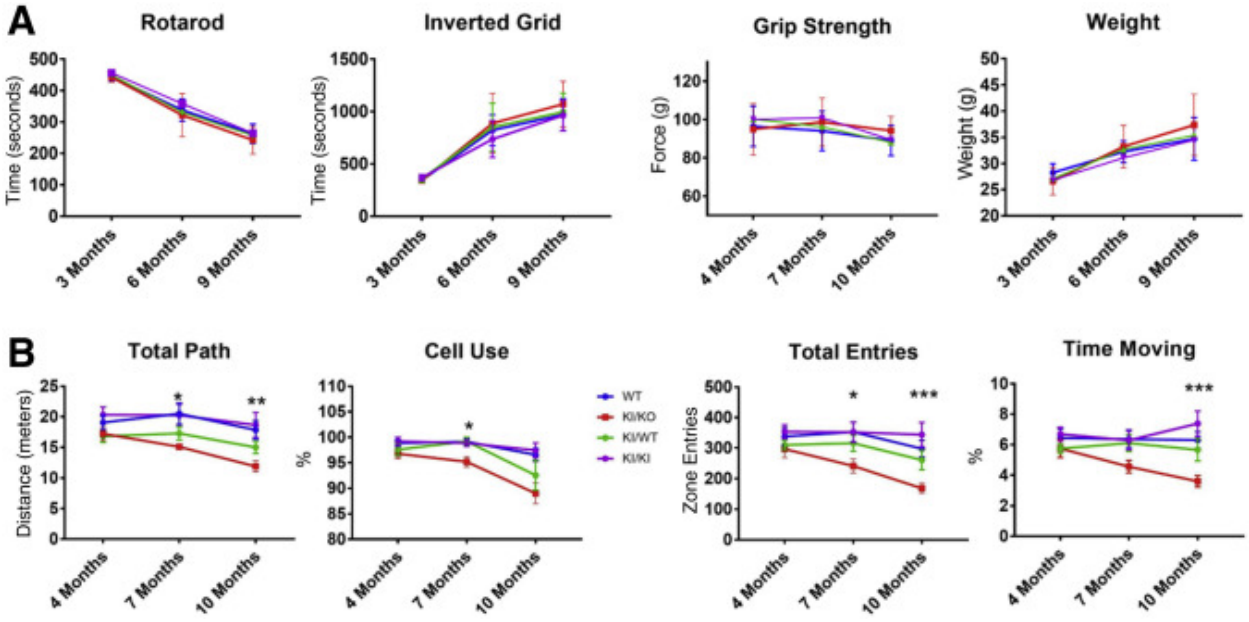

Figure 2.1. Clinical phenotyping of wild-type (WT), knock-in (KI)/knockout (KO), KI/WT, and KI/KI strains. A: Measures of weight, strength, and endurance, which included rotarod, grip strength, and inverted grid, show no difference. B: Open field measures show significant

difference between WT and KI/KO mice starting at 7 months of age. Data are expressed as means ± SEM. n = 14 WT; n = 15 KI/KO; n = 15 KI/WT; n = 14 KI/KI strains. *P < 0.05, **P < 0.01, and ***P < 0.001 versus WT (analysis of variance).

Myopathic Changes to the Muscle in P215L KI/KO Mice

The muscle of KI/KO mice has clear myopathic changes that are absent in KI/KI and KI/WT mice. A histologic examination of gastronomical muscle collected from 4-month–old male mice using H&E, Gomori trichrome, NADH, and immunohistochemical stains was conducted (Figure 2.2, A–C). H&E staining of cross-sections of the gastrocnemius of 4-month–old mice revealed centralized nuclei, splitting fibers, and angular fibers in areas near connective tissue in the KI/KO animals (Figure 2.2D). These abnormalities did not increase markedly with age up to 14 months (Supplemental Figure S2.2). The RRFs were visible on Gomori trichrome (Figure 2.2G) staining. The RRF count in KI/KO muscle is significantly increased (5.5%) compared with WT muscle (1.1%) (P < 0.05) (Supplemental Figure S3, A and B). Although the KI/KI mice also had a higher level of RRFs (2.09%) than the WT mice, this finding was not significant. NADH staining also found moth-eaten fibers (Figure 2H), indicating myofibrillar disruption and significantly higher disruption in KI/KO (0.54%) compared with WT (0.08%) mice (P < 0.05), with a nonsignificant increase in KI/KI mice (0.29%) (Supplemental Figure S2.3C). Aggregates were seen in immunohistochemical stainings of the Z-disk proteins BAG3, desmin, and filamin C (Figure 2.2, I–L) as well as Gomori trichrome (Figure 2.2, E and F). This finding was largely absent in KI/KI mice (not shown). Within the KI/KO mice, there was a higher concentration of abnormal and aggregate-containing fibers near large areas of connective tissue, such as epineurium or myotendinous junctions, which are sites of high stress that have greater damage levels and repair after stretch injury (Tidball 1984). The KI/KI and KI/WT muscle had little to no deviation from WT muscle and lacked the classic MFM pathologic findings of KI/KO muscle. The fiber cross-sectional area was reduced across all fiber types in KI/KO mice and in type 2A and 2B fibers in KI/KI mice (Figure 2.3 and Supplemental Figure S2.4). The reduction in KI/KO mice was by 19% in type 1, 22% in type 2B, and 25% in type 2A. In KI/KI mice, a 23% reduction in type 2B and 10% reduction in type 2A were observed. Otherwise, the KI/KI and KI/WT mice were histologically normal. In addition, H&E straining of muscle from 14-month–

old KO/WT mice did not have abnormalities (Supplemental Figure S2.2) or a fiber cross-sectional area reduction in KO/WT and KI/WT mice (Supplemental Figure S2.5).

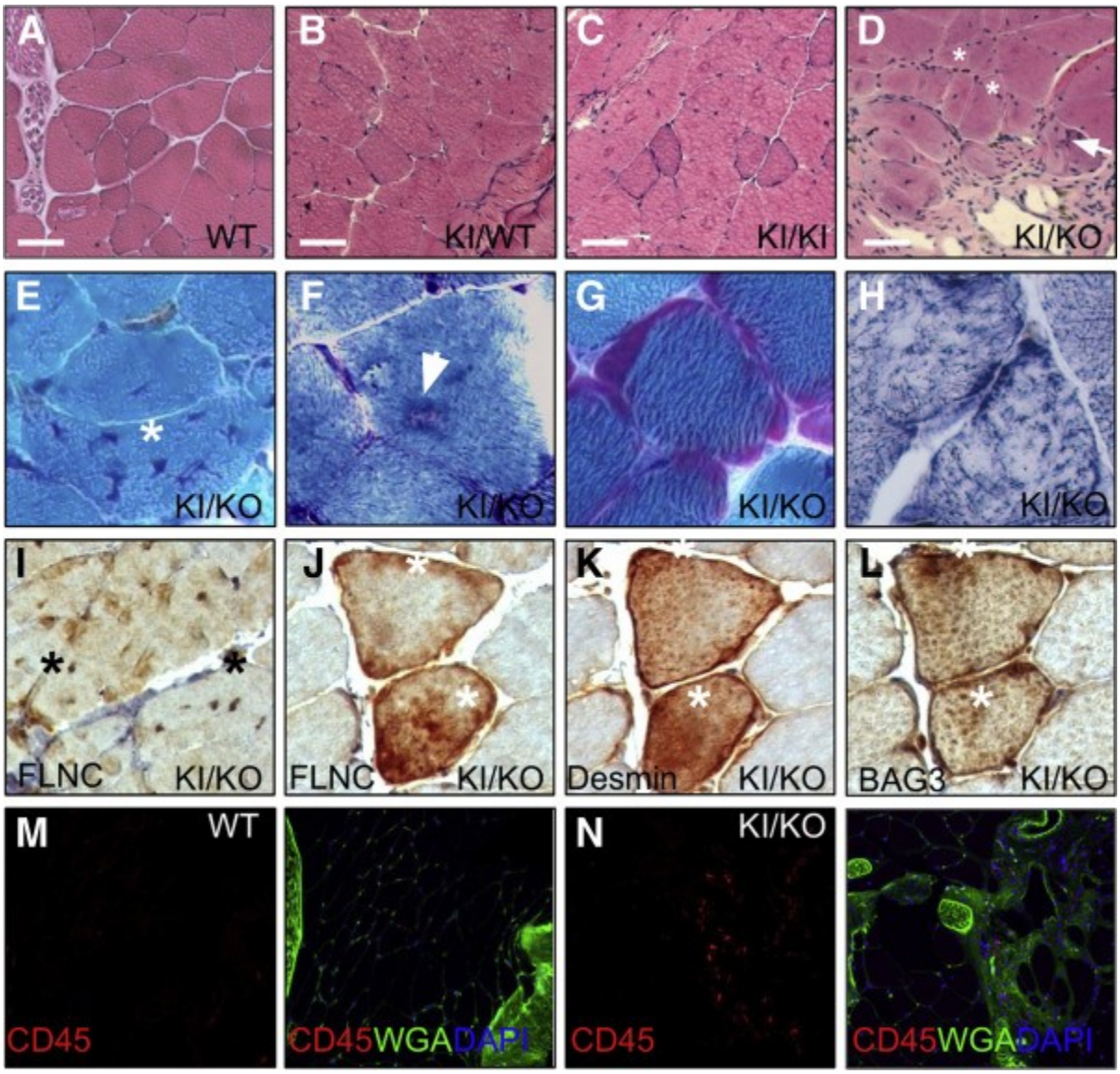

Figure 2.2. Histologic analysis of gastrocnemius muscles of 4-month–old mice. Hematoxylin and eosin staining of wild-type (WT) (A), knock-in (KI)/WT (B), KI/KI (C), and KI/knock-out (KO) (D) animals showing centralized nuclei and splitting (arrow in D) and angular fibers (stars) in KI/KO mice. Gomori trichrome findings in KI/KO mice, including aggregates (E and F; asterisk and arrow) and ragged red fibers (G). H: NADH of KI/KO mice showing moth-eaten fibers. I–L: Immunohistochemistry showing aggregates of filamin C (FLNC), desmin, and BCL-2–

associated athanogene 3 (BAG3) in KI/KO (asterisks); CD45 and wheat germ agglutinin (WGA) immunofluorescent labeling in WT (M) and KI/KO (N) animals, showing inflammation in KI/KO mice. Scale bars = 50 μm (A–D). Original magnification: ×20 (A–L); ×10 (M and N).

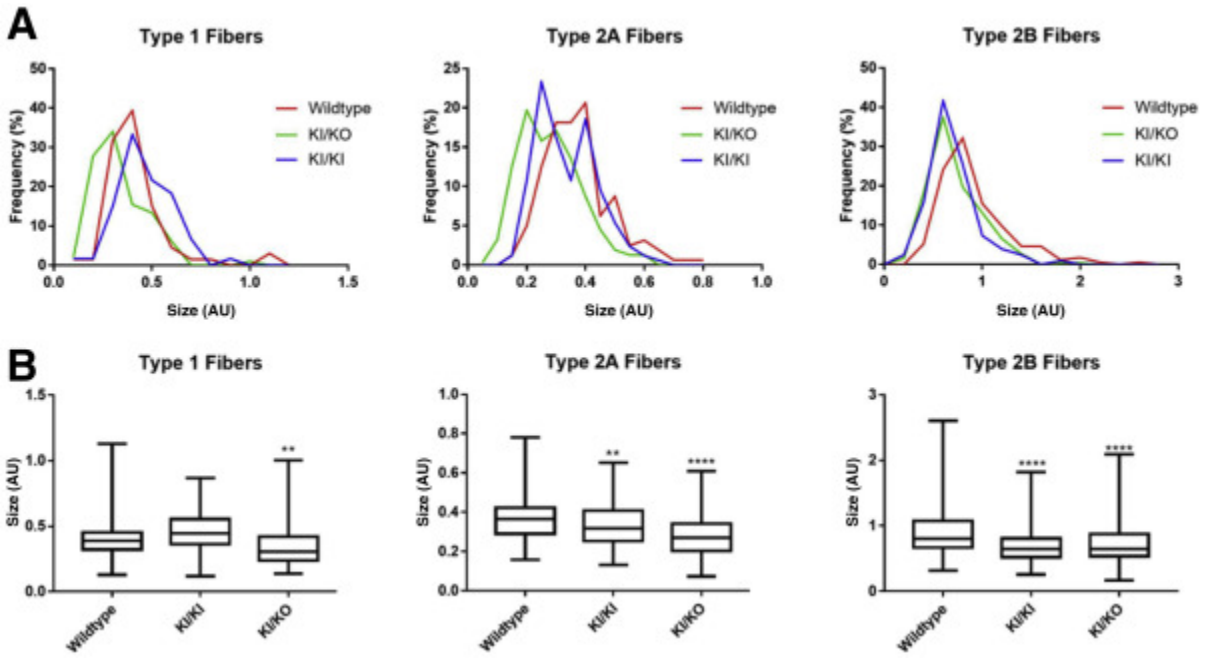

Figure 2.3. Fiber cross-sectional area comparison of gastrocnemius among wild-type, knock-in (KI)/KI, and KI/knockout (KO) mice shows a significant reduction in the size of all fibers between wild-type and KI/KO mice and a reduction in the size of type 2 fibers in KI/KI mice. Data are expressed as frequency distribution (A) and means ± SD (B). **P < 0.01, ****P < 0.0001 versus wildtype (analysis of variance). AU, arbitrary units.

To investigate whether an inflammatory response accompanied these pathologic changes, immunofluorescent staining for CD45, a pan-leukocyte cell surface antigen, was performed (Figure 2, M and N). Inflammatory infiltrate was seen in the connective tissue near areas of abnormal and disrupted fibers in the KI/KO strain, although it did not extend into the muscle fibers themselves in most cases. CD45-positive staining was rare in WT and KI/KI muscle.

To further explore the myofibrillar disruption, transmission electron microscopy was performed on muscle tissue from the gastrocnemius of 7-month–old animals to assess ultrastructural

changes to sarcomeres. Z-disk streaming and disruption, a classic feature of MFM, was seen in the tissue of KI/KO animals (Figure 4). Transmission electron microscopy also revealed the presence of megamitochondria, as well as other mitochondrial abnormalities, such as enlarged and mislocalized mitochondria, and subsarcolemmal accumulation, which corresponds to the increased RRFs. KI/KI animals were also assessed with transmission electron microscopy, which found some Z-disk disruption, although not as severely as in the KI/KO muscle and without the mitochondrial abnormalities.

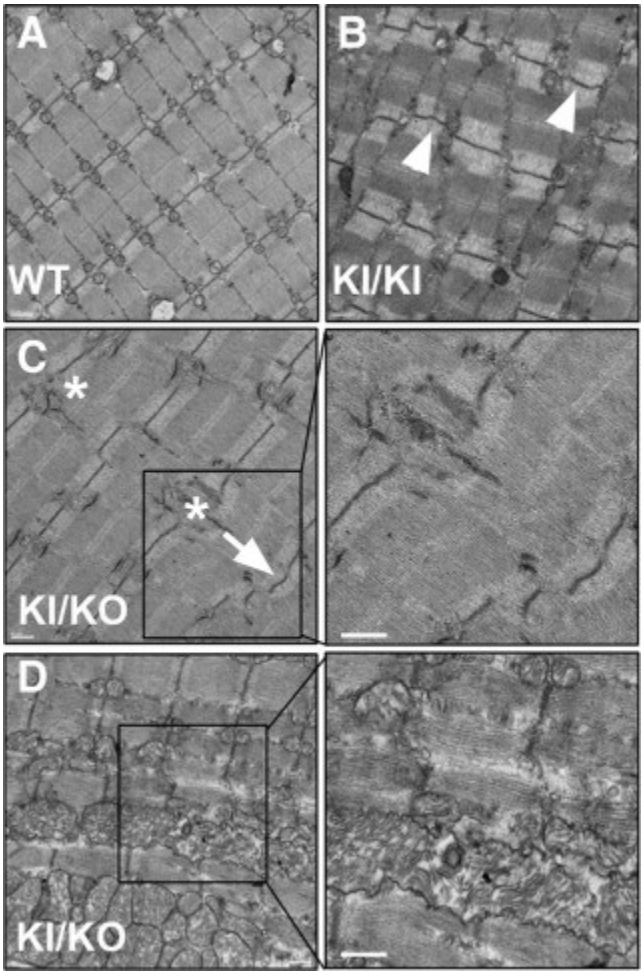

Figure 2.4. Transmission electron micrographs (TEMs) of longitudinally sectioned gastrocnemius muscle of 7-month–old mice wild-type (WT) (A), knock-in (KI)/KI (B), and KI/knockout (KO) (C and D) mice. Z-disk streaming (arrows in B and C) is observed in KI/KI and KI/KO mice with focal disruption and loss (asterisk) in KI/KO mice. Mitochondrial

abnormalities are also seen in KI/KO mice (D). Scale bars = 0.5 μm (A–D). Original magnification, ×6800 (A–D).

Altered Levels of BAG3-Associated Proteins

Western blots revealed deviation between mutant strains and WT in levels of BAG3 interactors (Figure 5, A and C). BAG3 levels decreased to approximately half in the KI/KO and KO/WT mice compared with the WT and KI/KI mice. The KO/KO mice had no evidence of any remaining protein when tested with a polyclonal antibody (Figure 5B).

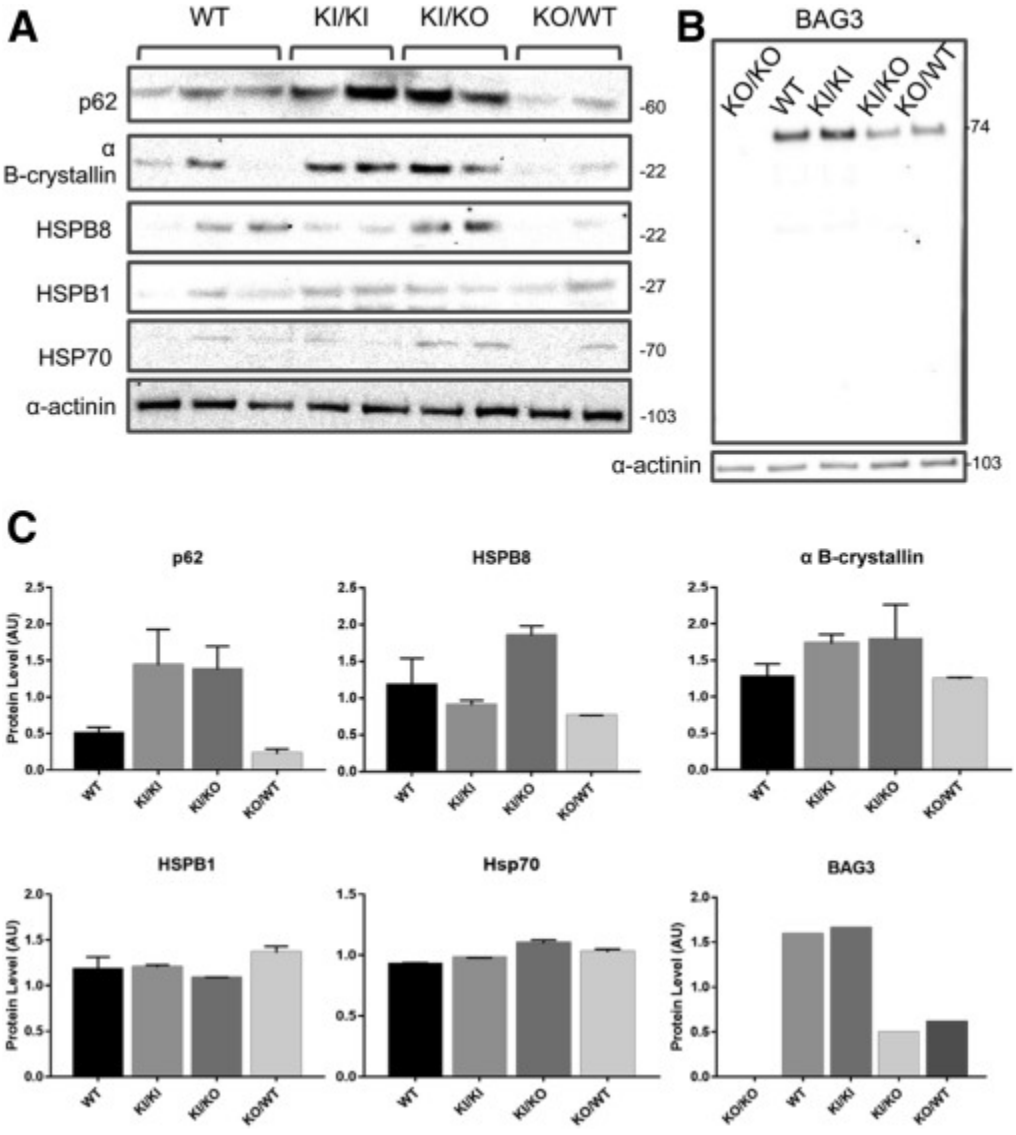

Figure 2.5. A: Western blot analysis of mouse muscle shows an increase in heat shock protein (HSP) B8, αB-crystallin, and p62 in knock-in (KI)/knockout (KO) animals, an increase in αB-crystallin and p62 in KI/KI animals, and a decrease in HSPB8 in KO/wild-type (WT) animals. B: BCL-2–associated athanogene 3 (BAG3) levels in KO, WT, KI/KI, KI/KO, and KO/WT mice. C: Protein levels normalized to loading controls (glyceraldehyde-3-phosphate dehydrogenase and actinin). Data are expressed as means ± SD (C).

The following proteins, previously reported to be increased in patients with BAG3 MFMs, were also increased in the KI/KO mice: p62, HSPB8, and αB-crystallin (Schänzer et al. 2018; Ruparelia et al. 2020). KI/KI mice also had an increase in p62 and αB-crystallin but not HSPB8. No increase was seen in HSPB1, a HSP known to have low affinity for BAG3 (Rauch et al. 2017; Carra et al. 2008). HSP70 levels also were not altered. These changes were not seen in KO/WT mice, which had levels of these proteins similar to that of WT mice except for HSPB8, which appeared to be lower in quantity.

Discussion

The BAG3 P215L/KO double mutant mouse is the first mouse model to recapitulate the skeletal muscle pathologic findings observed in patients with BAG3-P209L. Phenotypically, these mice do not have strength, coordination, or endurance deficits as measured by rotarod, grip strength, and inverted grid. However, they present with a significant reduction in voluntary movement with aging that appears at 7 months of age with further decline at 10 months. The decrease in voluntary movement seen may be an early clinical symptom of the muscle pathologic features, although heart, peripheral nerve, or even central nervous system pathologic findings cannot be ruled out as a cause because their investigation was beyond the scope of this study, which focuses on the skeletal muscle pathology. The absence of a strong phenotype likely reflects numerous physiologic differences between mice and humans, including much lower mechanical stress on the muscles of mice (Partridge 2013). These differences contribute to the often milder clinical phenotype seen in mice muscular dystrophy models. As such, additional mechanical stress may be needed to develop a phenotype that is more representative of what is seen clinically.

Despite only presenting with a reduction of movement with aging, histologically the KI/KO mice had many classic features of MFM, even before developing a clinical phenotype. These features include signs of muscle fiber damage, such as Z-disk streaming, myofibrillar disruption, inflammation, fiber atrophy, centralized nuclei, and Z-disk protein aggregates, which included filamin C, BAG3, and desmin (Selcen et al. 2009; Odgerel et al. 2010). Like the other MFMs, these same histologic features are present in patients with BAG3P209L (Selcen et al. 2009). Muscle is continually exposed to mechanical stress and has a number of repair mechanisms, including the CASA system in which BAG3 is essential (Ulbricht et al. 2015) and is negatively affected by the human P209L mutation (Meister-Broekema et al. 2018).

As in human BAG3 MFM cases, there appears to be a mitochondrial phenotype present. Swollen, mislocalized, and megamitochondria were seen on electron microscopy, and subsarcolemal clustering of mitochondria was noted in EM and in the form of RRFs on Gomori trichrome. Mitochondrial defects are a common feature of MFMs (Jackson et al. 2015; Vincent et al. 2016). Similar mitochondrial pathologic features, including megamitochondria, have been

observed in a mouse model of the human R350P desminopathy (Clemen et al. 2015). Patients with BAG3P209L have abnormalities in COX and NADH stainings (Selcen et al. 2009; Noury et al. 2018; Konersman et al. 2015), as well as clustered mitochondria as seen by electron microscopy (Selcen et al. 2009). BAG3 is implicated in mitochondrial quality control through activation of mitophagy (Tahrir et al. 2017), although it is unclear whether the presence of mitochondrial defects in the patients and mice is a primary or secondary effect of the myopathy.

Protein levels of various BAG3 interactors are affected in the KI/KO and KI/KI mice. A similar increase was not seen in KO/WT animals. In fact, they appeared to have lower levels of HSPB8. An increase was seen in p62 mice, αB-crystallin in KI/KI and KI/KO mice, and HSPB8 in KI/KO mice alone, all of which interact with BAG3. In contrast, HSPB1, a small HSP with little affinity for BAG3 (Rauch et al. 2017; Carra et al. 2008), is not affected. These increases may be attributable to increased stress response, stalling of the HSP70 machinery, and aggregate formation during CASA or a combination thereof. Stalling of the HSP70 machinery has been seen in human cell lines that express the BAG3P209L mutation (Meister-Broekema et al. 2018), leading to accumulation of components of the CASA system and its clients (Meister-Broekema et al. 2018; Guilbert et al. 2018). HSPB8 in particular is reliant on binding to BAG3 for stabilization; its levels are greatly decreased in BAG3 knock-down experiments in vitro (Carra et al. 2008), explaining the lower levels in KO/WT mice and making the increased levels in KI/KO mice even more striking. Alterations to levels of these proteins and autophagic dysregulation have been seen in patient muscle (Ruparelia et al. 2020) and heart (Schänzer et al. 2018), including an increase in small HSPs and p62. In addition, levels of HSP70 remain constant in mice and patient heart(Schänzer et al. 2018) despite HSP70's essential role in the CASA complex.

Although the KI/KO mice present with a myopathic phenotype, the homozygous and heterozygous P215L strains have little or no deviations from the WT mice, despite carrying the dominant mutation. The KI/KI animals present with some mild alterations, including a reduction in fiber cross-sectional area, a nonsignificant increase in RRFs, moth-eaten fibers, and some Z-disk disruption, but have no quantifiable clinical phenotype and are missing many of the classic myopathic features that the KI/KO animals have. This lack of phenotype supports the hypothesis

that BAG3 insufficiency in conjunction with the mutation is what leads to the MFM phenotype in humans.(Ruparelia et al. 2014) KO/WT mice have repeatedly been found to have no skeletal muscle or molecular phenotype (Youn et al. 2008; Homma et al. 2006), with only a mild heart phenotype and no histologic abnormalities (Myers et al. 2018). Human haploinsufficient patients also only have a heart phenotype (Norton et al. 2011). We found that the KO/WT mice do not exhibit similar molecular or histologic changes to the KI/KO mice, excluding haploinsufficiency alone as the cause of the phenotype. Although this disease is dominant in humans, the KI/KO genotype still reflects the loss of available and functional BAG3 in patients. It leads to a greater loss of functional BAG3, exacerbating the pathologic phenotype. Therefore, this KI/KO mouse overcomes some of the difficulties associated with using mice to model a human myopathy through exacerbating the phenotype via reduction of protein levels.

Although the KI/KO model presents with a myopathic phenotype, it still presents a milder phenotype than humans, without measurable loss of strength or endurance. Because of the significantly lower levels of mechanical stress on mouse muscle and their short lifespans compared with humans, this model likely represents the early stages of the disease. Early pathologic features of BAG3 MFM has not been well studied in humans because of the rarity of the disease and the fact that most patients are more advanced in terms of muscle damage at the time of biopsy. The KI/KO BAG3 model may well be a powerful tool to study the mechanisms involved in disease progression, in particular, for the repeated muscle injury caused by physical stress during exercise, while also serving as a model for preclinical trials.

Acknowledgements

We thank the Pigini family (Fondazione Roby) and the Bellini family (The Bellini Foundation) for inspiration and generous support; the Facility for Electron Microscopy Research (McGill University) for technical support and access to the FEI Tecnai G2 Spirit Twin 120 kV Cryo-TEM.

References

Rauch, J. N., *et al*. BAG3 is a modular, scaffolding protein that physically links heat shock protein 70 (Hsp70) to the small heat shock proteins, *Journal of Molecular Biology*, **429**, 128-141 (2017).

Hockenbery, D., Nuñez, G., Milliman, C., Schreiber, R & Korsmeyer, S. Bcl-2 is an inner mitochondrial membrane protein that blocks programmed cell death, *Nature*, **22**,334-336 (1990)**.**

Selcen, D., *et al*. Mutation in BAG3 causes severe dominant childhood muscular dystrophy, *Annals of Neurology*, **65**, 83-89 (2009).

Odgerel, Z., *et al.*. Inheritance patterns and phenotypic features of myofibrillar myopathy associated with a BAG3~mutation, *Neuromuscular Disorders*, **20**, 438-442 (2010).

Konersman, C. G., *et al.* BAG3 myofibrillar myopathy presenting with cardiomyopathy, Neuromuscular Disorders, **25**, 418 - 422 (2015).

Jaffer, F., *et al*. BAG3 mutations: another cause of giant axonal neuropathy, *Journal of the Peripheral Nervous System*, **17**, 210-216 (2012).

Lee, H., *et al*. BAG3-related myofibrillar myopathy in a Chinese family, *Clinical Genetics*, **81**, 394-398 (2012).

Kostera-Pruszczyk, A., *et al*. BAG3-related myopathy, polyneuropathy and cardiomyopathy with long QT syndrome, *Journal of Muscle Research and Cell Motility*, **36**, 423-432 (2015).

Noury, J., *et al*. Rigid spine syndrome associated with sensory-motor axonal neuropathy resembling Charcot–Marie-Tooth disease is characteristic of Bcl-2-associated athanogene-3 gene mutations even without cardiac involvement, *Muscle & Nerve*, **57**, 330-334 (2018).

Schänzer, A., *et al*. Dysregulated autophagy in restrictive cardiomyopathy due to Pro209Leu mutation in BAG3, *Molecular Genetics and Metabolism*, **123**, 388-399 (2018).

Quintana, M. T., *et al*. Cardiomyocyte-Specific Human Bcl2-Associated Anthanogene 3 P209L Expression Induces Mitochondrial Fragmentation, Bcl2-Associated Anthanogene 3~Haploinsufficiency, and Activates p38~Signaling, *The American Journal of Pathology*, **186**, 1989-2007 (2016).

Inomata, Y., *et al*. Bcl-2-associated athanogene 3 (BAG3) is an enhancer of small heat shock protein turnover via activation of autophagy in the heart, *Biochemical and Biophysical Research Communications*, **496**, 1141 - 1147 (2018).

Fang, X., *et al.* P209L Mutation in BAG3 Does Not Cause Cardiomyopathy in Mice, American Journal of Physiology-Heart and Circulatory Physiology, [Epub ahead of print] (2018).
Homma, S., *et al.* BAG3 Deficiency Results in Fulminant Myopathy and Early Lethality, The American Journal of Pathology, **169**, 761-773 (2006).
Youn, D. Y., *et al.* Bis deficiency results in early lethality with metabolic deterioration and involution of spleen and thymus, American Journal of Physiology-Endocrinology and Metabolism, **295**, E1349-E1357 (2008).
Myers, V. D., *et al.* Haplo-insufficiency of Bcl2-associated athanogene 3 in mice results in progressive left ventricular dysfunction, β-adrenergic insensitivity, and increased apoptosis, Journal of Cellular Physiology, **233**, 6319-6326 (2017).
Ruparelia, A. A., *et al*. Zebrafish models of BAG3~myofibrillar myopathy suggest a toxic gain of function leading to BAG3 insufficiency, Acta Neuropathologica, **128**, 821-833 (2014).
Meister-Broekema, M.,*et al*. Myopathy associated BAG3 mutations lead to protein aggregation by stalling Hsp70 networks, Nature Communications, **9**, 5342 (2018).
D'Avila, F., *et al*. Exome sequencing identifies variants in two genes encoding the LIM-proteins NRAP and FHL1 in an Italian patient with BAG3 myofibrillar myopathy, Journal of Muscle Research and Cell Motility, **37**, 101-115 (2016).
Selcen, D., Ohno, K. & Engel, A. G. Myofibrillar myopathy: clinical, morphological and genetic studies in 63 patients, Brain, **127**, 439-451 (2004).
Tidball, J. G. (**2011**). In: (Ed.), Mechanisms of Muscle Injury, Repair, and Regeneration, John Wiley & Sons, Inc..
Bjørkøy, G., *et al.* p62/SQSTM1 forms protein aggregates degraded by autophagy and has a protective effect on huntingtin-induced cell death, The Journal of Cell Biology, **171**, 603-614 (2005).
Whitehead, N., Streamer, M., I Lusambili, L., Sachs, F. & Allen, D. Streptomycin reduces stretch-induced membrane permeability in muscles from mdx mice, Neuromuscular Disorders, **16**, 845-54 (2007).
Gibbs, E. M. & Crosbie-Watson, R. H. A Simple and Low-cost Assay for Measuring Ambulation in Mouse Models of Muscular Dystrophy, Journal of Visual Experiments, **130**, e56772 (2017).

Chevessier, F., *et al*. Myofibrillar instability exacerbated by acute exercise in filaminopathy, Human Molecular Genetics, **24**, 7207-7220 (2015).
Murgia, M., *et al*. Single Muscle Fiber Proteomics Reveals Fiber-Type-Specific Features of Human Muscle Aging, Cell Reports, **19**, 2396-2409 (2017).
Hyzewicz, J., Ruegg, U. T. & Takeda, S. Comparison of Experimental Protocols of Physical Exercise for mdx Mice and Duchenne Muscular Dystrophy Patients, Journal of Muscular Dystrophy, **22**, 325-342 (2015).
Partridge, T. A. The mdx mouse model as a surrogate for Duchenne muscular dystrophy, The FEBS Journal, **280**, 4177-4186 (2013).
Guilbert, S. M., *et al.* HSPB8 and BAG3 cooperate to promote spatial sequestration of ubiquitinated proteins and coordinate the cellular adaptive response to proteasome insufficiency, The FASEB Journal, **32**, 3518-3535 (2018).
Hardie, D. G. & Carling, D. The AMP-Activated Protein Kinase, European Journal of Biochemistry, **246**, 259-273 (1997).
Owen, M. R., Doran, E. & Halestrap, A. P. Evidence that metformin exerts its anti-diabetic effects through inhibition of complex 1 of the mitochondrial respiratory chain, Biochemical Journal, 348, 607-614 (2000).
Kim, J., Kundu, M., Viollet, B. & Guan, K.L. AMPK and mTOR regulate autophagy through direct phosphorylation of Ulk1, Nature Cell Biology, **13**, 132-141 (2011).
Langone, F., *et al.* Metformin Protects Skeletal Muscle from Cardiotoxin Induced Degeneration, PLOS ONE, **9**, 1-19 (2014).
Ye, Y., Perez-Polo, J. R., Aguilar, D. & Birnbaum, Y. The potential effects of anti-diabetic medications on myocardial ischemia--reperfusion injury, Basic Research in Cardiology, **106**, 925-952 (2011).
Larivière, R., *et al.* Sacs knockout mice present pathophysiological defects underlying autosomal recessive spastic ataxia of Charlevoix-Saguenay, Human Molecular Genetics, **24**, 727-739 (2015).
Mantuano, P., *et al.* Effect of a long-term treatment with metformin in dystrophic mdx mice: A reconsideration of its potential clinical interest in Duchenne muscular dystrophy, Biochemical Pharmacology, **154**, 89 - 103 (2018).

Supplementary data

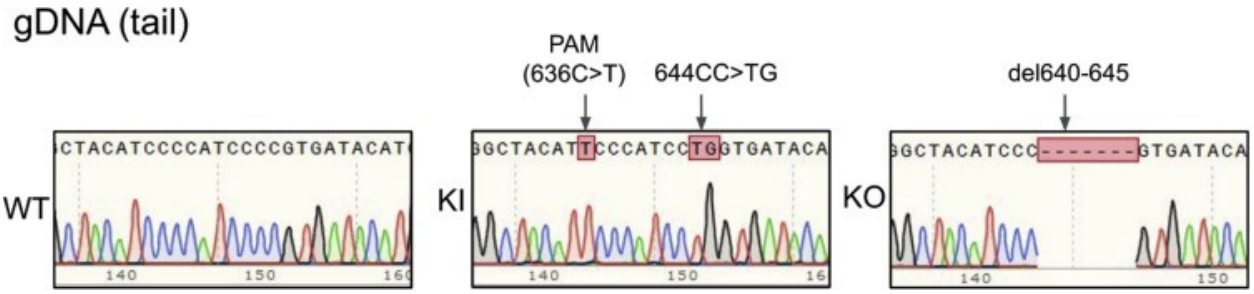

Supplemental Figure S2.1. Sequence chromatograms from wild-type (WT), knock-in (KI), and knockout (KO) mice, showing the presence of a 644CC>TG (p.P215L) and a silent point accepted mutation (PAM) (636C>T) in the KI allele and a 6-bp deletion from 640 to 645 in the KO allele.

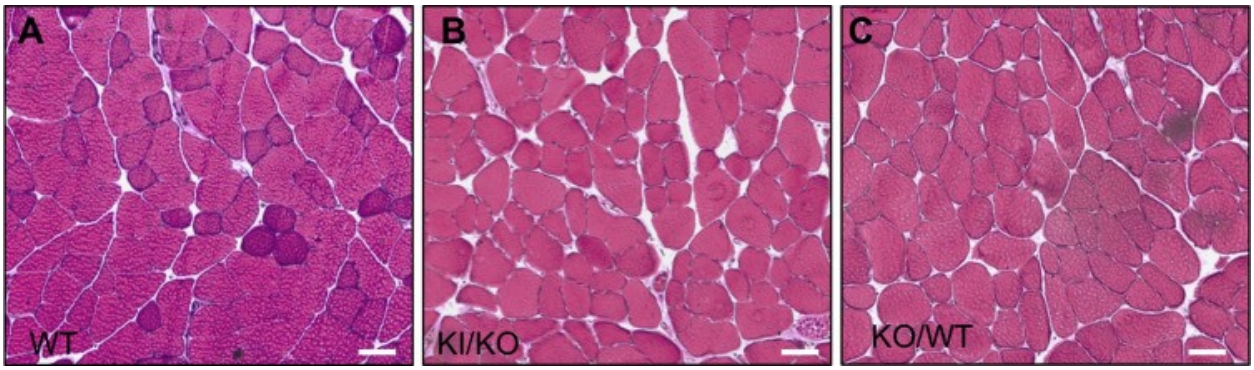

Supplemental Figure S2.2. Hematoxylin and eosin staining of images from 14-month–old wild-type (WT) (A), knock-in (KI)/knockout (KO) (B), and KO/WT (C) animals. Scale bars = 50 μm. Original magnification, ×20.

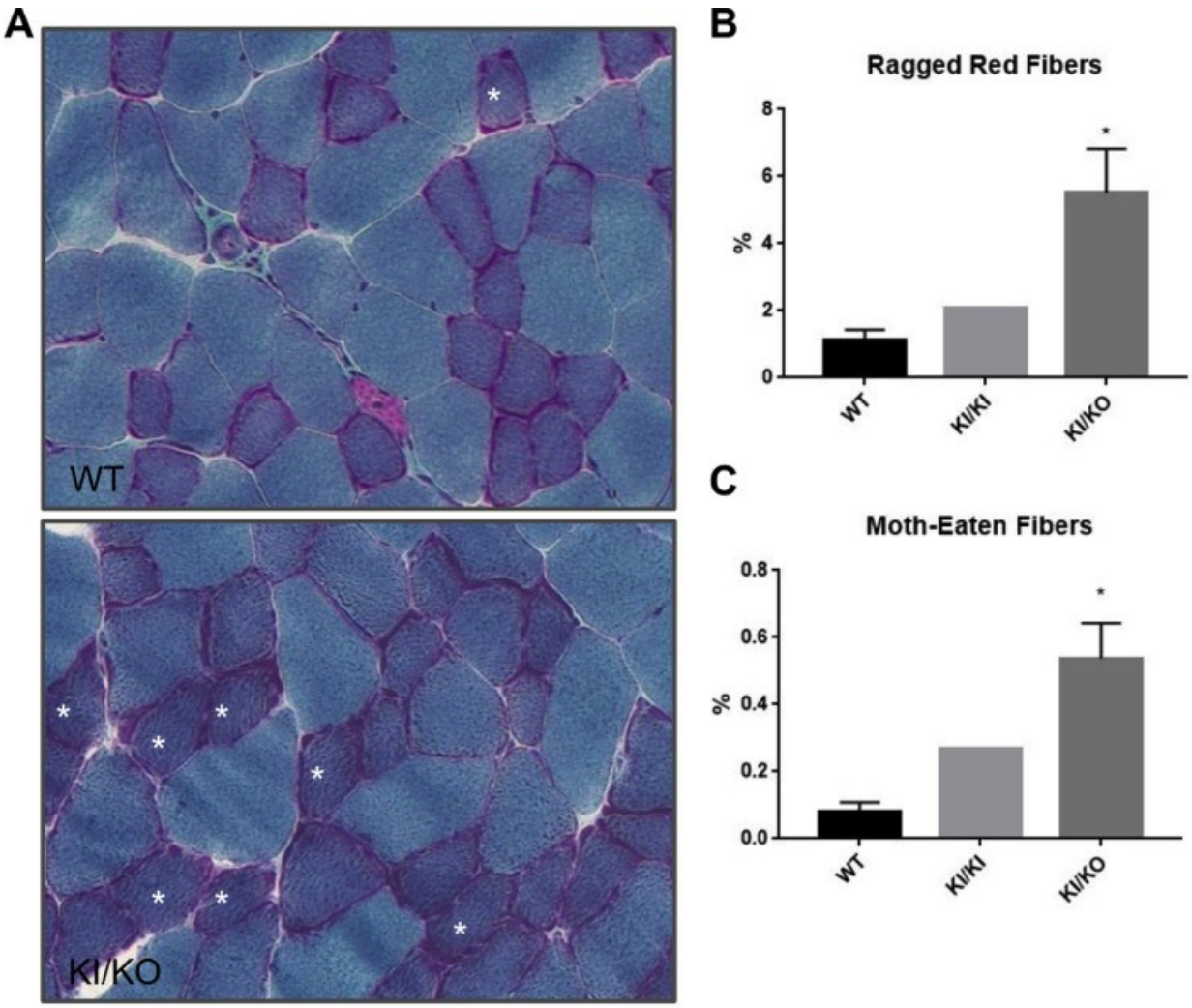

Supplemental Figure S2.3. A: Gomori trichrome of gastrocnemius of 4-month–old wild-type (WT) and knock-in (KI)/knockout (KO) mice with ragged red fibers (asterisks) B: Quantification of total ragged fibers in sections showing a significant increase in ragged red fibers in KI/KO mice. C: Quantification of moth-eaten fibers in NADH stain, showing an increase in KI/KO mice. n = 2 per genotype. *P < 0.05 versus WT (analysis of variance). Original magnification, ×20.

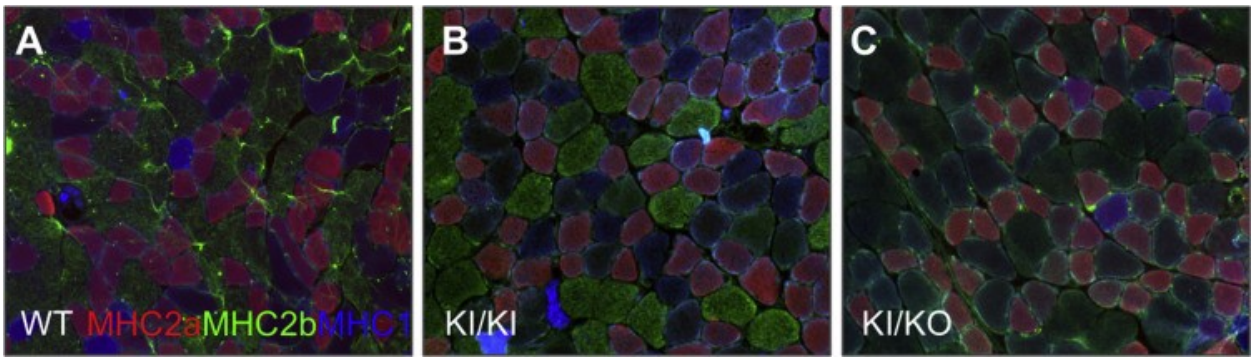

Supplemental Figure S2.4. Myosin heavy chain staining from wild-type (WT) (A), knock-in (KI)/KI (B), and KI/knockout (KO) (C) mice showing type 1 (blue), type 2a (red), and type 2b (green) fibers. Original magnification, ×20.

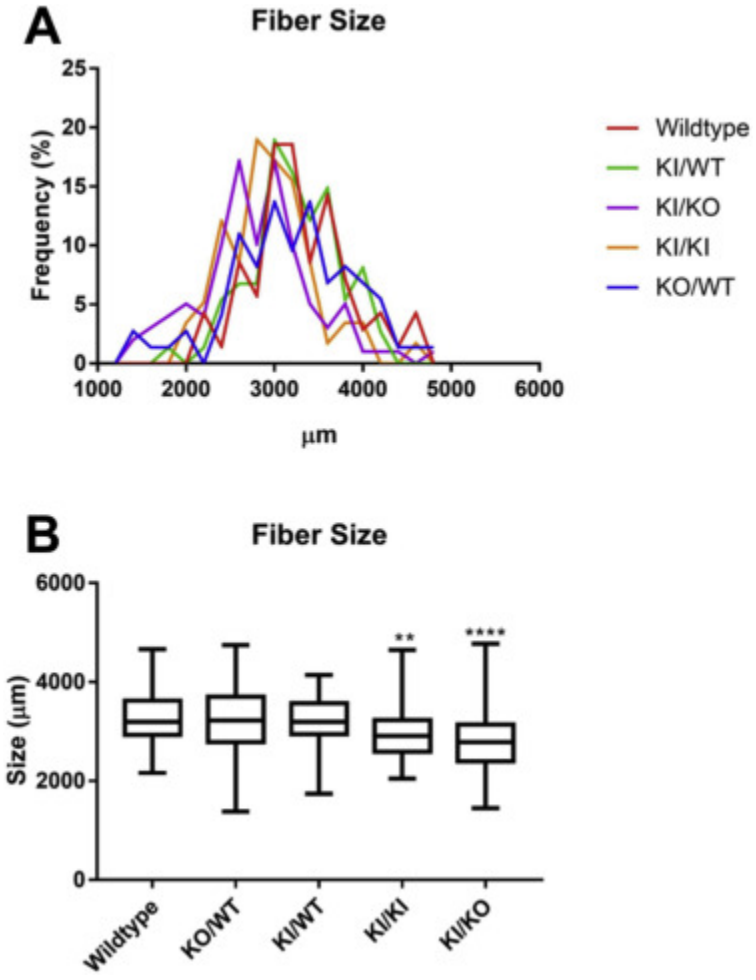

Supplemental Figure S2.5. Fiber cross-sectional area data from 14-month–old mice using hematoxylin and eosin staining of shallow area of gastrocnemius, which is predominately type

2b, show a significant reduction in size in knock-in (KI)/KI and KI/knockout (KO) mice. No size reduction was detected in KO/WT or KI/WT. Data are expressed as fiber cross-sectional area distribution (A) or as fiber cross-sectional area means ± SD. **P < 0.01, ****P < 0.0001 versus wildtype (analysis of variance).

PREFACE TO CHAPTER 3

With the establishment of the mouse model of BAG3 MFM in **Chapter 2**, there are still questions to be answered about the pathophysiology of disease. While the molecular basis of how this mutation affects CASA has been established, how this may affect structures beyond the sarcomere has not been well established, nor has the reason for the severity of this disease been discovered.

In Chapter 3, we aimed to explore how the BAG3 P209L mutation may affect actomyosin dynamics and nuclear-cytoskeletal coupling, leading into a self-feeding cycle of damage and failure to repair. This chapter is a manuscript in preparation, in which we use both our mouse model and a patient cell line to determine whether the BAG3 P209L mutation leads to impaired mechanotransduction.

CHAPTER 3: BAG3 P209L variant causes changes in nuclear and actomyosin dynamics and impairment of the transmission of mechanical signals

Rebecca Robertson [1,2], Marie-Josée Dicaire [1], Josée N Lavoie [3], Bernard Brais [1]

Affiliations:

1. Neurogenetics of Motion Laboratory, Department of Neurology and Neurosurgery, Montreal Neurological Institute, McGill University, Montreal, Quebec, Canada.
2. Department of Human Genetics, McGill University, Montreal, Quebec, Canada.
3. Centre de Recherche sur le Cancer, l'Université Laval, Québec, Quebec, Canada; Oncology Axis, Centre de Recherche du Centre Hospitalier Universitaire (CHU), Québec-Université Laval, Québec, Quebec, Canada; Département de Biologie Moléculaire, Biochimie Médicale et Pathologie, l'Université Laval, Québec, Quebec, Canada.

Manuscript in preparation

Abstract

The transmission of mechanical signals throughout the cell is important for cell function and cell fate decisions, turning mechanical tension into molecular signals and dynamic responses. This is achieved through the coupling of the nucleus and cytoskeleton via the LINC complex, mechanically integrating these structures. While BAG3 myofibrillar myopathy (MFM), caused by the Pro209Leu variant, is typically thought of as a disease which primarily affects the Z-disk, here we show evidence of a role for BAG3 in mechanotransduction. Our mPro215Leu knock-in/knock-out mouse model, as well as patient and mouse derived fibroblasts, show an increase in nuclear abnormalities. Patient cells show an abnormal nuclear/cytoplasmic ratio and impaired response to mechanical signals including slowed migration and defective actin remodeling. This is associated with impaired actin turnover and changes in active myosin II, and reducing myosin II activation results in improved migration and mechanosensing. These data suggest that BAG3 is important in maintaining proper cellular mechanotransduction, a role that may be important in the pathology of BAG3 MFM.

Introduction

BAG3 (BCL-2-associated athanogene 3) myofibrillar myopathy (MFM), resulting from the Pro209Leu (P209L) mutation, is a severe autosomal dominant childhood disease that results in progressive muscle weakness and atrophy(Selcen et al. 2009; Konersman et al. 2015; Kostera-Pruszczyk et al. 2015; Noury et al. 2018; Schänzer et al. 2018) and is often accompanied by peripheral neuropathy or a rigid spine(Noury et al. 2018; Jaffer et al. 2012). As the disease progresses, respiratory insufficiency and cardiomyopathy often develops, leading to death in the second or third decade of life(Selcen et al. 2009).

BAG3 is a highly multifunctional protein best known for its role in protein quality control. As a part of the chaperone assisted selective autophagy (CASA) machinery(Arndt et al. 2010), it acts as a co-chaperone to HSP70 and as a scaffold for this complex, which transports misfolded client proteins to the perinuclear region. Here, it stimulates formation of autophagosomes so that these clients may be processed. CASA is essential for the maintenance of muscle due to the high amounts of mechanical stress the tissue is subject to, resulting in damage and misfolding of force-bearing proteins like filamin C(Arndt et al. 2010) which anchors actin to the Z-disk. Impairment of CASA leads to Z-disk disintegration(Arndt et al. 2010), and complete loss of BAG3 leads to fulminant myopathy and early death in mice(Homma et al. 2006; Youn et al. 2008). It was shown *in vitro* that the P209L mutation results in the aggregation of the HSP70 client protein and subsequent sequestration of protein quality control (PQC) proteins into insoluble aggregates due to the formation of non-native BAG3 oligomers(Meister-Broekema et al. 2018; Adriaenssens et al. 2020).

While BAG3 MFM has largely been thought of as a disease primarily of the Z-disk, recent evidence has shown a role for BAG3 at the nuclear envelope (NE)(Gupta et al. 2019). BAG3 together with HSP70 were shown to interact with lamin B, a component of the NE which plays a role in maintaining its structural integrity(Bridger et al. 2007). Reduction of BAG3 in cardiomyocytes, particularly under proteotoxic stress, leads to changes in nuclear morphology and integrity such as enlargement, elongation, rupture, micronuclei formation and the

accumulation of lamin B in the perinuclear space (Gupta et al. 2019). Knockdown of BAG3 also results in the formation of chromatin bridges and multi-nucleation in HeLa cells due to mitotic defects (Fuchs et al. 2015). Moreover, expression of BAG3-P209L in HeLa cells results in cytoplasmic punctae of lamin A/C, the lamin type responsible for nuclear mechanical stability(Meister-Broekema et al. 2018). This suggests a role for BAG3 in the maintenance of the NE through protein quality control (PQC), and that MFM-associated mutations (P209L) may impair nuclear mechanical stability and cellular mechanics.

The cytoskeleton and nucleus are mechanically integrated structures, allowing for mechanical signals to be transmitted and quickly responded to. The NE is a double membraned structure that separates the nucleus from the cytoplasm. It plays a number of important roles, including structural support, mechanotransduction, transcriptional regulation and chromatin organization(Davidson and Lammerding 2014). A structure called the nuclear lamina is present on the nuclear face of the inner membrane. It is composed of a lattice of A and B type lamins which lends structural support to the nuclear membrane(Bridger et al. 2007). The nuclear lamina is connected through the Barrier to Autointegration Factor (BAF) to the chromatin. The envelope is tethered to the cytoskeleton through the Linker of Nucleoskeleton and Cytoskeleton (LINC) complex, which includes SUN (S ad1/UN C-84 homology) domain containing proteins(Zhang et al. 2001). SUN1/2 are integrated into the inner nuclear membrane and bridge the connection between cytoskeleton and nuclear lamina through the tethering of nesperins and A-type lamins(Crisp et al. 2006). The cytoskeleton is peripherally tethered to the integrins, receptors on the cell surface, that allow for interaction with the extracellular matrix (ECM), allowing the cell to sense tension changes in its environment and mechanotransduction(Alam et al. 2016). This allows mechanical signals to influence transcription and chromatin organization, which has implications for repair, migration, and cell fate decisions(Davidson and Lammerding 2014). As such, cellular mechanics are largely determined by these mechanically integrated structures.

Alterations to the LINC complex and cytoskeleton may lead to changes in tension at the NE that will influence transcription(Alam et al. 2016), as well as alter the shape and positioning of the nucleus within the cell(Lele, Dickinson, and Gundersen 2018; LOVETT et al. 2013). Similarly, loss of or mutation in the proteins of the nuclear lamina have been shown to result in defects of

morphology and function of the NE(Lammerding et al. 2005). This has implications for mechanosensitive pathways, such as that of YAP/TAZ, which rely on the transmission of forces, a process particularly important for muscle due to the high amounts of mechanical stress it experiences as a force producing tissue. Mechanosensitive repair pathways, including myogenic ones essential for the activation and commitment of muscle satellite cells, are important for cell function and survival(Bertrand et al. 2014; Dasgupta and McCollum 2019; Vogel and Sheetz 2006). This, in conjunction with the high mechanical stress muscle is subject to is why laminopathies frequently lead to myopathies such as Emery-Dreifuss muscular dystrophy(Emery 2000). BAG3 and the CASA machinery play a role in the maintenance of mechanosensitive functions in the cell, both through the aforementioned stimulation of autophagic processing of damaged filamin C and transcriptional regulation of YAP/TAZ signaling, which induce transcription of new filamin C(Ulbricht et al. 2013; Ulbricht, Arndt, and Höhfeld 2013). As such, BAG3 is responsible both for removal of damaged proteins and regulating the transcription of their replacements.

Given BAG3's role in maintenance of the NE and the known cytoskeletal defects in BAG3 MFM, we hypothesized that the failures of PQC caused by the P209L mutation would have implications for cellular tension and the integrity of the NE. While little investigation into the state of the nuclei in patients with BAG3 P209L has been done to date, it has been noted that they have an increase in nuclear apoptosis which is typically not seen in other MFMs except for αB-Crystallinopathy(Selcen 2011). Indeed, the first paper which described BAG3 MFM showed ultrastructural images of patient nuclei, which showed apoptotic, pyknotic and misshapen nuclei with increased chromatin clumps(Selcen et al. 2009). Here we describe the impact of the P209L BAG3 MFM mutation on nuclear morphology and mechanosensing which likely contributes to the disease's pathophysiology.

Methods

Mouse lines

The mouse lines used carried P215L knock-in allele or a knock-out allele, caused by a premature stop codon, on a C57Bl/6 background. Their generation is as described in Robertson *et al.* (2020)(Robertson et al. 2020). The KI allele carries the change c.644_645CC>TG, which results in the P215L mutation. The KO allele has a 7-bp deletion, c.639_645delCATCCCC, resulting in a premature stop codon.

Cell culture, treatments and transfections

The patient cell lines were obtained from Dr. Yvan Torrente(D'Avila et al. 2016) and the mutation was verified via Sanger Sequencing. Control fibroblasts MHC64 (control 64) and MHC74 (control 74) were obtained from the Montreal Children's Hospital cell repository (Montreal, Canada). Cell lines were immortalized as previously described(Lochmüller, Johns, and Shoubridge 1999). Cells were cultured in high-glucose DMEM with 10% fetal bovine serum (FBS) and penicillin/streptomycin. Cells used for imaging were plated on rat tail collagen I (Gibco; Thermo Fisher Scientific, Inc., Waltham, MA, USA) coated coverslips and fixed in 4% PFA for 10 minutes at 37°C. Collagen coating was done at a concentration of 0.3mg/ml in DMEM for 2h at 37°C, followed by a rinse with PBS prior to cell plating.

To generate primary mouse fibroblasts, ears from mice of 5 months of age were collected, diced and digested overnight in 400U/mL collagenase II (Thermofisher) in DMEM with 20% FBS and penicillin/streptomycin at 37°C. The following morning the collagenase containing media was removed, the tissue was further digested for 20 minutes with 0.05% trypsin. After digestion, the cells were passed through a 70 μm filter and plated. Cells were left to adhere for 48 hours before passaging, and cultured in DMEM with 10% FBS and penicillin/streptomycin. Experiments were done at passage 3.

Blebbistatin (Sigma-Aldrich, St. Louis, MO) was resuspended in DMSO. Treatments were done at a concentration of 2 μM, with controls treated with equivalent quantities of DMSO.

For cell substrate experiments, cells were plated at 4000 cells/cm² on glass coverslips coated with rat tail collagen (Gibco) or on hydrogel coated coverslips of 12 kPa stiffness with collagen coating (Matrigen, Irvine, CA, USA). The cells were allowed to adhere for 24 h, then fixed the next day with 4% PFA for 10 minutes at 37°C.

The EGFP-Actin and mCherry-Lamin A/C expression vectors were transfected into human fibroblasts using Lipofectamine 3000 (Invitrogen, Waltham, MA, USA), and cultured for 72 hours prior to imaging. EGFP-Actin-7 plasmid a gift from Michael Davidson (Addgene plasmid # 56421 ; http://n2t.net/addgene:56421)(Rizzo, Davidson, and Piston 2009)

For micropatterning experiments, cells were plated on micropatterned plates (4Dcell, Montreuil, France) that had either round or rectangular shaped patterns at 4000 cells/ cm². Cells were allowed to adhere overnight, then were fixed with 4% PFA for 10 minutes.

Wound healing assay

Cells were seeded at high confluency (30,000 cells/cm^2), allowed to adhere overnight, and then a pipette tip was used to scratch a wound through the monolayer in a straight line. To test polarity, cells were left for three hours and then fixed and immunolabeled for a marker of the Golgi apparatus (Giantin) and for actin (using phalloidin stain). Those cells whose Golgi apparatus were contained to the front third of the cell were defined as polarized. For the migration assay, migration was assessed by imaging the scratch every two hours over the course of six hours, and the distance between wound edges recorded(Cory 2011). Size of the wound was compared to time point 0 to obtain the distance the wound edge had migrated. Each cell line and each condition had at least 6 technical replicates.

Immunofluorescence

Coverslips with fixed cells were permeabilized for 15 minutes in 0.1% Triton in PBS, then blocked for 30 minutes with 5% normal donkey serum. Primary antibodies were applied for one hour at room temperature. Coverslips were washed three times in PBS, prior to secondary antibody incubation for one hour. For substrate experiments cells were incubated with Hoescht nuclear stain and mounted with ProLongTM Gold antifade reagent (Thermo Fisher). For all other cell experiments mounting was done with ProLongTM Gold antifade reagent with DAPI (Thermo Fisher).

For tissue sections, cryostat cross-sections of 10 μm were fixed with 4% paraformaldehyde for 10 minutes at room temperature. They were blocked and permeabilized for 1 hour in a buffered saline solution with 5% normal donkey serum, 0.25% Triton X-100, and 0.1 mol/l glycine. For nuclear aggregate immunostaining, sections were pretreated for 1h with 1M KCl to clear soluble proteins, as done previously for OPMD patient tissue to assess PABPN1 inclusions(Calado et al. 2000; Malerba et al. 2019), prior to immunolabeling.

Antibodies

Anti-YAP1 (Cell signaling 14074S, 1:1000), anti-Lamin A/C (Cell signaling 4c11, 1:200), Phalloidin (Abcam ab176756, 1:1000), anti-BAG3 (LP11)(1:100), anti-Giantin (Abcam ab37266 1:200), anti-pMLC ser19 (Cell signaling 3675S, 1:2000), anti-H3K9me3 (Cell signaling 13969T, 1:500)

Electron microscopy

Electron microscopy was performed as previously described(Robertson et al. 2020), and imaged using a FEI Tecnai G2 Spirit Twin 120 kV Cryo-TEM at the Facility of Electron Microscopy Research at McGill University. Nuclei were counted across a random axis through the section for two animals per genotype, with at least 60 nuclei counted per animal.

Microscopy and image analysis

Analysis of images was done with ImageJ software version 1.53 (NIH, Bethesda, MD; http://imagej.nih.gov/ij). Fluorescent microscopy was done with Zeiss Axio Imager M2. For confocal microscopy, cells were imaged with Olympus IX83 microscope connected with Yokogawa CSU-X confocal scanning unit, using UPLANSAPO 60x/1.40 Oil objective (Olympus) and Andor Neo sCMOS camera spinning disk, including FRAP (100x/1.40 Oil objective). Nuclear shape and size was calculated from fluorescent microscopy images taken with the 20x objective. Images were taken by tiling the entire coverslip to avoid selection bias. In ImageJ a threshold was applied on the DAPI channel, nuclei were selected with the wand tool and measurements of area and shape descriptors were taken for at least 300 nuclei per condition. Nuclear/cytoplasm size ratio was determined by taking this measurement (n) in addition to that of the entire cell body (c), and calculated as (n/(c-n)). To determine the YAP nuclear/cytoplasmic ratio, mean gray value measurements were taken from a section within the nucleus as well as directly adjacent to the nucleus where cytoplasmic YAP accumulates, and the nuclear measurement was divided by the cytoplasmic to determine the final value. Confocal images are presented as maximum projections, except where otherwise specified.

For FRAP, cells transfected with EGFP-Actin, viewed via the 100x oil objective, were photobleached via argon laser with 10 pulses of 30ms dwell time. Images were taken every 500ms for 30s, with four control images prior to photobleaching. Three intensity measurements were taken per frame: one of the site of photobleaching (Fs), one of a control site of similar initial intensity before (Fc0) and after (Fc) the photobleaching event, and a background region (Fb)("Fluorescence Recovery After Photobleaching (FRAP) of Fluorescence Tagged Proteins in Dendritic Spines of Cultured Hippocampal Neurons | Protocol" n.d.). Intensity data were normalized as follows to account for background and rate of photobleaching:

$$F = (Fs - Fb) / (Fc / Fc0).$$

and converted to percentage of initial intensity of the four control images.

Statistical analysis

Data are expressed as mean ± SD. The data analyses were performed using PRISM 7 software (GraphPad Software Inc., San Diego, California, USA) and Categorical data were analyzed using chi-squared analysis or Fisher's exact test. Quantitative data were analyzed using one way ANOVA followed by ad-hoc testing using Dunnett's multiple comparison test, or T-test for comparisons containing only two groups. Time course data was analyzed via two-way ANOVA. Python's scipy(Virtanen et al. 2020) package was used to calculate Pearson's correlation and perform linear regressions on data concerning the relationship between nuclear and cell size. A two-tailed P value below 0.05 was considered significant. The p value significance is represented as *, $p < 0.05$; **, $p < 0.01$; ***, $p< 0.001$; ****, $p< 0.0001$.

Results

Changes to the nucleus in BAG3 MFM mouse muscle

To assess the impact of BAG3-P209L MFM on nuclear integrity, transmission electron microscopy was performed on muscle tissue from the gastrocnemius of 7-month–old animals (Fig 1A). This revealed nuclei with a significant increase ($p<0.001$) of deformities of the NE including accumulations of chromatin at the envelope, chromatin clumps and nuclear inclusions in the KI/KO line, our model of BAG3 MFM(Robertson et al. 2020), as compared to wildtype (Fig 1B). These changes were not usually associated with an increase in nearby Z-disk damage, although some of the affected nuclei were positioned within mitochondrial accumulations, a common feature in the KI/KO animals(Robertson et al. 2020).

In order to assess whether the inclusions contained BAG3 and NE components, tissue from 6 month old mice was cleared of soluble protein using a KCl buffer (Fig 1C) so that only insoluble aggregates remained, and then labeled for BAG3 and lamin A/C. Confocal imaging revealed the presence of intranuclear accumulations positive for the two proteins within some of the nuclei of KI/KO animals (Fig 1C), suggesting that the inclusions seen via TEM (Fig 1A) are indeed in part composed of BAG3 and NE components.

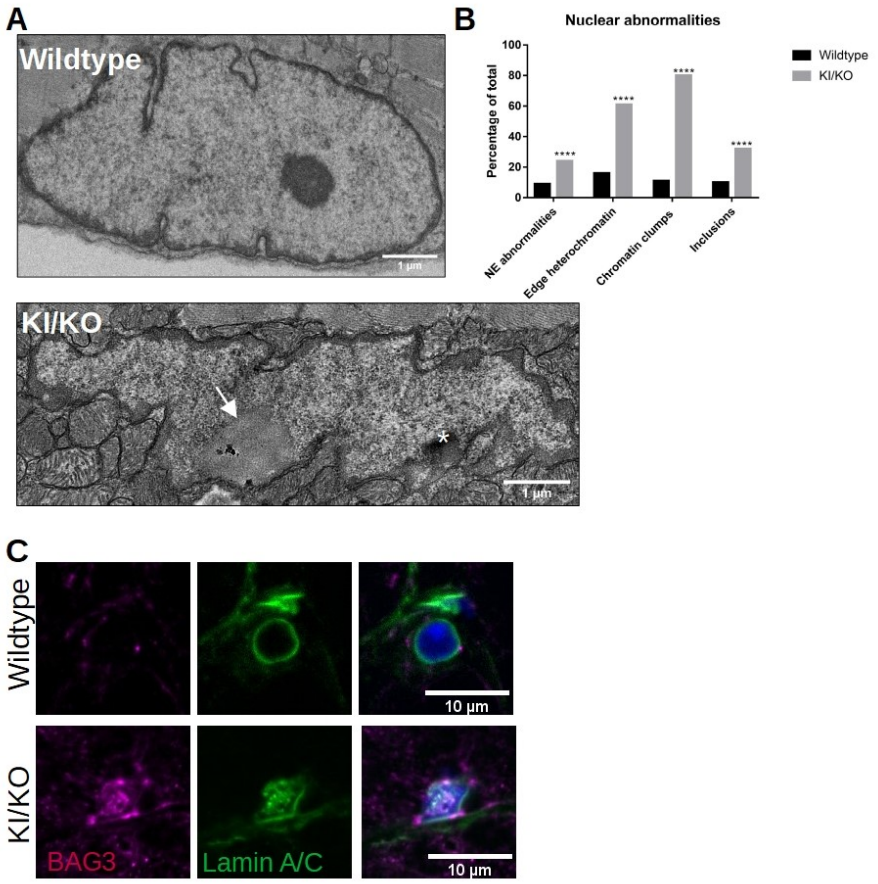

Figure 1. Nuclear abnormalities in muscle from KI/KO mice. A) EM images of nuclei in wildtype and KI/KO mice, showing irregularities in the KI/KO nuclei including an abnormal envelope contour, inclusion (arrow), accumulation of heterochromatin at the envelope and chromatin clump (*) B) quantification of abnormalities showing a significant increase in KI/KO lines (****, $p < 0.0001$; n=60 nuclei per genotype) C) single slices from confocal images of mouse muscle cleared of insoluble protein via KCl buffer, showing accumulations of insoluble BAG3 (magenta) and lamin A/C (green) in the nuclei (blue) of KI/KO mice.

Abnormalities and changes in response to tension in BAG3 P209L patient fibroblasts and BAG3 KI/KO mouse cells

To further analyze the impact of BAG3-P209L MFM on nuclear morphology, we used immortalized fibroblasts from a patient (D'Avila et al. 2016). Labeling for cytoskeletal actin and lamin A/C (Figure 2A) revealed that the patient's cells showed a significant increase in nuclear abnormalities (Fig. B-2C), including: micronuclei, blebbing, and honeycomb structures in the

NE (Fig. 2B). These nuclear changes were associated with disorganized stress fibers with large, rounded cell bodies compared to the smaller seen in controls (Fig. 2A). Similarly to the mouse muscle nuclei (Fig. 1A), nearly all patient cells displayed an increase in chromatin condensation as revealed by H3K9me3 labeling of compacted chromatin (Fig 2D).

Nuclear shape is coordinated with cell shape changes (Osorio and Gomes 2014). BAG3 MFM cells showed defects in both NE and cytoskeletal organization, suggesting that the disease variant may affect the transmission of cytoskeletal forces to the nucleus. To explore this possibility, we first sought to analyze how the nucleus of patient cells responds to changes in mechanical signals from the extracellular matrix (ECM). To do so, cells were plated on hard (collagen coated glass) and soft (matrigel, 12 kPa) substrates to test their response to changes in ECM stiffness. Remarkably, the cells carrying the P209L mutation had significantly larger nuclei than controls regardless of substrate stiffness ($p<0.0001$). While the nuclei of the control lines changed size between substrates (control 64: $p<0.0001$, control 74: $p=0.0003$), which is an expected response to ECM stiffness (Xia et al. 2019), the nuclei of patient cells showed no change in response between substrates ($p=0.49$) (Fig 2E). In cells plated on glass we also noted that despite being larger, patient cell nuclei are disproportionately smaller for their cell body size, with a low nuclear/cytoplasmic size ratio (Fig 2F; patient: 0.098 ± 0.063; control 64: 0.237 ± 0.059; control 74: 0.184 ± 0.06). Although nuclear and cell size are still well correlated (Pearson's correlation of 0.737 versus 0.776 and 0.698), the nuclear size changes were less pronounced compared to that of control cells with an increase in cell body size (Sup Fig 1A). Additionally, control cell roundness and nuclear roundness were moderately correlated (Pearson's correlation of 0.519 and 0.543), with very little correlation in patient cells (Pearson's correlation of 0.280) (Sup Fig 1B). Together these results suggest that in patient cells, nuclear shape is not responding normally to tensional forces from the cytoskeleton or the ECM.

Fibroblasts generated from mutant mouse lines also showed nuclear deformity (Sup Fig 1C). However, instead of showing an increase in nuclear size, on both substrates their nuclei became elongated with a change in aspect ratio ($p<0.05$ for all mutants on gel, KI/KO and KO/WT on glass), which is considered an abnormal finding[129,130]. The nuclei of both mutant and wildtype

lines changed size as expected between soft and hard substrates. All mutant lines also demonstrated an increase in nuclear abnormalities such as blebbing and micronuclei, similar to the human lines ($p<0.01$ for all mutant lines as compared to wildtype) (Sup Fig 1D).

To further probe whether mechanosensing is impaired in patient cells, the localization of the mechanosensitive protein YAP was examined (Fig. 2F). Typically, YAP localizes to the cytoplasm when inactive. When the cell receives a mechanical signal it translocates to the nucleus where it functions as a transcriptional co-activator(Dasgupta and McCollum 2019). As expected, control cells showed significantly less nuclear YAP on a soft gel substrate compared to hard glass ($p<0.001$), with a nuclear/cytoplasmic ratio of 2.51 ± 0.770 (control 64) and 2.245 ± 0.629 (control 74) on gel versus 5.266 ± 4.197 (control 64) and 5.07 ± 4.391 (control 74) on hard glass. Patient cells, however, did not significantly change YAP nuclear/cytoplasmic ratio between soft (1.946 ± 1.063) and hard (1.136 ± 0.923) substrates ($p=0.9234$), and had significantly less nuclear YAP compared to controls on the hard substrate ($p<0.0001$). Patient cells were not significantly different from control when plated on gel ($p>0.05$). This lack of YAP activation when on a hard surface suggests the cell is responding as if the surface is soft regardless of the actual surface rigidity, showing that mechanical response is impaired.

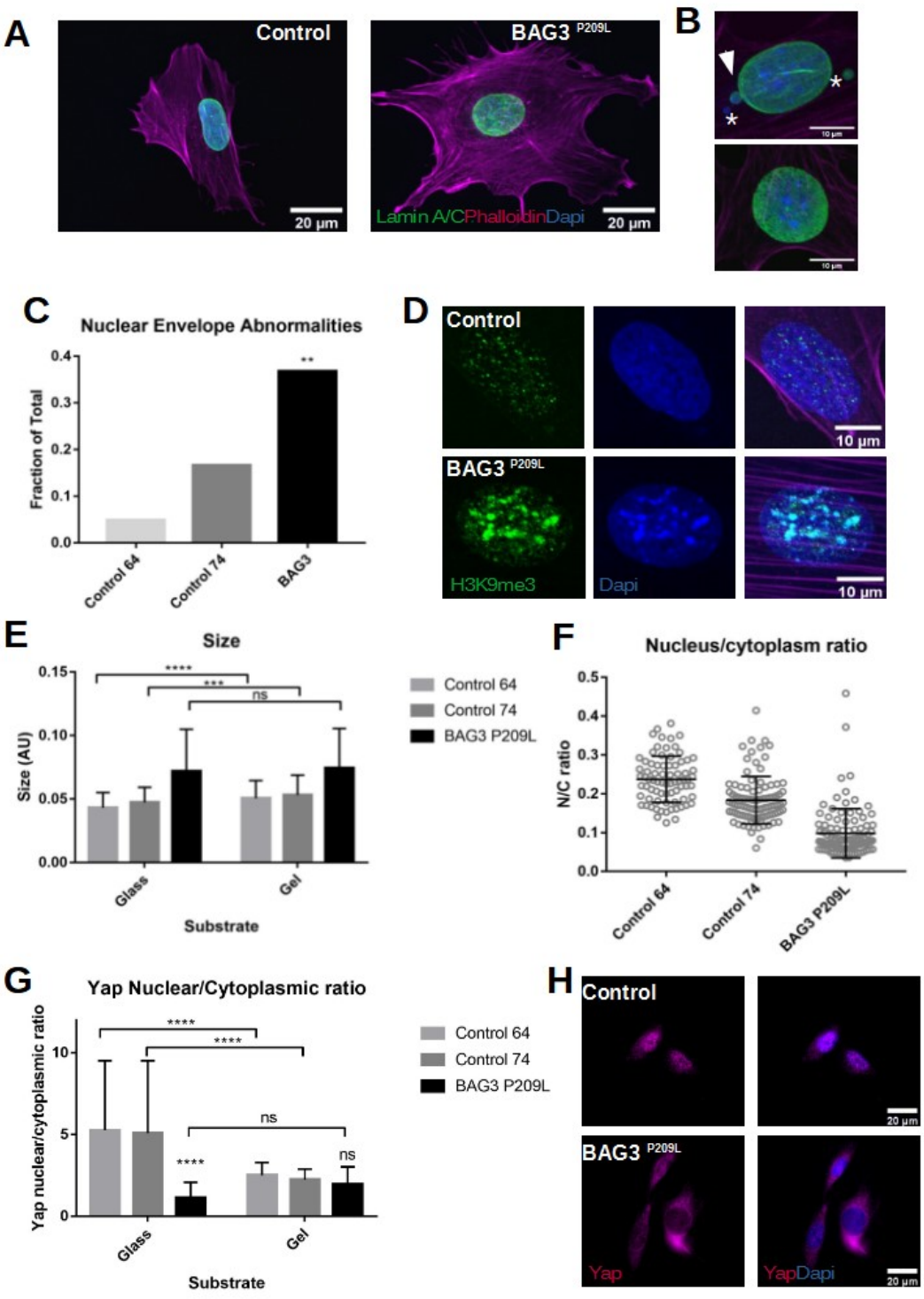

Figure 2. Changes in morphology and YAP localization in patient cells. A) Representative images of control and BAG3 P209L patient fibroblasts. B) Nuclear abnormalities: nuclei with blebbing (arrow), micronuclei (*), and nucleus demonstrating honeycombing (bottom panel)

(lamin A/C: green; phalloidin:magenta; DAPI, blue). C) Quantification of abnormalities in nuclei in patient and control lines, including: micronuclei, blebbing, honeycombing, and rupturing showing a significant increase in patient cells when compared to controls (**, $p<0.01$; $n>60$ per line). D) Representative images of H3K9me3 labeling showing an increase in condensed chromatin in patient fibroblasts. E) Comparison of nuclear size between patient and control lines, on hard glass or soft matrigel (12kPa) plates. Patient nuclei do not change in size between substrates unlike controls, but are significantly larger than controls on both substrates ($n>300$ per line). F) Nuclear/cytoplasmic size ratio, showing a disproportionately smaller nucleus in the patient line ($p<0.0001$, $n=40$ per line). G) Ratio of YAP in nucleus and cytoplasm on glass and soft gel substrate. Nuclear entry of YAP in patient lines is similar to control cells on gel, however entry does not increase on hard surfaces resulting in a significantly lower nuclear/cytoplasmic ratio than controls (****, $p < 0.0001$; $n=40$ per line). H) Representative images of YAP localization on glass. (data represented as mean ± SD)

Tension-induced cytoskeletal damage in BAG3 MFM cells is associated with reduced actin turnover

To further explore the effect of tension, patient and control cells were seeded on adhesive patterns of pre-defined geometry with patterning that was either round, which induces low tension, or rectangular, which induces higher tensions(Paul et al. 2016). Cells are confined in the pattern and forced to conform to the shape. In the lower tension round patterned coverslips, controls had primarily cortical actin that was circular in shape, following the confines of the well. In comparison, the patient cells appeared to have disorganized actin filaments (Fig 3A). When seeded on the rectangular patterning, controls again reorganized actin to follow the confines of the well while the actin filaments of the patient cells became further disorganized and often exhibited clumps of actin rather than filaments (Fig 3B), demonstrating clumping or significant disorganization in 61% of cells (n=28). The lamin A/C staining was discontinuous at the NE, and extranuclear lamin staining was frequently noted (Fig 3C). These NE defects were present in 64% of sampled BAG3 P209L cells in rectangular wells (n=28) despite not being seen in any other condition. Cells from the mice showed a similar, albeit less pronounced effect. While wildtype cells again conformed to the shape of the patterns, the KI/KO lines showed a

level of disorganization, both in round (Sup Fig 1E) and square (Sup Fig 1F) patterning, with some cells showing important deformation of the nuclear envelope.

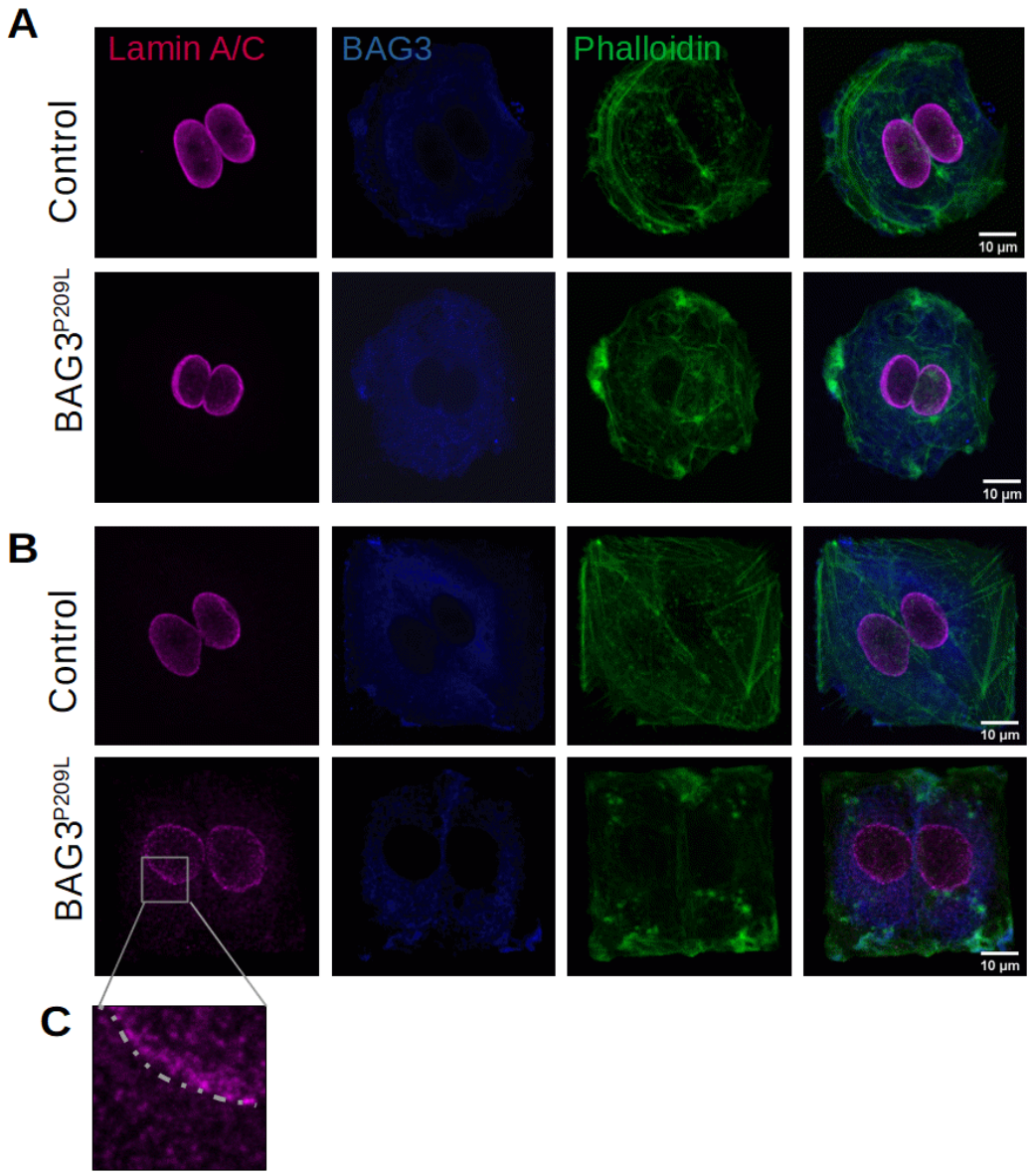

Figure 3. A defect of tension induced cytoskeletal remodeling in BAG3 P209L fibroblasts. Cells were plated on micropatterned coverslips. A) Round patterning, with control cells showing a ring of cortical actin conforming to the pattern shape and patient cells showing disorganized stress fibers with actin clumps. B) Rectangular patterning showing the stress fibers of control cells conforming to the shape of the pattern and highly disorganized and aggregated actin in the

patient cells, with a discontinuous nuclear envelope and C) extranuclear lamin (dashed line: nuclear membrane).

To assess whether there could be a defect of actin remodeling and turnover in response to tension given the tension induced damage and disorganization of the cytoskeleton, we analyzed the impact of BAG3 P209L on the turnover of actin. To measure this potential lack of turnover, Fluorescence Recovery After Photobleaching (FRAP) was performed in cells expressing EGFP-actin. Indeed, recovery was significantly impaired post-bleaching ($p<0.0001$) in patient cells (Fig 4A-B). While control cells recovered to 69±4.1% of the initial fluorescent intensity by the end of the 30s imaging period, BAG3 P209L cells had a significantly lower recovery with only 53.9±9.7% of initial intensity.

Moreover, we observed that activated myosin II (as detected by phosphorylated myosin light chain) accumulated in the perinuclear region (Fig 4C). These results suggest that BAG3 P209L variant impairs the dynamics of actomyosin structures and the ability of cells to properly respond to mechanical signals, which is in line with the defective nuclear mechanical response in these cells.

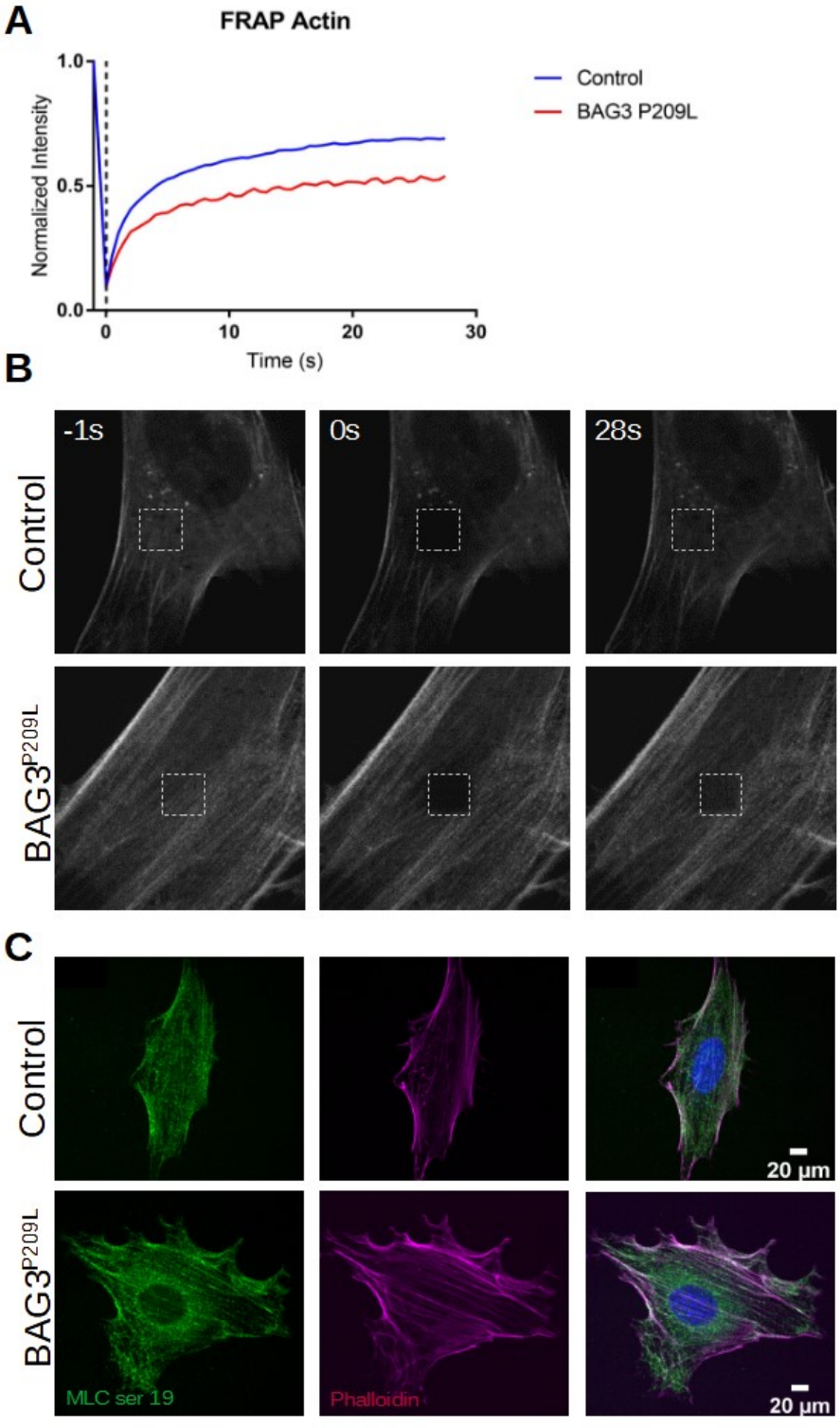

Figure 4. Disruption of actomyosin dynamics in BAG3 P209L fibroblasts. A-B) Fluorescence recovery after photobleaching of EGFP tagged actin. A) A time course of actin recovery in

BAG3 P209L cells compared to controls ($p<0.0001$). Data represented as mean normalized intensity (n=10 per line) B) Representative images of pre-bleaching (-1s), bleaching event (0s) and end of imaging (28s) showing a lack of recovery at the site of bleaching (white box) in patient cells. C) Active myosin was visualized by MLC ser19 labeling (green) in control and patient lines, showing an increased localization of myosin II to the area around the nucleus in patient cells.

Reducing actomyosin contractility alleviates the migration defect of BAG3 MFM cells

Myosin II contributes to the remodeling and turnover of actin filaments(Ideses et al. 2013). The ectopic accumulation of myosin II in the perinuclear region of patient cells, combined with poor actin turnover, could impact mechanical response in these cells. To assess whether there is impaired response, we used a wound healing assay to analyze the ability of patient cells to polarize and migrate. A wound healing assay involves creating a "wound" in a cell monolayer and tracking the movement of the cells as they fill the gap to assess migration, a process which relies on both cell-cell and cell-ECM interactions(Liang, Park, and Guan 2007).

First, we determined the polarization of the cells three hours post-scratch. While the control fibroblast lines showed evidence of polarization, as evidenced by the positioning of the golgi apparatus and lamellipodia, the BAG3 MFM fibroblasts had primarily fragmented golgi showing a lack of polarization and lacked lamellipodia extending into the wound space (Fig 5A). When tracked over a period of 6 hours, it was found that BAG3 patient cells migrated significantly slower than controls ($p=0.005$ at 5h post scratch), as measured by wound closure (Fig 5B).

Since patient cells displayed deregulated response to forces associated with ectopic accumulation of activated myosin II, we wondered whether inhibiting the action of myosin II could rescue the migration defect. As such, we treated control and patient cells with a low dose of blebbistatin (2μM), a myosin II inhibitor (Fig 5C,D). Indeed, inhibition of myosin resulted in a significantly increased rate of wound closure in the BAG3 P209L line ($p<0.0001$ at 6h), while there was no effect or a slight decrease in motility in control lines (Fig 5C). Polarity, however, did not recover after this treatment (data not shown).

Given the recovery of migration, we looked to see if mechanosignaling had increased with low dose blebbistatin treatment through assessing YAP nuclear entry (Fig 5E). While control cells either showed no change (control 74, $p>0.05$) or a reduction (control 64, $p<0.0001$) in YAP nuclear/cytoplasmic ratio, patient cells showed a significant increase with blebbistatin treatment ($p<0.0001$). This suggests that reducing myosin II activation in BAG3 patient cells leads to an increase in YAP activation and thus increasing mechanosensing.

Based on these results, we concluded that BAG3 P209L is impacting actomyosin dynamics, altering nuclear-cytoplasmic coupling and thus mechanotransduction.

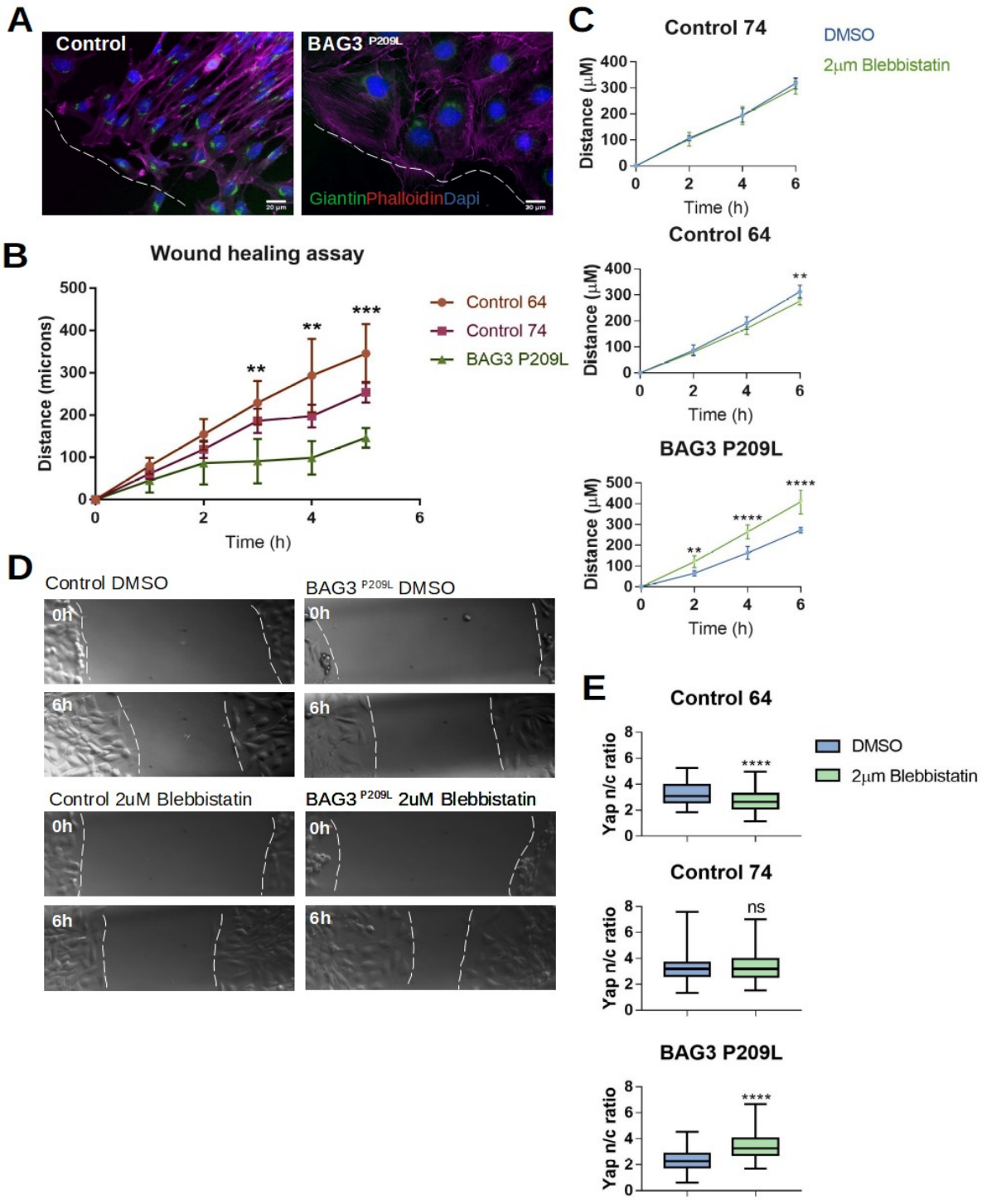

Figure 5. Decrease in migration and polarization of BAG3 P209L cells. A) Representative images of polarized cells at 3h post scratch, showing orientation and alignment of the golgi apparatus (Giantin, green) towards the wound edge (white line) in control cells, while patient

cells show fragmented golgi and no alignment. B) Wound healing assays in patient and control lines show a decrease in migration in BAG3 P209L cells compared to controls. C-D) The effect of blebbistatin treatment on control and patient cells. C) Graphs representing the cell migration time course indicating an increase in migration in patient cells. (n=6) D) Yap nuclear/cytoplasmic (N/C) ratio in cells treated with DMSO or low dose blebbistatin. Control cells either show no change or a reduction in YAP nuclear entry, while BAG3 P209L cells show a significant increase with blebbistatin treatment (n>60 per line). Data represented as mean ± SD *, $p < 0.05$; **, $p < 0.01$; ***, $p < 0.001$; ****, $p < 0.0001$.

Discussion

Here we identified mechanotransduction and nuclear mechanical response as novel cellular functions that are impaired by the BAG3 P209L variant in the context of patient cells. Transmission of mechanical signals throughout the cells appears to be impaired, resulting in reduction in migration, changes in cytoskeletal organization, tension-induced damage and lack of response to external mechanical changes or signals. The implication of BAG3 in actin and myosin dynamics(Fuchs et al. 2015; Hong et al. 2016) and NE integrity(Gupta et al. 2019) has been shown previously, however here we provide evidence that these functions are linked, impacting mechanotransduction. These structures are mechanically integrated, sending signals to each other in response to changes in mechanical stress(Stroud et al. 2014). This mechanosensing defect is associated with an increased vulnerability of the nucleus to mechanical signals, as revealed by the frequent finding of extranuclear lamin and discontinuous NE in patient cells on rectangular micropatterns. This is the first demonstration of human fibroblasts expressing the BAG3 P209L variant having a defect in mechanosensing and increased vulnerability to mechanical signals. While the exact mechanism remains to be deciphered, the BAG3-dependent regulation of mechanical coupling between the cytoskeleton and the nucleus has broad implications that are relevant to mechanically challenged tissues such as skeletal muscle.

We observed that the force-induced nuclear translocation of YAP is impaired in BAG3 MFM cells. YAP nuclear/cytoplasmic ratio remained low in BAG3 MFM fibroblasts despite changes in extracellular tension and actin-dynamics. This suggests that BAG3 MFM cells may have a mechanosensing defect reminiscent of myoblasts with *LMNA* mutations that show a paradoxical response to mechanical strain. Indeed in these cells, YAP nuclear translocation in response to forces is reduced upon cyclical strain(Bertrand et al. 2014). YAP nuclear translocation can be regulated by nuclear-cytoskeletal mechanical coupling independently of the Hippo pathway(Elosegui-Artola et al. 2017), and disruption of the LINC complex reduces YAP nuclear entry, presumably preventing the transmission of actomyosin-generated cytoskeletal tension(Elosegui-Artola et al. 2017; Driscoll et al. 2015). This has broad implications for the ability of the cell and muscle tissue at large to respond and repair after mechanically induced damage. YAP influences cell fate decisions, as well as homeostasis and regeneration in mature

tissue(Varelas 2014). It influences the expression of myogenic factors, specifically Pax7 and MyoD which induce the activation and proliferation of quiescent satellite cells(Watt et al. 2018), which may impair muscle repair and regeneration.

Our finding that BAG3 MFM cells display a reduced actin turnover is consistent with recent work supporting a role for BAG3 in the regulation of actin dynamics. Indeed, BAG3 depletion impairs mitotic actin remodeling and the assembly of a mechanically rigid actin cortex, a defect that can be alleviated by limiting actin polymerization(Fuchs et al. 2015; Luthold et al. 2020). Additionally, motility is impaired in BAG3 deficient cells due to loss of this remodelling(Fontanella et al. 2010; Iwasaki et al. 2007). We suggest that the poor turnover of actin is related to a reduction in BAG3's co-chaperoning activity and thus an impairment in BAG3's role in regulating actin dynamics and cytoskeletal organization(Fuchs et al. 2015; Fontanella et al. 2010). Both our previous work(Robertson et al. 2020) and that in zebrafish(Ruparelia et al. 2014) suggests that the pathology of BAG3 P209L results from a toxic gain of function that leads to a loss of function. As such, a loss of processing of specific client cytoskeletal proteins by BAG3 may be responsible for this impairment of actin turnover. BAG3 was reported to regulate the stability of myosin II heavy chain in skeletal muscle(Hong et al. 2016), Moreover, BAG3 was also shown to tune the mitotic activity of HDAC6, a deacetylase with several cytoskeletal targets, including myosin II(Luthold et al. 2020). We see an increase in the activation of myosin II in the perinuclear region, which may alter the tensile forces around the nucleus(Goeckeler and Wysolmerski 1995) and impair actomyosin turnover and thus the transmission of mechanical signals(Houben et al. 2007). Indeed, reducing myosin II activation increased YAP activation in patient cells, suggesting that it is contributing to the deregulation of force transmission to the nucleus. The increased accumulation of heterochromatin in mouse muscle as well as in patient lines may either be a protective response against these nearby changes in tension(Stephens, Banigan, and Marko 2019; Stephens et al. 2017), or a disorganization caused by impaired mechanosensing.

Previous work has shown that BAG3 P209L results in stalling of HSP70 chaperoning activity, including within the context of CASA, showing a toxic gain of function with aggregate formation and trapping of model client proteins(Meister-Broekema et al. 2018; Adriaenssens et

al. 2020). Previous work studying this gain of function have all involved overexpression of BAG3 P209L, making it rather difficult to interpret, as other studies have shown negative effects of overexpression of wild type BAG3(Inomata et al. 2018) and a surplus of the mutant protein may overload PQC systems. Thus, investigation within the context of the endogenous levels of BAG3 in patient cells is particularly important. Insoluble intranuclear inclusions positive for both BAG3 and lamin A/C in the absence of extensive muscle pathology implies that the previously described stalling of the HSP70 machinery and loss of PQC activity(Meister-Broekema et al. 2018) may also be occurring at the NE and results in the reduction of its stability. As such, potentially relevant targets are those that regulate the connections of LINC complex, such as myosin II, emerin and lamin A/C. Identification of the full repertoire of CASA as well as BAG3-HSPB8 clients will be required in order to decipher the mechanism behind the impairment we have described.

This work has uncovered a novel role for BAG3 in the regulation of nuclear-cytoskeletal coupling and mechanotransduction, which may explain the greater severity of BAG3 MFM in comparison to other MFMs. It also has implications for both laminopathies and muscular dystrophies which affect cytoskeletal components that are mechanically integrated with the nucleus through the LINC complex. We show a phenotypic overlap between BAG3 MFM and laminopathies, with similar nuclear abnormalities and defects in mechanotransduction. Emerging evidence shows that laminopathies are also linked to defects in the transmission and of mechanical signals and nuclear-cytoskeletal coupling, resulting in poor response to mechanical tension(Lammerding et al. 2005; Bertrand et al. 2014; Verstraeten et al. 2008). The novel findings presented here thus have implications for future work on both BAG3 MFM and laminopathies. Uncovering the mechanism behind BAG3's role in nuclear-cytoskeletal coupling and potential co-chaperoning clients in the lamin A/C-LINC-cytoskeleton signaling axis, including ones responsible for laminopathies, may provide important insight into the pathology of both.

Acknowledgements

We thank the Pigini family (Fondazione Roby) and the Bellini family (The Bellini Foundation) for inspiration and generous support; the Facility for Electron Microscopy Research (McGill University) for technical support and access to the FEI Tecnai G2 Spirit Twin 120 kV Cryo-TEM.

References

Selcen D, Muntoni F, Burton BK, et al. Mutation in BAG3 causes severe dominant childhood muscular dystrophy. Ann Neurol. 2009;65(1):83-89. doi:10.1002/ana.21553

Konersman CG, Bordini BJ, Scharer G, et al. BAG3 myofibrillar myopathy presenting with cardiomyopathy. Neuromuscul Disord NMD. 2015;25(5):418-422. doi:10.1016/j.nmd.2015.01.009

Kostera-Pruszczyk A, Suszek M, Płoski R, et al. BAG3-related myopathy, polyneuropathy and cardiomyopathy with long QT syndrome. J Muscle Res Cell Motil. 2015;36(6):423-432. doi:10.1007/s10974-015-9431-3

Noury JB, Maisonobe T, Richard P, Delague V, Malfatti E, Stojkovic T. Rigid spine syndrome associated with sensory-motor axonal neuropathy resembling Charcot–Marie-Tooth disease is characteristic of Bcl-2-associated athanogene-3 gene mutations even without cardiac involvement. Muscle Nerve. 2018;57(2):330-334. doi:10.1002/mus.25631

Schänzer A, Rupp S, Gräf S, et al. Dysregulated autophagy in restrictive cardiomyopathy due to Pro209Leu mutation in BAG3. Mol Genet Metab. 2018;123(3):388-399. doi:10.1016/j.ymgme.2018.01.001

Jaffer F, Murphy SM, Scoto M, et al. BAG3 mutations: another cause of giant axonal neuropathy. J Peripher Nerv Syst JPNS. 2012;17(2):210-216. doi:10.1111/j.1529-8027.2012.00409.x

Arndt V, Dick N, Tawo R, et al. Chaperone-Assisted Selective Autophagy Is Essential for Muscle Maintenance. Curr Biol. 2010;20(2):143-148. doi:10.1016/j.cub.2009.11.022

Homma S, Iwasaki M, Shelton GD, Engvall E, Reed JC, Takayama S. BAG3 Deficiency Results in Fulminant Myopathy and Early Lethality. Am J Pathol. 2006;169(3):761-773. doi:10.2353/ajpath.2006.060250

Youn DY, Lee DH, Lim MH, et al. Bis deficiency results in early lethality with metabolic deterioration and involution of spleen and thymus. Am J Physiol-Endocrinol Metab. 2008;295(6):E1349-E1357. doi:10.1152/ajpendo.90704.2008

Meister-Broekema M, Freilich R, Jagadeesan C, et al. Myopathy associated BAG3 mutations lead to protein aggregation by stalling Hsp70 networks. Nat Commun. 2018;9(1):5342. doi:10.1038/s41467-018-07718-5

Adriaenssens E, Tedesco B, Mediani L, et al. BAG3 Pro209 mutants associated with myopathy and neuropathy relocate chaperones of the CASA-complex to aggresomes. Sci Rep. 2020;10(1):8755. doi:10.1038/s41598-020-65664-z

Gupta MK, Gordon J, Glauser GM, et al. Lamin B is a target for selective nuclear PQC by BAG3: implication for nuclear envelopathies. Cell Death Dis. 2019;10(1):1-11. doi:10.1038/s41419-018-1255-9

Bridger JM, Foeger N, Kill IR, Herrmann H. The nuclear lamina. FEBS J. 2007;274(6):1354-1361. doi:https://doi.org/10.1111/j.1742-4658.2007.05694.x

Fuchs M, Luthold C, Guilbert SM, et al. A Role for the Chaperone Complex BAG3-HSPB8 in Actin Dynamics, Spindle Orientation and Proper Chromosome Segregation during Mitosis. PLoS Genet. 2015;11(10):e1005582. doi:10.1371/journal.pgen.1005582

Davidson PM, Lammerding J. Broken nuclei – lamins, nuclear mechanics and disease. Trends Cell Biol. 2014;24(4):247-256. doi:10.1016/j.tcb.2013.11.004

Stroud MJ, Banerjee I, Veevers J, Chen J. Linker of Nucleoskeleton and Cytoskeleton Complex Proteins in Cardiac Structure, Function, and Disease. Circ Res. 2014;114(3):538-548. doi:10.1161/CIRCRESAHA.114.301236

Crisp M, Liu Q, Roux K, et al. Coupling of the nucleus and cytoplasm. J Cell Biol. 2006;172(1):41-53. doi:10.1083/jcb.200509124

Alam SG, Zhang Q, Prasad N, et al. The mammalian LINC complex regulates genome transcriptional responses to substrate rigidity. Sci Rep. 2016;6(1):38063. doi:10.1038/srep38063

Lele TP, Dickinson RB, Gundersen GG. Mechanical principles of nuclear shaping and positioning. J Cell Biol. 2018;217(10):3330-3342. doi:10.1083/jcb.201804052

Lovett DB, Shekhar N, Nickerson JA, Roux KJ, Lele TP. Modulation of Nuclear Shape by Substrate Rigidity. Cell Mol Bioeng. 2013;6(2):230-238. doi:10.1007/s12195-013-0270-2

Lammerding J, Hsiao J, Schulze PC, Kozlov S, Stewart CL, Lee RT. Abnormal nuclear shape and impaired mechanotransduction in emerin-deficient cells. J Cell Biol. 2005;170(5):781-791. doi:10.1083/jcb.200502148

Bertrand AT, Ziaei S, Ehret C, et al. Cellular microenvironments reveal defective mechanosensing responses and elevated YAP signaling in LMNA-mutated muscle precursors. J Cell Sci. 2014;127(Pt 13):2873-2884. doi:10.1242/jcs.144907

Dasgupta I, McCollum D. Control of cellular responses to mechanical cues through YAP/TAZ regulation. J Biol Chem. 2019;294(46):17693-17706. doi:10.1074/jbc.REV119.007963
Vogel V, Sheetz M. Local force and geometry sensing regulate cell functions. Nat Rev Mol Cell Biol. 2006;7(4):265-275. doi:10.1038/nrm1890
Emery AEH. Emery–Dreifuss muscular dystrophy – a 40 year retrospective. Neuromuscul Disord. 2000;10(4):228-232. doi:10.1016/S0960-8966(00)00105-X
Ulbricht A, Eppler FJ, Tapia VE, et al. Cellular Mechanotransduction Relies on Tension-Induced and Chaperone-Assisted Autophagy. Curr Biol. 2013;23(5):430-435. doi:10.1016/j.cub.2013.01.064
Ulbricht A, Arndt V, Höhfeld J. Chaperone-assisted proteostasis is essential for mechanotransduction in mammalian cells. Commun Integr Biol. 2013;6(4):e24925. doi:10.4161/cib.24925
Selcen D. Myofibrillar myopathies. Neuromuscul Disord NMD. 2011;21(3):161-171. doi:10.1016/j.nmd.2010.12.007
Robertson R, Conte TC, Dicaire MJ, et al. BAG3P215L/KO Mice as a Model of BAG3P209L Myofibrillar Myopathy. Am J Pathol. 2020;190(3):554-562. doi:10.1016/j.ajpath.2019.11.005
D'Avila F, Meregalli M, Lupoli S, et al. Exome sequencing identifies variants in two genes encoding the LIM-proteins NRAP and FHL1 in an Italian patient with BAG3 myofibrillar myopathy. J Muscle Res Cell Motil. 2016;37(3):101-115. doi:10.1007/s10974-016-9451-7
Lochmüller H, Johns T, Shoubridge EA. Expression of the E6 and E7 genes of human papillomavirus (HPV16) extends the life span of human myoblasts. Exp Cell Res. 1999;248(1):186-193. doi:10.1006/excr.1999.4407
Rizzo MA, Davidson MW, Piston DW. Fluorescent protein tracking and detection: fluorescent protein structure and color variants. Cold Spring Harb Protoc. 2009;2009(12):pdb.top63. doi:10.1101/pdb.top63
Cory G. Scratch-Wound Assay. In: Wells CM, Parsons M, eds. Cell Migration: Developmental Methods and Protocols. Methods in Molecular Biology. Humana Press; 2011:25-30. doi:10.1007/978-1-61779-207-6_2
Calado A, Tomé FM, Brais B, et al. Nuclear inclusions in oculopharyngeal muscular dystrophy consist of poly(A) binding protein 2 aggregates which sequester poly(A) RNA. Hum Mol Genet. 2000;9(15):2321-2328. doi:10.1093/oxfordjournals.hmg.a018924

Malerba A, Klein P, Lu-Nguyen N, et al. Established PABPN1 intranuclear inclusions in OPMD muscle can be efficiently reversed by AAV-mediated knockdown and replacement of mutant expanded PABPN1. Hum Mol Genet. 2019;28(19):3301-3308. doi:10.1093/hmg/ddz167
Fluorescence Recovery After Photobleaching (FRAP) of Fluorescence Tagged Proteins in Dendritic Spines of Cultured Hippocampal Neurons | Protocol. Accessed December 6, 2021. https://www.jove.com/t/2568/fluorescence-recovery-after-photobleaching-frap-fluorescence-tagged
Virtanen P, Gommers R, Oliphant TE, et al. SciPy 1.0: fundamental algorithms for scientific computing in Python. Nat Methods. 2020;17(3):261-272. doi:10.1038/s41592-019-0686-2
Osorio DS, Gomes ER. Connecting the nucleus to the cytoskeleton for nuclear positioning and cell migration. Adv Exp Med Biol. 2014;773:505-520. doi:10.1007/978-1-4899-8032-8_23
Xia Y, Cho S, Vashisth M, Ivanovska IL, Dingal PCDP, Discher DE. Manipulating the mechanics of extracellular matrix to study effects on the nucleus and its structure. Methods San Diego Calif. 2019;157:3-14. doi:10.1016/j.ymeth.2018.12.009
Paul CD, Hung WC, Wirtz D, Konstantopoulos K. Engineered Models of Confined Cell Migration. Annu Rev Biomed Eng. 2016;18:159-180. doi:10.1146/annurev-bioeng-071114-040654
Ideses Y, Sonn-Segev A, Roichman Y, Bernheim-Groswasser A. Myosin II does it all: assembly, remodeling, and disassembly of actin networks are governed by myosin II activity. Soft Matter. 2013;9(29):7127-7137. doi:10.1039/C3SM50309G
Liang CC, Park AY, Guan JL. In vitro scratch assay: a convenient and inexpensive method for analysis of cell migration in vitro. Nat Protoc. 2007;2(2):329-333. doi:10.1038/nprot.2007.30
Hong J, Park JS, Lee H, et al. Myosin heavy chain is stabilized by BCL-2 interacting cell death suppressor (BIS) in skeletal muscle. Exp Mol Med. 2016;48(4):e225-e225. doi:10.1038/emm.2016.2
Elosegui-Artola A, Andreu I, Beedle AEM, et al. Force Triggers YAP Nuclear Entry by Regulating Transport across Nuclear Pores. Cell. 2017;171(6):1397-1410.e14. doi:10.1016/j.cell.2017.10.008
Driscoll TP, Cosgrove BD, Heo SJ, Shurden ZE, Mauck RL. Cytoskeletal to Nuclear Strain Transfer Regulates YAP Signaling in Mesenchymal Stem Cells. Biophys J. 2015;108(12):2783-2793. doi:10.1016/j.bpj.2015.05.010

Varelas X. The Hippo pathway effectors TAZ and YAP in development, homeostasis and disease. Development. 2014;141(8):1614-1626. doi:10.1242/dev.102376
Watt KI, Goodman CA, Hornberger TA, Gregorevic P. The Hippo Signaling Pathway in the Regulation of Skeletal Muscle Mass and Function. Exerc Sport Sci Rev. 2018;46(2):92-96. doi:10.1249/JES.0000000000000142
Judson RN, Gray SR, Walker C, et al. Constitutive Expression of Yes-Associated Protein (Yap) in Adult Skeletal Muscle Fibres Induces Muscle Atrophy and Myopathy. PLOS ONE. 2013;8(3):e59622. doi:10.1371/journal.pone.0059622
Judson RN, Tremblay AM, Knopp P, et al. The Hippo pathway member Yap plays a key role in influencing fate decisions in muscle satellite cells. J Cell Sci. 2012;125(24):6009-6019. doi:10.1242/jcs.109546
Luthold C, Varlet AA, Lambert H, Bordeleau F, Lavoie JN. Chaperone-Assisted Mitotic Actin Remodeling by BAG3 and HSPB8 Involves the Deacetylase HDAC6 and Its Substrate Cortactin. Int J Mol Sci. 2020;22(1). doi:10.3390/ijms22010142
Fontanella B, Birolo L, Infusini G, et al. The co-chaperone BAG3 interacts with the cytosolic chaperonin CCT: New hints for actin folding. Int J Biochem Cell Biol. 2010;42(5):641-650. doi:10.1016/j.biocel.2009.12.008
Iwasaki M, Homma S, Hishiya A, Dolezal SJ, Reed JC, Takayama S. BAG3 Regulates Motility and Adhesion of Epithelial Cancer Cells. Cancer Res. 2007;67(21):10252-10259. doi:10.1158/0008-5472.CAN-07-0618
Ruparelia AA, Oorschot V, Vaz R, Ramm G, Bryson-Richardson RJ. Zebrafish models of BAG3 myofibrillar myopathy suggest a toxic gain of function leading to BAG3 insufficiency. Acta Neuropathol (Berl). 2014;128(6):821-833. doi:10.1007/s00401-014-1344-5
Goeckeler ZM, Wysolmerski RB. Myosin light chain kinase-regulated endothelial cell contraction: the relationship between isometric tension, actin polymerization, and myosin phosphorylation. J Cell Biol. 1995;130(3):613-627. doi:10.1083/jcb.130.3.613
Houben F, Ramaekers FCS, Snoeckx LHEH, Broers JLV. Role of nuclear lamina-cytoskeleton interactions in the maintenance of cellular strength. Biochim Biophys Acta BBA - Mol Cell Res. 2007;1773(5):675-686. doi:10.1016/j.bbamcr.2006.09.018
Stephens AD, Banigan EJ, Marko JF. Chromatin's physical properties shape the nucleus and its functions. Curr Opin Cell Biol. 2019;58:76-84. doi:10.1016/j.ceb.2019.02.006

Stephens AD, Banigan EJ, Adam SA, Goldman RD, Marko JF. Chromatin and lamin A determine two different mechanical response regimes of the cell nucleus. Mol Biol Cell. 2017;28(14):1984-1996. doi:10.1091/mbc.e16-09-0653

Inomata Y, Nagasaka S, Miyate K, et al. Bcl-2-associated athanogene 3 (BAG3) is an enhancer of small heat shock protein turnover via activation of autophagy in the heart. Biochem Biophys Res Commun. 2018;496(4):1141-1147. doi:10.1016/j.bbrc.2018.01.158

Verstraeten VLRM, Ji JY, Cummings KS, Lee RT, Lammerding J. Increased mechanosensitivity and nuclear stiffness in Hutchinson–Gilford progeria cells: effects of farnesyltransferase inhibitors. Aging Cell. 2008;7(3):383-393. doi:10.1111/j.1474-9726.2008.00382.x

Supplementary data

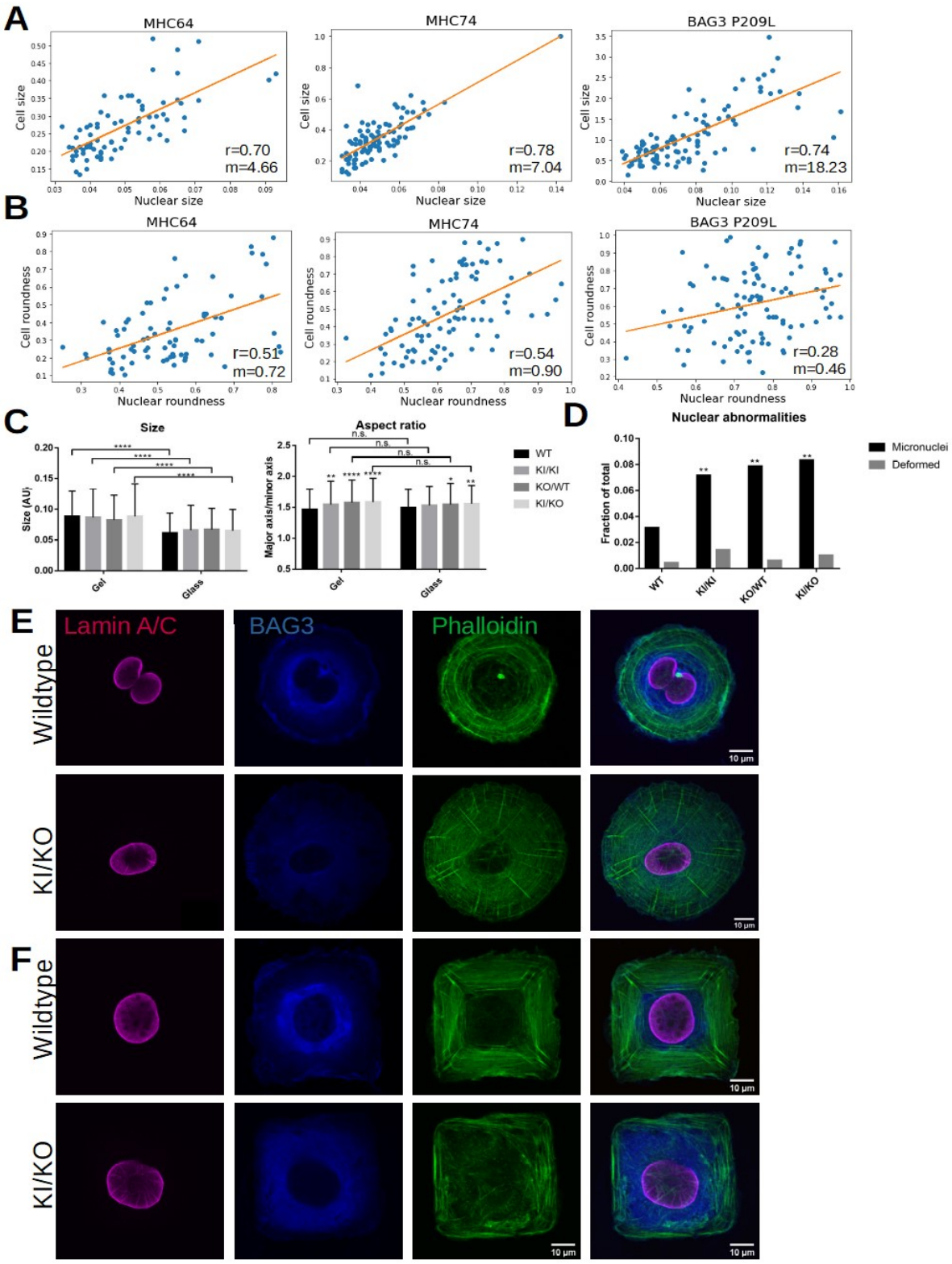

Supplemental Figure 1. Changes in nuclear morphology and defective tension induced actin remodeling in KI/KO mouse cells. A) Relationship between cell size and nuclear size in control and patient fibroblasts, showing good correlation but a large change in slope (m) in patient cells compared to controls, implying the nuclear size does not increase at the same rate as in control cells with an increase in cell body size B) Relationship between nuclear roundness and cell roundness, showing a moderate correlation in control lines and low correlation in the patient cell lines. C) Size and aspect ratio changes of mouse fibroblast nuclei on hard glass or soft matrigel (12 kPa) plates, showing that the nuclei change size as expected in all lines, however the nuclear aspect ratio has increased in all mutant lines compared to wildtype (WT), indicating elongation of the nuclei (n=400 per line). D) Abnormalities in mouse fibroblast lines, showing an increase in micronuclei in mutant lines as compared to wildtype controls (n=400 per line). Micropatterned coverslips with E)round and F)square patterns, showing changes in cytoskeletal organization in KI/KO

CHAPTER 4: General discussion

4.1 Summary

The goal of this thesis was to create and characterize a mouse model of BAG3 MFM, as well as to explore the pathophysiology of this disease. This study contributes to the neuromuscular field by putting forth a murine model of the disease with both full-body expression of the mutant protein and a measurable phenotype, something not previously accomplished.

In **chapter 2** we described the characterization of the mouse model. This model carries a P215L knock-in and a knock-out mutation, developing a phenotype that is more severe than that of mice carrying a knock-in mutation alone. In **chapter 3**, we describe a novel nuclear phenotype in BAG3 MFM, as well as defective cellular response to tension related to changes in actomyosin dynamics.

4.2 Models of BAG3 myofibrillar myopathy

4.2.1 Limitations of mouse models of degenerative muscle disease

Mice, while a convenient model to use due to their size and fast reproductive cycle, are not always perfect models of human disease. Numerous successful models of muscle disease have been produced using mice, such as that of R120G αB-crystallin myopathy[131] ; a model of limb-girdle muscular dystrophy type 1A[132] and SMA, for which multiple successful models have been developed and used in therapeutic testing[133]. Many mouse models of muscular dystrophy, however, do not exhibit a phenotype until late in life[98] or, in the case of the well-known mdx mice, show little phenotype[134] in contrast with the relatively severe phenotype seen in human patients. Previous attempts to model BAG3 MFM in mice have had limited success, with a previous mP215L KI/KI showing no phenotype[97]. Our KI/KO model of BAG3 MFM does demonstrate a phenotype, likely representing an early stage of the disease.

The KI/KO line has a number of advantages but also some limitations as a model. A major disadvantage is that they display a very mild phenotype compared to the high severity and early onset seen in humans. In terms of behavioural phenotyping, they only show a reduction in voluntary movement, and their strength and fatigue levels appear otherwise normal. Unfortunately, this makes them a poor model for candidate molecule testing unless a stressor such as exercise can be used to produce measurable defects and to detect pathological changes the mouse must be sacrificed for analysis using methods such as histology.

This discrepancy in phenotype often comes from the differences in size and tension of their respective muscle, which may be an important factor in model development in BAG3 MFM. As relative muscle length increases there is greater stress put on the muscle, as the relationship between the size and stress is not a linear one[135,136]. Due to this, it becomes more difficult for larger muscles to handle force and morphological changes such as thicker tendons and more fibrous septa results[9]. Regeneration is also an easier feat in mouse muscle due to its decreased size. While myoblasts proliferate and move at a similar pace in mice and humans, the increased size of human muscle fibers can make for a longer journey, and thus slower recovery[9] . These factors can make the creation of a mouse model for degenerative muscle disease difficult.

If damage in BAG3 MFM comes from failure to repair after damage due to mechanical stress, then this lower stress would mean less opportunity for the toxic aggregations to form as the CASA complex assembles with cargo and stalls. As shown in our *in vitro* work, tension appears to heavily influence the severity of the phenotype in patient cells, and reducing tension associated with actomyosin complexes ameliorates some of the phenotype. Our heterozygous knock-in mice, which have the same genotype as patients, have virtually no phenotype and our homozygous knock-ins have very little. This was also seen in a previously published model which had the mP215L mutation[97]. Despite this site being highly conserved in animals[1], clearly the effect of this mutation is not sufficient to produce a strong phenotype in mice, either due to the aforementioned physiological differences or another compensatory mechanism not present in humans.

4.2.2 Use of murine and patient derived fibroblasts as a model

Despite BAG3 MFM primarily being a disease of skeletal muscle, cardiac muscle and peripheral nerve, we have used fibroblasts as our cellular model. While there are disadvantages to using a non myogenic cell type to study a disease that affects the muscle, this is still an informative model. We hypothesize that, like in many laminopathies, the primarily skeletal muscle phenotype is due to the increased mechanical stress in this tissue, posing a greater need for the NE to both resist damage and transmit mechanical signals[21]. Indeed, fibroblasts are commonly used to study laminopathies with success for this reason[106,117,122,124]. It is possible to modulate the amount of tension the cells are subject to with greater ease than in a tissue, as we have done through the use of substrates of different stiffness and micropatterned plates. Through this we have been able to show the impact of tension on the phenotype in our fibroblast model and we observe a distinct, measurable phenotype in these cells that is distinct from control lines.

The major disadvantage of using fibroblasts is the inability to explore the effect on myogenesis. BAG3 appears to play a role in mitosis[53], as well as ensuring cell survival during myogenesis[90] and modulating myogenin expression which is important for the end stages of myogenesis. Proper assembly of the muscle Z-disk is also reliant on BAG3, including proper

capping of actin with CapZ[55,79]. It is probable then that this process is affected in BAG3 MFM, however, we cannot directly study how it affects this process, only extrapolate from our data on fibroblasts. While they share many similar characteristics, and fibroblasts can be differentiated into myogenic or myoblast-like cells under the correct conditions[137], they still cannot differentiate to form myotubes. A myoblast cell line would have to be generated for this to be possible.

The use of murine fibroblast lines also has its own advantages and disadvantages. These lines are practically isogenic, from mice with the same genetic background, eliminating some of the interindividual variability seen with our human lines. They are certainly easier to obtain than murine myoblasts, with less need for specialized equipment or the use of very young mice[138]. They only survive for a limited number of passages and cannot be immortalized except in the case of spontaneous immortalization[139]. In our hands by passage four these cells begin to differentiate into something more epithelial-like, changing their morphology and necessitating that they be used quickly after isolation.

There are also inherent disadvantages to using patient lines. The first most obvious issue is that we only have access to one patient line, limiting our statistical power to identify differences between patients and controls and necessitating that we use other models to confirm our findings. While they are still useful tools, coming from patients who have a well documented phenotype, differences in genetic background between patient and control lines can have a major impact on gene expression and result in increased variability between lines. Indeed, the control lines often vary significantly from each other, thus necessitating the use of more than one so that inter-individual variability is not mistaken for pathological changes. The differences in the patient bearing the BAG3 P209L variant are fortunately often stark and very clearly pathological, strongly suggesting that they are biologically meaningful, however we had to show caution when interpreting less overt changes. While we have supporting data from the mouse lines, the ideal control in this scenario would have been an isogenic control line.

4.3 Insights from the mouse model

4. 3. 1 BAG3 P209L: a toxic gain of function leading to loss of function

The nature of the P209L mutation has been extensively investigated. Despite being present at one of the IPV domains, its impact on the binding of small heat shock proteins is not significantly reduced; instead it causes a conformational change which causes the protein to become more hydrophobic, inducing the formation of non-native oligomers and stalling the CASA complex[78,81]. There is some disagreement about whether this causes an increase in BAG3 due to its accumulation, or a loss of it as it is no longer available to function. Two other groups have taken the overexpression approach to modeling this disease[95,140], while we opted for a model which is haploinsufficient for the mutant protein (KI/KO).

We propose that by reducing the overall level of the mutant protein, we mimic disease progression in humans by reducing the amount of available, functional BAG3. The P209L mutation indeed results in a partially functional protein, despite stalling of the CASA complex, as in a zebrafish model the mutant protein can partially rescue the myofibrillar disintegration phenotype caused by knocking out BAG3[80]. It is not a true loss of function mutation, as simply reducing the level of BAG3 does not result in the same phenotype as BAG3 MFM. Our KO/WT mice do not develop characteristic aggregates nor a loss in fiber size as the mice that carry a knock-in allele (KI/KO) do. They also lack the molecular changes seen in animals with P215L knock-in alleles (KI/KI, KI/KO)[4]. Knock-down fish models, which develop an impaired swimming phenotype, also lack aggregates which those expressing the mutant protein do develop[80]. Additionally, haploinsufficient humans only develop cardiac issues, specifically dilated cardiomyopathy typically with late onset[141] . Likewise, mice models which are either haploinsufficient for the protein or carry knockdown mutations only have cardiac symptoms[86,92] .

The mutated protein is semi functional as well, as its overexpression is able to rescue a knockout fiber[80]. BAG3 P209L is able to form the full CASA complex, however its rate of cycling at the ATPase domain is significantly slowed, thus causing the aggregate pathology[78]. Our mice who are homozygous for the murine version of the mutation, mP215L, do not show significant defects in the muscle despite showing some similarities to the KI/KO model in terms of fiber size defect and molecular changes. Similarly, phenotypic assessment of the heart of mice

with KI/KI mP215L mutation showed no phenotype[97]. This shows that the MFM phenotype we see in our KI/KO is not due to either haploinsufficiency or the mP215L mutation alone but the combination of the two. This supports the hypothesis that BAG3 P209L MFM is a toxic gain of function variant which leads to a loss of function.

Two other models of BAG3 myofibrillar myopathy have been published since the beginning of this work, both using transgenic animals which overexpress the human version of the protein[95,140]. One is cardiomyocyte specific, leading to the development of significant systolic and diastolic dysfunction, as well as dilation, by eight months of age. This, however, did not lead to congestive heart failure, nor the restrictive cardiomyopathy or aggregation typically seen in patients[95]. The second model, published after ours, used the same strategy however expression was more broadly within striated muscle cells. This model resulted in restrictive cardiomyopathy with prominent fibrosis, aggregate formation and z-disk disruption within just 1-2 months of life[140], closer mimicking the patient phenotype. While these indeed produce a more severe phenotype than in our KI/KO mice, there are questions about how increasing autophagy through overexpression may diverge from the human disease which is thought to be related to stalling of autophagy[78]. Overexpressing the wildtype human form of the protein can cause a heart phenotype, specifically fractional shortening and an increase in atrial natriuretic peptide within one model[96]. This is due to an increase in autophagy as seen in the increased turnover of small heat shock proteins[96], which typically do not turnover properly in BAG3 MFM due to increased stabilization[67]. While this was controlled for in one paper with control lines expressing the wildtype human version[140], the other did not[95]. In this aspect our KI/KO model may better reflect the conditions seen in patients, in which an increase in autophagy has not been reported.

Ultimately, as this is a gain of function leading to loss of function, BAG3 MFM has features of both a loss of the protein and too much of the protein. BAG3 P209L's autophagic function is diminished due to the stalling of its co-chaperoning activity, but the protein is still present and is responsible for increased stabilization of small heat shock proteins[67] and perhaps MHC[142].

4.3.2 Could the KI/KO line represent an early stage of disease?

While it is difficult to use our murine model to study the later stages of disease due to its mild phenotype, it may represent the earlier stages, which are poorly documented in patients due to the rapid onset of disease. Only a few documented patients have had mild skeletal muscle phenotypes, and these patients were atypical examples of the disease that were more reminiscent of Charcot-Marie-Tooth disease[74,75]. In a highly disrupted tissue, such as the skeletal muscle of BAG3 MFM patients, it is difficult to determine if some of the pathology seen is a primary or secondary effect of the disease. The KI/KO mice, which have a mild phenotype, could thus represent an early stage of the disease before the accumulation of damage has caused large-scale breakdown of the muscle.

In the mice, we see that there is significant fiber atrophy in all fiber types, even in the absence of extensive damage to the fiber. This suggests that atrophy may proceed the disintegration of the sarcomeres, suggesting it is not the accumulation of damage that leads to atrophy, although we are unable to do more than speculate as to the cause at this time. We also see early changes to the mitochondria. There is a significant accumulation of mitochondria in the mouse muscles, as well as the presence of abnormal mitochondria such as megamitochondria. It remains to be seen whether this is a primary effect, perhaps due to BAG3's role in mitophagy[143], or due to changes to respiratory chain insufficiencies and the mtDNA damage that occurs in many MFMs[144]. It is rare, however, to see an increase in ragged red fibers in MFMs, although it is sometimes seen in MFMs caused by filamin mutations, a major client of BAG3[145]. In patients with advanced BAG3 MFM we see aggregations of mitochondria[1], however ragged red fibers have not been noted, so care should be taken when investigating this to ensure relevance to the human disease.

4.4 Implications of defects in tension response

4.4.1 The complicated connections between nucleus and cytoskeleton

In Chapter 3, we showed that there are changes in nuclear and actomyosin dynamics that contribute to the cell's inability to respond to changes in tension, both from the ECM and

intracellularly. The nucleus and cytoskeleton are mechanically integrated, sending signals to each other in response to changes in mechanical stress[146]. It is apparent that BAG3 is important in the maintenance of both cytoskeleton and nuclear envelope as well as their coupling, which means that damage caused by impaired PQC likely occurs in tandem to both. We hypothesize that this is followed by a cycle of continued dysfunction as aberrant cytoskeletal organization and turnover leads to changes in tension within the cell. This affects the nucleus through changes in tension, and this leads to damage and poor initiation of repair and aberrant signaling, leading to further cytoskeletal disorganization. Proteins of the nuclear envelope such as lamins and emerin have been shown to impact both the quantity and organization of stress fibers, with their loss creating more stress fibers and displacing nuclear actin[147]. We see that, as we reduce myosin II activation we increase YAP activation in patient cells, while the control fibroblasts either do not change or decrease activation. This would imply that the signals reaching the nucleus through the LINC complex from the cytoskeleton are aberrant, and this is in relation to changes in actomyson dynamics.

4.4.2 The role of myosin in BAG3 myofibrillar myopathy

Our work has shown that myosin appears to be a player in the pathophysiology of BAG3 MFM. While we have not determined why there is a change in myosin activation, there are two potential causes. The first is increased stabilization of myosin by BAG3. MHC has been shown to be stabilized by BAG3, and a loss of BAG3 suppresses MHC levels through increased ubiquitination and degradation[142]. Non-muscle myosin II plays an important role in the formation and organization of stress fibers, particularly the ventral stress fibers residing under the nucleus and transverse arcs, which are curved bundles in the lamellae[148,149]. We see an increase in the activation of myosin II around the nucleus, as well as an increase in the amount of stress fibers in the transverse arcs and an apparent disorganization of them. If myosin II activation is increased through the phosphorylation of myosin light chain, this would increase the tensile forces within the cell[150]. These tensile forces in the cell must be balanced in order to resist mechanical forces without inducing excess internal forces, as well as for the correct transmission of mechanical signals[151]. The increase of tensile forces caused by excess myosin and associated stress fibers

could mean impaired mechanosensing, as we see with the change in YAP localization, and an increase in mechanical damage within the cell, which may be leading to an increase in misfolded proteins that must be turned over. The rescue of the migration phenotype that we see during blebbistatin treatment in the patient lines supports this idea.

A role for myosin in BAG3 MFM is particularly important in the context of muscle. While actomyosin bundles become stress fibers in non-muscle cells, they make up the contractile apparatus of sarcomeres in the mature muscle which is capable of generating large amounts of force. Dysregulation of the activation of myosin could lead to damaging changes in tension, increasing the burden upon BAG3 and the CASA complex, further driving the damage seen in BAG3 MFM.

4.4.3 An impact on satellite cell activation?

Of particular pertinence to skeletal muscle is how repair and myogenesis may be affected by a defect in mechanotransduction. The muscle stem cells, known as satellite cells, typically sit quiescent at the basal lamina of the mature skeletal muscle until they are activated. After activation, they first begin a cycle of self-renewal, giving rise to myoblasts which then go through asymmetrical division. One of these daughter cells returns to quiescence, while the other proceeds through myogenesis. They can be activated through a variety of cues, the most important of which for this discussion is mechanical cues such as disruption of the muscle fiber and exercise[152,153]. YAP, a mechanosensitive transcriptional co-activator[108] that we have shown to have reduced activation in BAG3 MFM, is a regulator of the initiation of myogenesis and muscle homeostasis. In regulating myogenesis both its activation and subsequent deactivation are important for successfully progressing through differentiation[154]. YAP's activation leads to the expression of Pax7 and MyoD, activating quiescent satellite cells and causing their proliferation; however, constitutive activation of YAP prevents these cells from progressing past this self-renewal process and proceeding through differentiation[114]. This leads to atrophy and myopathy in mice with a non-phosphorylatable form of the protein[155]. The impairment in mechanotransduction and alterations in YAP activation that we have shown in BAG3 MFM would likely therefore have implications for satellite cell activation and proliferation in the

muscle of patients. A reduction in YAP activation may lead to poor satellite cell activation after stretch injury, affecting recovery and potentially resulting in the fiber atrophy we see, as well as segmental loss due to poor repair.

In DMD models, impairment of satellite cell function has been a subject of interest. Similarly to BAG3 MFM, this may be a two-fold issue involving failure of both PQC and mechanotransduction. Dystrophin physically links the intermediate filaments of muscle to the sarcolemma, and as the disease progresses there is a progressive loss of autophagic activity which coincides with the exhaustion of satellite-cell mediated regeneration of damaged muscle[156]. The satellite cells in these models fail to correctly polarize, showing impaired mitotic spindle orientation and delayed mitosis[157]. A reduction in active YAP is also present in muscle biopsies from DMD patients, with both less overall YAP and less YAP nuclear entry, preventing transcription of YAP-mediated targets such as myogenic factors[158]. A similar issue may arise in BAG3 MFM given the alteration in YAP localization, and as such this should be a future area of study.

4.4.4 An impact on myogenesis?

Once activated, satellite cells must differentiate into myoblasts which then fuse to form multinucleated myotubes. Careful modulation of tension is required not only for activation of satellite cells but for myogenic progenitors to differentiate and eventually form mature muscle[114,159,160]. Additionally, careful organization and alignment of the cytoskeleton of myoblasts is important for this process to be successful[161,162]. Stress fibers must successfully align to the long axis of the cells, and the cells themselves must align to each other for end-to-end fusion and the formation of myotubes. Tight control of the activation of myosin II, as well as levels of RhoA which modulates its activation, is important to the proper formation of adult skeletal muscle, controlling the timing of fusion and their bipolar alignment[163]. BAG3 controls MHC stabilization independently of the expression of myogenic factors during differentiation, and a loss of BAG3 results in muscle wasting and loss of myotube diameter[142]. Disruption of cytoskeletal organization, myosin activation and mechanotransduction in BAG3 MFM would then likely result in impaired differentiation of myogenic precursors, impairing myogenesis.

4.5 Relevance to other diseases and insights into the treatment of BAG3 MFM

4.5.1 Laminopathies

Our work has shown previously unexplored overlap between laminopathies and BAG3 MFM. We see nuclear changes more typical of laminopathies than traditional MFMs, such as wrinkling of the membrane, changes in chromatin dynamics and NE honeycombing; as well as evidence of poor stability of the envelope, particularly under tension. While we cannot exclude the cytoskeletal defects as a contributor to these abnormalities, it seems that the nucleus is not able to compensate adequately for this implying that there is an inherent weakness in the NE. This, as well as previously published work[128], suggests that BAG3 is important in the maintenance of the NE. Our work also suggests that there may be phenotypic and mechanistic overlap between laminopathies and BAG3 MFM. While EDMD is not a severe or early onset disease like BAG3 MFM, if BAG3 MFM has both NE and cytoskeletal pathophysiology and an impairment in the relationship between the two this could explain its severity compared to other MFMs. NE maintenance by BAG3 could also be a subject of interest in laminopathies, particularly those in which there is a disorganization or excess of NE proteins where modulating their turnover may improve pathological phenotypes.

4.5.2 Muscular dystrophies involving structural proteins

Our findings in BAG3 MFM have implications for other types of myopathies. While the study of the role of mechanosensing in many diseases outside of laminopathies[164] is in its infancy, with the field of mechanobiology emerging in the last decade and a half[165], the connection between mutations to sarcomeric proteins and defective mechanosensing has been made[62,166,167]. The mechanical integration of nucleus, cytoskeleton and the integrins which interact with the ECM most certainly mean that pathologies which affect structures within this group may have defects of mechanotransduction. While we have shown a nuclear phenotype in BAG3 MFM, the most severe aspect of this disease remains its impact on the structural integrity of the contractile apparatus, which is likely contributing to the nuclear phenotype. By addressing the cytoskeletal defects alone through the inhibition of myosin, we show an improvement in

mechanosensing and cell migration, demonstrating how cytoskeletal defects can cause issues with tension within the cell that affect mechanosensing and the nucleus.

4.5.3 Treatment of BAG3 myofibrillar myopathy

There are still no effective treatments available for BAG3 MFM, despite the work done to elucidate the mechanism of disease. It is a complicated pathology, and therapeutic strategies being proposed for other myopathies may not be applicable here. The BAG3 P209L protein is prone to aggregation, meaning that the gene editing solutions in mature muscle used in myopathies such as in DMD[168], in which even a small restoration of the protein is effective, may not be as effective here. Reducing the mutant protein without completely knocking it out, something not feasible with current technologies, would likely still result in the toxic aggregation and segmental loss. Increasing the levels of wildtype version does not address the aggregation issue as wildtype BAG3 is also sequestered in the toxic aggregates[80], and overexpression of BAG3 on its own may lead to damaging effects[96]. Despite using blebbistatin with some success in the cell lines, use of this drug *in vivo* is not ideal due to both its poor solubility and stability and off-target toxicity[169]. While analogues are in development, it remains to be seen how drugs in this category may perform *in vivo* due to these limitations.

Work done in the lab of Dr. Robert Bryson-Richardson has suggested that metformin may be a potential treatment, having published work on it in zebrafish and human myoblasts[170] showing that it cleared much of the aggregates and improved the fiber disintegration and swimming phenotype in the fish. Metformin has been proposed as a potential treatment for a variety of myopathies, including DMD[171] and CMD[172], although it has never made it past clinical trials. Metformin acts through its effects on AMPK, an energy sensing protein that regulates metabolism to maintain energy homeostasis[173]. Metformin inhibits complex I of the mitochondrial respiratory chain[174], which alters the AMP/ATP ratio, activating AMPK. This activation can result in a variety of physiological changes, including the activation of autophagy through the phosphorylation and thus activation of ULK1[175]. Metformin has been shown to have protective effects in muscle[176] and heart tissue[177]. This broad upregulation of autophagy, which is independent of BAG3, may compensate for the impairment of chaperone assisted selective

autophagy in the muscle of BAG3 P209L patients and our animal models. It does not address the loss of some of BAG3's functions outside of CASA, such as transcriptional regulation under stress[126], regulation of actin capping and dynamics[53–55], and motility and adhesion regulation[178]. So, while metformin would address the most pressing issue, the failure of PQC, it is not a cure.

If indeed there is a defect in satellite cell activation and myogenesis, that could present a possible therapeutic target. Repairing the mutation in satellite cell derived myoblasts from patients and grafting them back into patient tissue, while still experimental, could allow for more efficient repair of the muscle and possibly the formation of "normal" myofibers. This kind of therapy has been a subject of interest in recent years and has shown promise in mouse and primate studies, although a number of hurdles remain before it can move to humans, such as the issue of graft rejection and whether it can restore fibrotic and badly degenerated tissue[179].

Figures

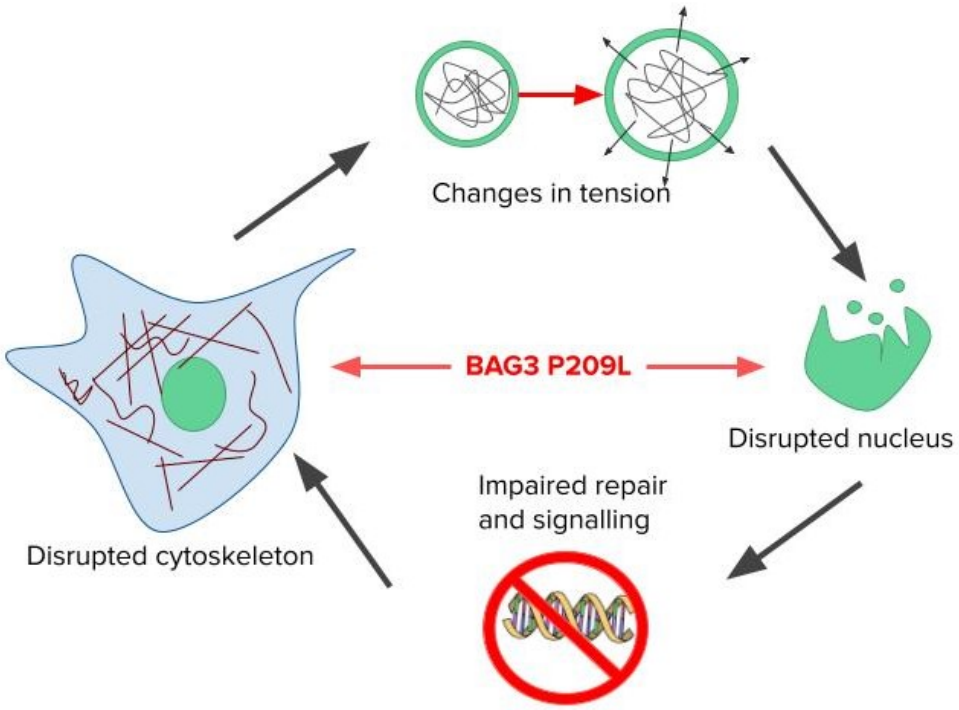

Figure 4.1 Proposed mechanism of damage due to defects in nuclear-cytoskeletal coupling due to the BAG3 P209L mutation. BAG3 P209L negatively impacts the cytoskeleton, nucleus and the

connection between them due to failures in protein quality control and changes in actomyosin and nuclear dynamics. This causes cyclical damage due to changes in the transmission of tension within the cell, contributing to further disorganization and damage; and a hampering of the cells ability to respond to mechanical signals.

CHAPTER 5: Conclusion and Future Directions

5.1 Conclusion

BAG3 MFM is a severe disease with a complicated pathophysiology due to the many roles of BAG3. Identifying novel aspects of this pathophysiology can help us understand the mechanisms behind them and identify novel therapeutic targets. We have developed and characterized a murine model of BAG3 MFM which can be used to further explore the pathophysiology of BAG3 MFM, and if the phenotype can be modulated by additional stress then perhaps useful for candidate molecule testing for the treatment of BAG3 MFM. This model revealed nuclear abnormalities, which we further explored in fibroblast lines from both the mice and a patient bearing the P209L mutation. Through this we were able to show a novel aspect of the pathophysiology of BAG3 MFM involving the NE and mechanotransduction. We showed that these cells respond poorly to changes in ECM tension, not modulating NE size and cytoskeletal organization as expected nor migrating. We showed that there is a change in tension within the cell, and reducing that tension through the inhibition of myosin can reduce some of its negative impacts on mechanosensing. Altogether, our findings provide additional insight into and understanding of the pathophysiology of BAG3 MFM, a severe childhood MFM without cure. We also show that there may be unexplored overlaps between laminopathies and muscular dystrophies which affect proteins that are mechanically integrated with the nucleus.

5.2 Future directions

There are a number of unresolved questions concerning the specific nature of the tension related defect in BAG3 MFM, as well as how exactly the nuclear-cytoplasmic coupling is impaired beyond a likely PQC issue. Here we have studied the effect of the defect in mechanotransduction, but the molecular basis of it has not been determined. It would be of interest both for BAG3 MFM and laminopathies to investigate whether members of the lamin A/C-LINC-cytoskeleton signaling axis potential are co-chaperoning clients of BAG3, determined through immunoprecipitation or 2D electrophoresis, and whether they are components of the

insoluble aggregates in BAG3 MFM through separating protein lysates into soluble and insoluble fractions. It would also be of interest to study the mechanistic properties of the nucleus in BAG3 MFM. We cannot say with certainty whether there is a stiffening or lack of tension at the envelope. Progeroid syndromes, which cause increased stiffening[124] and EDMD, which causes a loss of stiffness[115], frequently show overlapping phenotypes. While we would assume there is an increase in stiffness in the cytoskeleton, we were not able to directly mechanistically show this because of technical limitations. A crucial step in studying the impact of these defects would be to determine how satellite cell activation and myogenesis is impacted in BAG3 MFM. Profiling the population of myogenic precursor cells both in a resting state as well as in damaged muscle in a model of BAG3 MFM, ideally due to stretch injury, may help give insight into the pathophysiology of this disease including help to explain its severity, as well as potentially providing a target for treatment. Profiling gene expression under these conditions would also give insight into the downstream effects of poor mechanosensing, showing which repair pathways may be impacted. Ultimately, uncovering the mechanisms and consequences of the changes in nuclear-cytoplasmic coupling and mechanotransduction we have described here has significant implications for both BAG3 MFM and other disorders involving the cytoskeletal-LINC-NE signaling axis.

CHAPTER 6: references

1. Selcen D, Muntoni F, Burton BK, et al. Mutation in BAG3 causes severe dominant childhood muscular dystrophy. *Ann Neurol*. 2009;65(1):83-89. doi:10.1002/ana.21553
2. Odgerel Z, Sarkozy A, Lee HS, et al. Inheritance patterns and phenotypic features of myofibrillar myopathy associated with a BAG3 mutation. *Neuromuscul Disord*. 2010;20(7):438-442. doi:10.1016/j.nmd.2010.05.004
3. Ulbricht A, Gehlert S, Leciejewski B, Schiffer T, Bloch W, Höhfeld J. Induction and adaptation of chaperone-assisted selective autophagy CASA in response to resistance exercise in human skeletal muscle. *Autophagy*. 2015;11(3):538-546. doi:10.1080/15548627.2015.1017186
4. Robertson R, Conte TC, Dicaire MJ, et al. BAG3P215L/KO Mice as a Model of BAG3P209L Myofibrillar Myopathy. *Am J Pathol*. 2020;190(3):554-562. doi:10.1016/j.ajpath.2019.11.005
5. Frontera WR, Ochala J. Skeletal Muscle: A Brief Review of Structure and Function. *Calcif Tissue Int*. 2015;96(3):183-195. doi:10.1007/s00223-014-9915-y
6. Wolfe RR. The underappreciated role of muscle in health and disease. *Am J Clin Nutr*. 2006;84(3):475-482. doi:10.1093/ajcn/84.3.475
7. Evans WJ. What Is Sarcopenia? *J Gerontol Ser A*. 1995;50A(Special_Issue):5-8. doi:10.1093/gerona/50A.Special_Issue.5
8. Bertorini TE. 1 - Neuromuscular Anatomy and Function. In: Bertorini TE, ed. *Neuromuscular Case Studies*. Butterworth-Heinemann; 2008:1-25. doi:10.1016/B978-0-7506-7332-7.50005-2
9. Partridge TA. The mdx mouse model as a surrogate for Duchenne muscular dystrophy. *FEBS J*. 2013;280(17):4177-4186. doi:https://doi.org/10.1111/febs.12267
10. Peter AK, Cheng H, Ross RS, Knowlton KU, Chen J. The costamere bridges sarcomeres to the sarcolemma in striated muscle. *Prog Pediatr Cardiol*. 2011;31(2):83-88. doi:10.1016/j.ppedcard.2011.02.003
11. Luther PK. The vertebrate muscle Z-disc: sarcomere anchor for structure and signalling. *J Muscle Res Cell Motil*. 2009;30(5):171-185. doi:10.1007/s10974-009-9189-6
12. Lieber RL, Fridén J. Mechanisms of muscle injury gleaned from animal models. *Am J Phys Med Rehabil*. 2002;81(11 Suppl):S70-79. doi:10.1097/00002060-200211001-00008
13. Schiaffino S, Reggiani C. Fiber Types in Mammalian Skeletal Muscles. *Physiol Rev*. 2011;91(4):1447-1531. doi:10.1152/physrev.00031.2010
14. Emery AE. The muscular dystrophies. *The Lancet*. 2002;359(9307):687-695. doi:10.1016/S0140-6736(02)07815-7
15. Gao Q, McNally EM. The Dystrophin Complex: structure, function and implications for therapy. *Compr Physiol*. 2015;5(3):1223-1239. doi:10.1002/cphy.c140048
16. Meryon E. On fatty degeneration of the voluntary muscles. *Lancet*. 1851;2:588-589.
17. Hoffman EP, Fischbeck KH, Brown RH, et al. Characterization of dystrophin in muscle-biopsy specimens from patients with Duchenne's or Becker's muscular dystrophy. *N Engl J Med*. 1988;318(21):1363-1368. doi:10.1056/NEJM198805263182104

18. Straub V, Murphy A, Udd B, et al. 229th ENMC international workshop: Limb girdle muscular dystrophies – Nomenclature and reformed classification Naarden, the Netherlands, 17–19 March 2017. *Neuromuscul Disord*. 2018;28(8):702-710. doi:10.1016/j.nmd.2018.05.007
19. Hack AA, Groh ME, McNally EM. Sarcoglycans in muscular dystrophy. *Microsc Res Tech*. 2000;48(3-4):167-180. doi:10.1002/(SICI)1097-0029(20000201/15)48:3/4<167::AID-JEMT5>3.0.CO;2-T
20. Adam MP, Ardinger HH, Pagon RA, et al., eds. *GeneReviews®*. University of Washington, Seattle; 1993. Accessed April 29, 2021. http://www.ncbi.nlm.nih.gov/books/NBK1116/
21. Emery AEH. Emery–Dreifuss muscular dystrophy – a 40 year retrospective. *Neuromuscul Disord*. 2000;10(4):228-232. doi:10.1016/S0960-8966(00)00105-X
22. Buckley AE, Dean J, Mahy IR. Cardiac involvement in Emery Dreifuss muscular dystrophy: a case series. *Heart*. 1999;82(1):105-108. doi:10.1136/hrt.82.1.105
23. Fidziańska A, Hausmanowa-Petrusewicz I. Architectural abnormalities in muscle nuclei. Ultrastructural differences between X-linked and autosomal dominant forms of EDMD. *J Neurol Sci*. 2003;210(1):47-51. doi:10.1016/S0022-510X(03)00012-1
24. Fidziańska A, Toniolo D, Hausmanowa-Petrusewicz I. Ultrastructural abnormality of sarcolemmal nuclei in Emery-Dreifuss muscular dystrophy (EDMD). *J Neurol Sci*. 1998;159(1):88-93. doi:10.1016/S0022-510X(98)00130-0
25. Sabatelli P, Lattanzi G, Ognibene A, et al. Nuclear alterations in autosomal-dominant Emery-Dreifuss muscular dystrophy. *Muscle Nerve*. 2001;24(6):826-829. doi:10.1002/mus.1076
26. Selcen D. Myofibrillar myopathies. *Neuromuscul Disord NMD*. 2011;21(3):161-171. doi:10.1016/j.nmd.2010.12.007
27. Olivé M, Kley RA, Goldfarb LG. Myofibrillar myopathies: new developments. *Curr Opin Neurol*. 2013;26(5):527-535. doi:10.1097/WCO.0b013e328364d6b1
28. Béhin A, Salort-Campana E, Wahbi K, et al. Myofibrillar myopathies: State of the art, present and future challenges. *Rev Neurol (Paris)*. 2015;171(10):715-729. doi:10.1016/j.neurol.2015.06.002
29. Goldfarb LG, Park KY, Cervenáková L, et al. Missense mutations in desmin associated with familial cardiac and skeletal myopathy. *Nat Genet*. 1998;19(4):402-403. doi:10.1038/1300
30. Vicart P, Caron A, Guicheney P, et al. A missense mutation in the alphaB-crystallin chaperone gene causes a desmin-related myopathy. *Nat Genet*. 1998;20(1):92-95. doi:10.1038/1765
31. Selcen D, Engel AG. Mutations in ZASP define a novel form of muscular dystrophy in humans. *Ann Neurol*. 2005;57(2):269-276. doi:10.1002/ana.20376
32. Vorgerd M, van der Ven PFM, Bruchertseifer V, et al. A mutation in the dimerization domain of filamin c causes a novel type of autosomal dominant myofibrillar myopathy. *Am J Hum Genet*. 2005;77(2):297-304. doi:10.1086/431959
33. Selcen D, Engel AG. Mutations in myotilin cause myofibrillar myopathy. *Neurology*. 2004;62(8):1363-1371. doi:10.1212/01.wnl.0000123576.74801.75
34. Schessl J, Zou Y, McGrath MJ, et al. Proteomic identification of FHL1 as the protein mutated in human reducing body myopathy. *J Clin Invest*. 2008;118(3):904-912. doi:10.1172/JCI34450
35. Ohlsson M, Hedberg C, Brådvik B, et al. Hereditary myopathy with early respiratory failure associated with a mutation in A-band titin. *Brain J Neurol*. 2012;135(Pt 6):1682-1694.

doi:10.1093/brain/aws103
36. Capetanaki Y, Bloch RJ, Kouloumenta A, Mavroidis M, Psarras S. Muscle intermediate filaments and their links to membranes and membranous organelles. *Exp Cell Res*. 2007;313(10):2063-2076. doi:10.1016/j.yexcr.2007.03.033
37. O'Neill A, Williams MW, Resneck WG, Milner DJ, Capetanaki Y, Bloch RJ. Sarcolemmal Organization in Skeletal Muscle Lacking Desmin: Evidence for Cytokeratins Associated with the Membrane Skeleton at Costameres. *Mol Biol Cell*. 2002;13(7):2347-2359. doi:10.1091/mbc.01-12-0576
38. Palmio J, Udd B. Myofibrillar and distal myopathies. *Rev Neurol (Paris)*. 2016;172(10):587-593. doi:10.1016/j.neurol.2016.07.019
39. Sacconi S, Féasson L, Antoine JC, et al. A novel CRYAB mutation resulting in multisystemic disease. *Neuromuscul Disord*. 2012;22(1):66-72. doi:10.1016/j.nmd.2011.07.004
40. Takayama S, Xie Z, Reed JC. An Evolutionarily Conserved Family of Hsp70/Hsc70 Molecular Chaperone Regulators*. *J Biol Chem*. 1999;274(2):781-786. doi:10.1074/jbc.274.2.781
41. Takayama S, Sato T, Krajewski S, et al. Cloning and functional analysis of BAG-1: a novel Bcl-2-binding protein with anti-cell death activity. *Cell*. 1995;80(2):279-284. doi:10.1016/0092-8674(95)90410-7
42. Coulson M, Robert S, Saint R. Drosophila starvin Encodes a Tissue-Specific BAG-Domain Protein Required for Larval Food Uptake. *Genetics*. 2005;171(4):1799-1812. doi:10.1534/genetics.105.043265
43. Doukhanina EV, Chen S, van der Zalm E, Godzik A, Reed J, Dickman MB. Identification and functional characterization of the BAG protein family in Arabidopsis thaliana. *J Biol Chem*. 2006;281(27):18793-18801. doi:10.1074/jbc.M511794200
44. Bruno AP, Festa M, Dal Piaz F, et al. Identification of a synaptosome-associated form of BAG3 protein. *Cell Cycle Georget Tex*. 2008;7(19):3104-3105. doi:10.4161/cc.7.19.6774
45. Lee JH, Takahashi T, Yasuhara N, Inazawa J, Kamada S, Tsujimoto Y. Bis, a Bcl-2-binding protein that synergizes with Bcl-2 in preventing cell death. *Oncogene*. 1999;18(46):6183-6190. doi:10.1038/sj.onc.1203043
46. Gamerdinger M, Kaya AM, Wolfrum U, Clement AM, Behl C. BAG3 mediates chaperone-based aggresome-targeting and selective autophagy of misfolded proteins. *EMBO Rep*. 2011;12(2):149-156. doi:10.1038/embor.2010.203
47. Arndt V, Dick N, Tawo R, et al. Chaperone-Assisted Selective Autophagy Is Essential for Muscle Maintenance. *Curr Biol*. 2010;20(2):143-148. doi:10.1016/j.cub.2009.11.022
48. Rauch JN, Tse E, Freilich R, et al. BAG3 Is a Modular, Scaffolding Protein that physically Links Heat Shock Protein 70 (Hsp70) to the Small Heat Shock Proteins. *J Mol Biol*. 2017;429(1):128-141. doi:10.1016/j.jmb.2016.11.013
49. Ulbricht A, Eppler FJ, Tapia VE, et al. Cellular Mechanotransduction Relies on Tension-Induced and Chaperone-Assisted Autophagy. *Curr Biol*. 2013;23(5):430-435. doi:10.1016/j.cub.2013.01.064
50. Totaro A, Panciera T, Piccolo S. YAP/TAZ upstream signals and downstream responses. *Nat Cell Biol*. 2018;20(8):888-899. doi:10.1038/s41556-018-0142-z
51. Kathage B, Gehlert S, Ulbricht A, et al. The cochaperone BAG3 coordinates protein synthesis and autophagy under mechanical strain through spatial regulation of mTORC1. *Biochim Biophys Acta BBA - Mol Cell Res*. 2017;1864(1):62-75.

doi:10.1016/j.bbamcr.2016.10.007
52. Iwasaki M, Tanaka R, Hishiya A, Homma S, Reed JC, Takayama S. BAG3 directly associates with guanine nucleotide exchange factor of Rap1, PDZGEF2, and regulates cell adhesion. *Biochem Biophys Res Commun*. 2010;400(3):413-418. doi:10.1016/j.bbrc.2010.08.092
53. Fuchs M, Luthold C, Guilbert SM, et al. A Role for the Chaperone Complex BAG3-HSPB8 in Actin Dynamics, Spindle Orientation and Proper Chromosome Segregation during Mitosis. *PLoS Genet*. 2015;11(10):e1005582. doi:10.1371/journal.pgen.1005582
54. Varlet AA, Fuchs M, Luthold C, Lambert H, Landry J, Lavoie JN. Fine-tuning of actin dynamics by the HSPB8-BAG3 chaperone complex facilitates cytokinesis and contributes to its impact on cell division. *Cell Stress Chaperones*. 2017;22(4):553-567. doi:10.1007/s12192-017-0780-2
55. Hishiya A, Kitazawa T, Takayama S. BAG3 and Hsc70 interact with actin capping protein CapZ to maintain myofibrillar integrity under mechanical stress. *Circ Res*. 2010;107(10):1220-1231. doi:10.1161/CIRCRESAHA.110.225649
56. Sarparanta J, Jonson PH, Golzio C, et al. Mutations affecting the cytoplasmic functions of the co-chaperone DNAJB6 cause limb-girdle muscular dystrophy. *Nat Genet*. 2012;44(4):450-S2. doi:10.1038/ng.1103
57. Sondermann H, Scheufler C, Schneider C, Hohfeld J, Hartl FU, Moarefi I. Structure of a Bag/Hsc70 complex: convergent functional evolution of Hsp70 nucleotide exchange factors. *Science*. 2001;291(5508):1553-1557. doi:10.1126/science.1057268
58. Young JC. Mechanisms of the Hsp70 chaperone system. *Biochem Cell Biol Biochim Biol Cell*. 2010;88(2):291-300. doi:10.1139/o09-175
59. Rauch JN, Gestwicki JE. Binding of Human Nucleotide Exchange Factors to Heat Shock Protein 70 (Hsp70) Generates Functionally Distinct Complexes in Vitro. *J Biol Chem*. 2014;289(3):1402-1414. doi:10.1074/jbc.M113.521997
60. Brehmer D, Rüdiger S, Gässler CS, et al. Tuning of chaperone activity of Hsp70 proteins by modulation of nucleotide exchange. *Nat Struct Biol*. 2001;8(5):427-432. doi:10.1038/87588
61. Haslbeck M, Franzmann T, Weinfurtner D, Buchner J. Some like it hot: the structure and function of small heat-shock proteins. *Nat Struct Mol Biol*. 2005;12(10):842-846. doi:10.1038/nsmb993
62. Ulbricht A, Arndt V, Höhfeld J. Chaperone-assisted proteostasis is essential for mechanotransduction in mammalian cells. *Commun Integr Biol*. 2013;6(4):e24925. doi:10.4161/cib.24925
63. Gamerdinger M, Hajieva P, Kaya AM, Wolfrum U, Hartl FU, Behl C. Protein quality control during aging involves recruitment of the macroautophagy pathway by BAG3. *EMBO J*. 2009;28(7):889-901. doi:10.1038/emboj.2009.29
64. Minoia M, Boncoraglio A, Vinet J, et al. BAG3 induces the sequestration of proteasomal clients into cytoplasmic puncta: implications for a proteasome-to-autophagy switch. *Autophagy*. 2014;10(9):1603-1621. doi:10.4161/auto.29409
65. Franceschelli S, Rosati A, Lerose R, Nicola SD, Turco MC, Pascale M. bag3 gene expression is regulated by heat shock factor 1. *J Cell Physiol*. 2008;215(3):575-577. doi:10.1002/jcp.21397
66. Lee KK, Haraguchi T, Lee RS, Koujin T, Hiraoka Y, Wilson KL. Distinct functional domains in emerin bind lamin A and DNA-bridging protein BAF. *J Cell Sci*. 2001;114(Pt 24):4567-4573.

67. Carra S, Seguin SJ, Lambert H, Landry J. HspB8 chaperone activity toward poly(Q)-containing proteins depends on its association with Bag3, a stimulator of macroautophagy. *J Biol Chem*. 2008;283(3):1437-1444. doi:10.1074/jbc.M706304200
68. Lei Z, Brizzee C, Johnson GVW. BAG3 facilitates the clearance of endogenous tau in primary neurons. *Neurobiol Aging*. 2015;36(1):241-248. doi:10.1016/j.neurobiolaging.2014.08.012
69. L. Phan, Y. Jin, H. Zhang, et al. ALFA: Allele Frequency Aggregator. ALFA: Allele Frequency Aggregator. Published March 10, 2020. Accessed April 22, 2022. https://www.ncbi.nlm.nih.gov/snp/docs/gsr/alfa/
70. Carvalho AA de S, Lacene E, Brochier G, et al. Genetic Mutations and Demographic, Clinical, and Morphological Aspects of Myofibrillar Myopathy in a French Cohort. *Genet Test Mol Biomark*. 2018;22(6):374-383. doi:10.1089/gtmb.2018.0004
71. Jaffer F, Murphy SM, Scoto M, et al. BAG3 mutations: another cause of giant axonal neuropathy. *J Peripher Nerv Syst JPNS*. 2012;17(2):210-216. doi:10.1111/j.1529-8027.2012.00409.x
72. Konersman CG, Bordini BJ, Scharer G, et al. BAG3 myofibrillar myopathy presenting with cardiomyopathy. *Neuromuscul Disord NMD*. 2015;25(5):418-422. doi:10.1016/j.nmd.2015.01.009
73. Schänzer A, Rupp S, Gräf S, et al. Dysregulated autophagy in restrictive cardiomyopathy due to Pro209Leu mutation in BAG3. *Mol Genet Metab*. 2018;123(3):388-399. doi:10.1016/j.ymgme.2018.01.001
74. Noury JB, Maisonobe T, Richard P, Delague V, Malfatti E, Stojkovic T. Rigid spine syndrome associated with sensory-motor axonal neuropathy resembling Charcot–Marie-Tooth disease is characteristic of Bcl-2-associated athanogene-3 gene mutations even without cardiac involvement. *Muscle Nerve*. 2018;57(2):330-334. doi:10.1002/mus.25631
75. Kim SJ, Nam SH, Kanwal S, et al. BAG3 mutation in a patient with atypical phenotypes of myofibrillar myopathy and Charcot–Marie–Tooth disease. *Genes Genomics*. 2018;40(12):1269-1277. doi:10.1007/s13258-018-0721-1
76. Semmler AL, Sacconi S, Bach JE, et al. Unusual multisystemic involvement and a novel BAG3 mutation revealed by NGS screening in a large cohort of myofibrillar myopathies. *Orphanet J Rare Dis*. 2014;9(1):121. doi:10.1186/s13023-014-0121-9
77. Shy M, Rebelo AP, Feely SM, et al. Mutations in BAG3 cause adult-onset Charcot-Marie-Tooth disease. *J Neurol Neurosurg Psychiatry*. 2018;89(3):313-315. doi:10.1136/jnnp-2017-315929
78. Meister-Broekema M, Freilich R, Jagadeesan C, et al. Myopathy associated BAG3 mutations lead to protein aggregation by stalling Hsp70 networks. *Nat Commun*. 2018;9(1):5342. doi:10.1038/s41467-018-07718-5
79. Arimura T, Ishikawa T, Nunoda S, Kawai S, Kimura A. Dilated cardiomyopathy-associated BAG3 mutations impair Z-disc assembly and enhance sensitivity to apoptosis in cardiomyocytes. *Hum Mutat*. 2011;32(12):1481-1491. doi:https://doi.org/10.1002/humu.21603
80. Ruparelia AA, Oorschot V, Vaz R, Ramm G, Bryson-Richardson RJ. Zebrafish models of BAG3 myofibrillar myopathy suggest a toxic gain of function leading to BAG3 insufficiency. *Acta Neuropathol (Berl)*. 2014;128(6):821-833. doi:10.1007/s00401-014-1344-5
81. Adriaenssens E, Tedesco B, Mediani L, et al. BAG3 Pro209 mutants associated with

myopathy and neuropathy relocate chaperones of the CASA-complex to aggresomes. *Sci Rep*. 2020;10(1):8755. doi:10.1038/s41598-020-65664-z
82. Johnston JA, Ward CL, Kopito RR. Aggresomes: a cellular response to misfolded proteins. *J Cell Biol*. 1998;143(7):1883-1898. doi:10.1083/jcb.143.7.1883
83. Corboy MJ, Thomas PJ, Wigley WC. Aggresome Formation. In: Patterson C, Cyr DM, eds. *Ubiquitin-Proteasome Protocols*. Methods in Molecular Biology™. Humana Press; 2005:305-327. doi:10.1385/1-59259-895-1:305
84. Mahmaljy H, Yelamanchili VS, Singhal M. Dilated Cardiomyopathy. In: *StatPearls*. StatPearls Publishing; 2021. Accessed September 7, 2021. http://www.ncbi.nlm.nih.gov/books/NBK441911/
85. Dilated Cardiomyopathy Due to BLC2-Associated Athanogene 3 (BAG3) Mutations - ClinicalKey. Accessed September 7, 2021. https://www.clinicalkey.com/#!/content/playContent/1-s2.0-S0735109718385176?returnurl=https:%2F%2Flinkinghub.elsevier.com%2Fretrieve%2Fpii%2FS0735109718385176%3Fshowall%3Dtrue&referrer=https:%2F%2Fwww.nature.com%2F
86. Fang X, Bogomolovas J, Wu T, et al. Loss-of-function mutations in co-chaperone BAG3 destabilize small HSPs and cause cardiomyopathy. *J Clin Invest*. 127(8):3189-3200. doi:10.1172/JCI94310
87. Martin TG, Myers VD, Dubey P, et al. Cardiomyocyte contractile impairment in heart failure results from reduced BAG3-mediated sarcomeric protein turnover. *Nat Commun*. 2021;12(1):2942. doi:10.1038/s41467-021-23272-z
88. Feldman AM, Begay RL, Knezevic T, et al. Decreased Levels of BAG3 in a Family With a Rare Variant and in Idiopathic Dilated Cardiomyopathy. *J Cell Physiol*. 2014;229(11):1697-1702. doi:10.1002/jcp.24615
89. Chami N, Tadros R, Lemarbre F, et al. Nonsense Mutations in BAG3 are Associated With Early-Onset Dilated Cardiomyopathy in French Canadians. *Can J Cardiol*. 2014;30(12):1655-1661. doi:10.1016/j.cjca.2014.09.030
90. Homma S, Iwasaki M, Shelton GD, Engvall E, Reed JC, Takayama S. BAG3 Deficiency Results in Fulminant Myopathy and Early Lethality. *Am J Pathol*. 2006;169(3):761-773. doi:10.2353/ajpath.2006.060250
91. Youn DY, Lee DH, Lim MH, et al. Bis deficiency results in early lethality with metabolic deterioration and involution of spleen and thymus. *Am J Physiol-Endocrinol Metab*. 2008;295(6):E1349-E1357. doi:10.1152/ajpendo.90704.2008
92. Myers VD, Tomar D, Madesh M, et al. Haplo-insufficiency of Bcl2-associated athanogene 3 in mice results in progressive left ventricular dysfunction, β-adrenergic insensitivity, and increased apoptosis. *J Cell Physiol*. 2018;233(9):6319-6326. doi:https://doi.org/10.1002/jcp.26482
93. Feldman AM, Gordon J, Wang J, et al. BAG3 regulates contractility and Ca(2+) homeostasis in adult mouse ventricular myocytes. *J Mol Cell Cardiol*. 2016;92:10-20. doi:10.1016/j.yjmcc.2016.01.015
94. Diofano F, Weinmann K, Schneider I, Thiessen KD, Rottbauer W, Just S. Genetic compensation prevents myopathy and heart failure in an in vivo model of Bag3 deficiency. *PLOS Genet*. 2020;16(11):e1009088. doi:10.1371/journal.pgen.1009088
95. Quintana MT, Parry TL, He J, et al. Cardiomyocyte-Specific Human Bcl2-Associated Anthanogene 3 P209L Expression Induces Mitochondrial Fragmentation, Bcl2-Associated

Anthanogene 3 Haploinsufficiency, and Activates p38 Signaling. *Am J Pathol*. 2016;186(8):1989-2007. doi:10.1016/j.ajpath.2016.03.017
96. Inomata Y, Nagasaka S, Miyate K, et al. Bcl-2-associated athanogene 3 (BAG3) is an enhancer of small heat shock protein turnover via activation of autophagy in the heart. *Biochem Biophys Res Commun*. 2018;496(4):1141-1147. doi:10.1016/j.bbrc.2018.01.158
97. Fang X, Bogomolovas J, Zhou PS, et al. P209L mutation in Bag3 does not cause cardiomyopathy in mice. *Am J Physiol Heart Circ Physiol*. 2019;316(2):H392-H399. doi:10.1152/ajpheart.00714.2018
98. Clemen CS, Stöckigt F, Strucksberg KH, et al. The toxic effect of R350P mutant desmin in striated muscle of man and mouse. *Acta Neuropathol (Berl)*. 2015;129(2):297-315. doi:10.1007/s00401-014-1363-2
99. Mierzejewski B, Archacka K, Grabowska I, Florkowska A, Ciemerych MA, Brzoska E. Human and mouse skeletal muscle stem and progenitor cells in health and disease. *Semin Cell Dev Biol*. 2020;104:93-104. doi:10.1016/j.semcdb.2020.01.004
100. Bareja A, Holt JA, Luo G, et al. Human and Mouse Skeletal Muscle Stem Cells: Convergent and Divergent Mechanisms of Myogenesis. *PLOS ONE*. 2014;9(2):e90398. doi:10.1371/journal.pone.0090398
101. Banks GB, Combs AC, Odom GL, Bloch RJ, Chamberlain JS. Muscle structure influences utrophin expression in mdx mice. *PLoS Genet*. 2014;10(6):e1004431. doi:10.1371/journal.pgen.1004431
102. Zhang Q, Skepper JN, Yang F, et al. Nesprins: a novel family of spectrin-repeat-containing proteins that localize to the nuclear membrane in multiple tissues. *J Cell Sci*. 2001;114(Pt 24):4485-4498.
103. Crisp M, Liu Q, Roux K, et al. Coupling of the nucleus and cytoplasm. *J Cell Biol*. 2006;172(1):41-53. doi:10.1083/jcb.200509124
104. Schirmer EC, Florens L, Guan T, Yates JR, Gerace L. Nuclear Membrane Proteins with Potential Disease Links Found by Subtractive Proteomics. *Science*. 2003;301(5638):1380-1382. doi:10.1126/science.1088176
105. Jaalouk DE, Lammerding J. Mechanotransduction gone awry. *Nat Rev Mol Cell Biol*. 2009;10(1):63-73. doi:10.1038/nrm2597
106. Lee JSH, Hale CM, Panorchan P, et al. Nuclear Lamin A/C Deficiency Induces Defects in Cell Mechanics, Polarization, and Migration. *Biophys J*. 2007;93(7):2542-2552. doi:10.1529/biophysj.106.102426
107. Wang N, Butler JP, Ingber DE. Mechanotransduction across the cell surface and through the cytoskeleton. *Science*. 1993;260(5111):1124-1127. doi:10.1126/science.7684161
108. Dupont S, Morsut L, Aragona M, et al. Role of YAP/TAZ in mechanotransduction. *Nature*. 2011;474(7350):179-183. doi:10.1038/nature10137
109. Elosegui-Artola A, Andreu I, Beedle AEM, et al. Force Triggers YAP Nuclear Entry by Regulating Transport across Nuclear Pores. *Cell*. 2017;171(6):1397-1410.e14. doi:10.1016/j.cell.2017.10.008
110. Bertrand AT, Ziaei S, Ehret C, et al. Cellular microenvironments reveal defective mechanosensing responses and elevated YAP signaling in LMNA-mutated muscle precursors. *J Cell Sci*. 2014;127(Pt 13):2873-2884. doi:10.1242/jcs.144907
111. Dasgupta I, McCollum D. Control of cellular responses to mechanical cues through YAP/TAZ regulation. *J Biol Chem*. 2019;294(46):17693-17706. doi:10.1074/jbc.REV119.007963

112. Varelas X. The Hippo pathway effectors TAZ and YAP in development, homeostasis and disease. *Development*. 2014;141(8):1614-1626. doi:10.1242/dev.102376
113. Watt KI, Goodman CA, Hornberger TA, Gregorevic P. The Hippo Signaling Pathway in the Regulation of Skeletal Muscle Mass and Function. *Exerc Sport Sci Rev*. 2018;46(2):92-96. doi:10.1249/JES.0000000000000142
114. Judson RN, Tremblay AM, Knopp P, et al. The Hippo pathway member Yap plays a key role in influencing fate decisions in muscle satellite cells. *J Cell Sci*. 2012;125(24):6009-6019. doi:10.1242/jcs.109546
115. Worman HJ, Bonne G. "Laminopathies": A wide spectrum of human diseases. *Exp Cell Res*. 2007;313(10):2121-2133. doi:10.1016/j.yexcr.2007.03.028
116. Bione S, Maestrini E, Rivella S, et al. Identification of a novel X-linked gene responsible for Emery-Dreifuss muscular dystrophy. *Nat Genet*. 1994;8(4):323-327. doi:10.1038/ng1294-323
117. Lammerding J, Schulze PC, Takahashi T, et al. Lamin A/C deficiency causes defective nuclear mechanics and mechanotransduction. *J Clin Invest*. 2004;113(3):370-378. doi:10.1172/JCI19670
118. Lammerding J, Hsiao J, Schulze PC, Kozlov S, Stewart CL, Lee RT. Abnormal nuclear shape and impaired mechanotransduction in emerin-deficient cells. *J Cell Biol*. 2005;170(5):781-791. doi:10.1083/jcb.200502148
119. Davidson PM, Lammerding J. Broken nuclei – lamins, nuclear mechanics and disease. *Trends Cell Biol*. 2014;24(4):247-256. doi:10.1016/j.tcb.2013.11.004
120. Sullivan T, Escalante-Alcalde D, Bhatt H, et al. Loss of A-type lamin expression compromises nuclear envelope integrity leading to muscular dystrophy. *J Cell Biol*. 1999;147(5):913-920. doi:10.1083/jcb.147.5.913
121. van Engelen BGM, Muchir A, Hutchison CJ, van der Kooi AJ, Bonne G, Lammens M. The lethal phenotype of a homozygous nonsense mutation in the lamin A/C gene. *Neurology*. 2005;64(2):374-376. doi:10.1212/01.WNL.0000149763.15180.00
122. Zwerger M, Jaalouk DE, Lombardi ML, et al. Myopathic lamin mutations impair nuclear stability in cells and tissue and disrupt nucleo-cytoskeletal coupling. *Hum Mol Genet*. 2013;22(12):2335-2349. doi:10.1093/hmg/ddt079
123. Decostre V, Ben Yaou R, Bonne G. Laminopathies affecting skeletal and cardiac muscles: clinical and pathophysiological aspects. *Acta Myol Myopathies Cardiomyopathies Off J Mediterr Soc Myol*. 2005;24(2):104-109.
124. Verstraeten VLRM, Ji JY, Cummings KS, Lee RT, Lammerding J. Increased mechanosensitivity and nuclear stiffness in Hutchinson–Gilford progeria cells: effects of farnesyltransferase inhibitors. *Aging Cell*. 2008;7(3):383-393. doi:10.1111/j.1474-9726.2008.00382.x
125. Dahl KN, Scaffidi P, Islam MF, Yodh AG, Wilson KL, Misteli T. Distinct structural and mechanical properties of the nuclear lamina in Hutchinson–Gilford progeria syndrome. *Proc Natl Acad Sci*. 2006;103(27):10271-10276. doi:10.1073/pnas.0601058103
126. Jin YH, Ahn SG, Kim SA. BAG3 affects the nucleocytoplasmic shuttling of HSF1 upon heat stress. *Biochem Biophys Res Commun*. 2015;464(2):561-567. doi:10.1016/j.bbrc.2015.07.006
127. Santoro A, Nicolin V, Florenzano F, Rosati A, Capunzo M, Nori SL. BAG3 is involved in neuronal differentiation and migration. *Cell Tissue Res*. 2017;368(2):249-258. doi:10.1007/s00441-017-2570-7

128. Gupta MK, Gordon J, Glauser GM, et al. Lamin B is a target for selective nuclear PQC by BAG3: implication for nuclear envelopathies. *Cell Death Dis*. 2019;10(1):1-11. doi:10.1038/s41419-018-1255-9
129. Steele-Stallard HB, Pinton L, Sarcar S, et al. Modeling Skeletal Muscle Laminopathies Using Human Induced Pluripotent Stem Cells Carrying Pathogenic LMNA Mutations. *Front Physiol*. 2018;9. Accessed April 26, 2022. https://www.frontiersin.org/article/10.3389/fphys.2018.01332
130. Scharner J, Brown CA, Bower M, et al. Novel LMNA mutations in patients with Emery-Dreifuss muscular dystrophy and functional characterization of four LMNA mutations. *Hum Mutat*. 2011;32(2):152-167. doi:10.1002/humu.21361
131. Wignes JA, Goldman JW, Weihl CC, Bartley MG, Andley UP. p62 expression and autophagy in αB-crystallin R120G mutant knock-in mouse model of hereditary cataract. *Exp Eye Res*. 2013;115:263-273. doi:10.1016/j.exer.2013.06.026
132. Garvey SM, Miller SE, Claflin DR, Faulkner JA, Hauser MA. Transgenic mice expressing the myotilin T57I mutation unite the pathology associated with LGMD1A and MFM. *Hum Mol Genet*. 2006;15(15):2348-2362. doi:10.1093/hmg/ddl160
133. Bebee TW, Dominguez CE, Chandler DS. Mouse models of SMA: tools for disease characterization and therapeutic development. *Hum Genet*. 2012;131(8):1277-1293. doi:10.1007/s00439-012-1171-5
134. Bulfield G, Siller WG, Wight PA, Moore KJ. X chromosome-linked muscular dystrophy (mdx) in the mouse. *Proc Natl Acad Sci U S A*. 1984;81(4):1189-1192. doi:10.1073/pnas.81.4.1189
135. Mayer E. On growth and form. By D'Arcy Wentworth Thompson. A new edition. Cambridge and New York, University Press and Macmillan, 1942, 1116 pp., 554 illustrations, 21½ cm. Price, $12.50. *Anat Rec*. 1943;85(1):111-116. doi:10.1002/ar.1090850108
136. Abzhanov A. The old and new faces of morphology: the legacy of D'Arcy Thompson's 'theory of transformations' and 'laws of growth'. *Development*. 2017;144(23):4284-4297. doi:10.1242/dev.137505
137. Wakao J, Kishida T, Fumino S, et al. Efficient direct conversion of human fibroblasts into myogenic lineage induced by co-transduction with MYCL and MYOD1. *Biochem Biophys Res Commun*. 2017;488(2):368-373. doi:10.1016/j.bbrc.2017.05.059
138. Hindi L, McMillan JD, Afroze D, Hindi SM, Kumar A. Isolation, Culturing, and Differentiation of Primary Myoblasts from Skeletal Muscle of Adult Mice. *Bio-Protoc*. 2017;7(9):e2248. doi:10.21769/BioProtoc.2248
139. Amand MMSt, Hanover JA, Shiloach J. A comparison of strategies for immortalizing mouse embryonic fibroblasts. *J Biol Methods*. 2016;3(2):e41. doi:10.14440/jbm.2016.110
140. Kimura K, Ooms A, Graf-Riesen K, et al. Overexpression of human BAG3P209L in mice causes restrictive cardiomyopathy. *Nat Commun*. 2021;12(1):3575. doi:10.1038/s41467-021-23858-7
141. Norton N, Li D, Rieder MJ, et al. Genome-wide Studies of Copy Number Variation and Exome Sequencing Identify Rare Variants in BAG3 as a Cause of Dilated Cardiomyopathy. *Am J Hum Genet*. 2011;88(3):273-282. doi:10.1016/j.ajhg.2011.01.016
142. Hong J, Park JS, Lee H, et al. Myosin heavy chain is stabilized by BCL-2 interacting cell death suppressor (BIS) in skeletal muscle. *Exp Mol Med*. 2016;48(4):e225-e225. doi:10.1038/emm.2016.2

143. Tahrir FG, Knezevic T, Gupta MK, et al. Evidence for the Role of BAG3 in Mitochondrial Quality Control in Cardiomyocytes. *J Cell Physiol*. 2017;232(4):797-805. doi:https://doi.org/10.1002/jcp.25476
144. Vincent AE, Grady JP, Rocha MC, et al. Mitochondrial dysfunction in myofibrillar myopathy. *Neuromuscul Disord*. 2016;26(10):691-701. doi:10.1016/j.nmd.2016.08.004
145. Jackson S, Schaefer J, Meinhardt M, Reichmann H. Mitochondrial abnormalities in the myofibrillar myopathies. *Eur J Neurol*. 2015;22(11):1429-1435. doi:https://doi.org/10.1111/ene.12814
146. Stroud MJ, Banerjee I, Veevers J, Chen J. Linker of Nucleoskeleton and Cytoskeleton Complex Proteins in Cardiac Structure, Function, and Disease. *Circ Res*. 2014;114(3):538-548. doi:10.1161/CIRCRESAHA.114.301236
147. Ranade D, Pradhan R, Jayakrishnan M, Hegde S, Sengupta K. Lamin A/C and Emerin depletion impacts chromatin organization and dynamics in the interphase nucleus. *BMC Mol Cell Biol*. 2019;20(1):11. doi:10.1186/s12860-019-0192-5
148. Kuragano M, Uyeda TQP, Kamijo K, Murakami Y, Takahashi M. Different contributions of nonmuscle myosin IIA and IIB to the organization of stress fiber subtypes in fibroblasts. *Mol Biol Cell*. 2018;29(8):911-922. doi:10.1091/mbc.E17-04-0215
149. Lehtimäki JI, Rajakylä EK, Tojkander S, Lappalainen P. Generation of stress fibers through myosin-driven reorganization of the actin cortex. *eLife*. 10:e60710. doi:10.7554/eLife.60710
150. Goeckeler ZM, Wysolmerski RB. Myosin light chain kinase-regulated endothelial cell contraction: the relationship between isometric tension, actin polymerization, and myosin phosphorylation. *J Cell Biol*. 1995;130(3):613-627. doi:10.1083/jcb.130.3.613
151. Houben F, Ramaekers FCS, Snoeckx LHEH, Broers JLV. Role of nuclear lamina-cytoskeleton interactions in the maintenance of cellular strength. *Biochim Biophys Acta BBA - Mol Cell Res*. 2007;1773(5):675-686. doi:10.1016/j.bbamcr.2006.09.018
152. Fu X, Wang H, Hu P. Stem cell activation in skeletal muscle regeneration. *Cell Mol Life Sci*. 2015;72(9):1663-1677. doi:10.1007/s00018-014-1819-5
153. Masschelein E, D'Hulst G, Zvick J, et al. Exercise promotes satellite cell contribution to myofibers in a load-dependent manner. *Skelet Muscle*. 2020;10(1):21. doi:10.1186/s13395-020-00237-2
154. Watt KI, Judson R, Medlow P, et al. Yap is a novel regulator of C2C12 myogenesis. *Biochem Biophys Res Commun*. 2010;393(4):619-624. doi:10.1016/j.bbrc.2010.02.034
155. Judson RN, Gray SR, Walker C, et al. Constitutive Expression of Yes-Associated Protein (Yap) in Adult Skeletal Muscle Fibres Induces Muscle Atrophy and Myopathy. *PLOS ONE*. 2013;8(3):e59622. doi:10.1371/journal.pone.0059622
156. Fiacco E, Castagnetti F, Bianconi V, et al. Autophagy regulates satellite cell ability to regenerate normal and dystrophic muscles. *Cell Death Differ*. 2016;23(11):1839-1849. doi:10.1038/cdd.2016.70
157. Dumont NA, Wang YX, von Maltzahn J, et al. Dystrophin expression in muscle stem cells regulates their polarity and asymmetric division. *Nat Med*. 2015;21(12):1455-1463. doi:10.1038/nm.3990
158. Vita GL, Polito F, Oteri R, et al. Hippo signaling pathway is altered in Duchenne muscular dystrophy. *PLoS ONE*. 2018;13(10). doi:10.1371/journal.pone.0205514
159. Mazelet L, Parker MO, Li M, Arner A, Ashworth R. Role of Active Contraction and Tropomodulins in Regulating Actin Filament Length and Sarcomere Structure in Developing

Zebrafish Skeletal Muscle. *Front Physiol*. 2016;7. Accessed February 10, 2022. https://www.frontiersin.org/article/10.3389/fphys.2016.00091
160. Cameron AR, Frith JE, Gomez GA, Yap AS, Cooper-White JJ. The effect of time-dependent deformation of viscoelastic hydrogels on myogenic induction and Rac1 activity in mesenchymal stem cells. *Biomaterials*. 2014;35(6):1857-1868. doi:10.1016/j.biomaterials.2013.11.023
161. Clark P, Dunn GA, Knibbs A, Peckham M. Alignment of myoblasts on ultrafine gratings inhibits fusion in vitro. *Int J Biochem Cell Biol*. 2002;34(7):816-825. doi:10.1016/s1357-2725(01)00180-7
162. Tassin AM, Maro B, Bornens M. Fate of microtubule-organizing centers during myogenesis in vitro. *J Cell Biol*. 1985;100(1):35-46. doi:10.1083/jcb.100.1.35
163. Duan R, Gallagher PJ. Dependence of myoblast fusion on a cortical actin wall and nonmuscle myosin IIA. *Dev Biol*. 2009;325(2):374-385. doi:10.1016/j.ydbio.2008.10.035
164. Fedorchak GR, Kaminski A, Lammerding J. Cellular Mechanosensing: Getting to the nucleus of it all. *Prog Biophys Mol Biol*. 2014;115(0):76-92. doi:10.1016/j.pbiomolbio.2014.06.009
165. Iskratsch T, Wolfenson H, Sheetz MP. Appreciating force and shape—the rise of mechanotransduction in cell biology. *Nat Rev Mol Cell Biol*. 2014;15(12):825-833. doi:10.1038/nrm3903
166. Clippinger SR, Cloonan PE, Greenberg L, Ernst M, Stump WT, Greenberg MJ. Disrupted mechanobiology links the molecular and cellular phenotypes in familial dilated cardiomyopathy. *Proc Natl Acad Sci*. 2019;116(36):17831-17840. doi:10.1073/pnas.1910962116
167. Dewulf M, Köster DV, Sinha B, et al. Dystrophy-associated caveolin-3 mutations reveal that caveolae couple IL6/STAT3 signaling with mechanosensing in human muscle cells. *Nat Commun*. 2019;10(1):1974. doi:10.1038/s41467-019-09405-5
168. Olson EN. Toward the correction of muscular dystrophy by gene editing. *Proc Natl Acad Sci*. 2021;118(22). doi:10.1073/pnas.2004840117
169. Roman BI, Verhasselt S, Stevens CV. Medicinal Chemistry and Use of Myosin II Inhibitor (S)-Blebbistatin and Its Derivatives. *J Med Chem*. 2018;61(21):9410-9428. doi:10.1021/acs.jmedchem.8b00503
170. Ruparelia AA, McKaige EA, Williams C, et al. Metformin rescues muscle function in BAG3 myofibrillar myopathy models. *Autophagy*. Published online October 19, 2020:1-17. doi:10.1080/15548627.2020.1833500
171. Hafner P, Bonati U, Erne B, et al. Improved Muscle Function in Duchenne Muscular Dystrophy through L-Arginine and Metformin: An Investigator-Initiated, Open-Label, Single-Center, Proof-Of-Concept-Study. *PLOS ONE*. 2016;11(1):e0147634. doi:10.1371/journal.pone.0147634
172. Fontes-Oliveira CC, M. Soares Oliveira B, Körner Z, M. Harandi V, Durbeej M. Effects of metformin on congenital muscular dystrophy type 1A disease progression in mice: a gender impact study. *Sci Rep*. 2018;8(1):16302. doi:10.1038/s41598-018-34362-2
173. Hardie DG, Carling D. The AMP-activated protein kinase--fuel gauge of the mammalian cell? *Eur J Biochem*. 1997;246(2):259-273. doi:10.1111/j.1432-1033.1997.00259.x
174. Owen MR, Doran E, Halestrap AP. Evidence that metformin exerts its anti-diabetic effects through inhibition of complex 1 of the mitochondrial respiratory chain. *Biochem J*. 2000;348 Pt 3:607-614.

175. Kim J, Kundu M, Viollet B, Guan KL. AMPK and mTOR regulate autophagy through direct phosphorylation of Ulk1. *Nat Cell Biol*. 2011;13(2):132-141. doi:10.1038/ncb2152
176. Langone F, Cannata S, Fuoco C, et al. Metformin Protects Skeletal Muscle from Cardiotoxin Induced Degeneration. *PLOS ONE*. 2014;9(12):e114018. doi:10.1371/journal.pone.0114018
177. Ye Y, Perez-Polo JR, Aguilar D, Birnbaum Y. The potential effects of anti-diabetic medications on myocardial ischemia-reperfusion injury. *Basic Res Cardiol*. 2011;106(6):925-952. doi:10.1007/s00395-011-0216-6
178. Iwasaki M, Homma S, Hishiya A, Dolezal SJ, Reed JC, Takayama S. BAG3 Regulates Motility and Adhesion of Epithelial Cancer Cells. *Cancer Res*. 2007;67(21):10252-10259. doi:10.1158/0008-5472.CAN-07-0618
179. Skuk D, Tremblay JP. Chapter 55 - Myoblast Transplantation in Skeletal Muscles. In: Atala A, Lanza R, Mikos AG, Nerem R, eds. *Principles of Regenerative Medicine (Third Edition)*. Academic Press; 2019:971-986. doi:10.1016/B978-0-12-809880-6.00055-2

APPENDIX

Appendix 1: Significant contributions to other projects

a) Peer-reviewed articles

Pellerin, D., Aykanat, A., Ellezam, B., Troiano, E.C., Karamchandani, J., Dicaire, M.J., Petitclerc, M., **Robertson, R.**, Allard-Chamard, X., Brunet, D., Konersman, C.G., Mathieu, J., Warman Chardon, J., Gupta, V.A., Beggs, A.H., Brais, B., Chrestian, N. Novel Recessive TNNT1 Congenital Core-Rod Myopathy in French Canadians. *Ann Neurol.* 2020 Apr;87(4):568-583.

R.R. helped with the sectioning, processing and imaging of human muscle tissue.

b) Manuscripts in preparation

Pellerin, D., Danzi, M.C., Wilke, C., Renaud, R., Fazal, S., Scriba, C., Ashton, C., Yanick, C., Dicaire, M.J., Choquet, K., Sakalla, R., Sonnen, J.A., Provost, S., **Robertson, R**., Allard-Chamard, X., Tétreault, M., Mathieu, J.; Massie, R,. Chalk, C.H., Lafontaine, A.L., Evoy, F., Rioux, M.F., Boycott, K.M., Dubé, M.P., Duquette, A.,Ravenscroft, G., Laing, N., Lamont, P., Schüle, R., Schöls, L., La Piana, R., Synofzik, M., Züchner, S.L., Brais, B. A Novel Mutation in FGF gene causes Cerebellar Ataxia. *Manuscript in preparation.*

R.R. helped with the processing and analysis of nanopore sequencing data